

PROBABILISTIC MODELING OF FAILURE IN ROCK SLOPES

A THESIS SUBMITTED TO
THE GRADUATE SCHOOL OF NATURAL AND APPLIED SCIENCES
OF
MIDDLE EAST TECHNICAL UNIVERSITY

BY

MOHAMED MOHIELDIN FADLELMULA FADLELSEED

IN PARTIAL FULFILLMENT OF THE REQUIREMENTS
FOR
THE DEGREE OF MASTER OF SCIENCE
IN
MINING ENGINEERING

JULY 2007

Approval of the Graduate School of Natural and Applied Sciences

Prof. Dr. Canan Özgen
Director

I certify that this thesis satisfies all the requirements as a thesis for the degree of Master of Science.

Prof. Dr. Celal Karpuz
Head of Department

This is to certify that we have read this thesis and that in our opinion it is fully adequate, in scope and quality, as a thesis for the degree of Master of Science.

Assoc. Prof. Dr. H. Ş. Düzgün
Co-Supervisor

Prof. Dr. Celal Karpuz
Supervisor

Examining Committee Members

Prof. Dr. Bahtiyar Ünver (Hacettepe Univ., Mine) _____

Prof. Dr. Celal Karpuz (METU, Mine) _____

Assoc. Prof. Dr. H. Ş. Düzgün (METU, Mine) _____

Assoc. Prof. Dr. Harun Sönmez (Hacettepe Univ.,GEO) _____

Dr. Nuray Demirel (METU, Mine) _____

I hereby declare that all information in this document has been obtained and presented in accordance with academic rules and ethical conduct. I also declare that, as required by these rules and conduct, I have fully cited and referenced all material and results that are not original to this work.

Name, Last name: Mohamed Mohieldin Fadlelmula Fadlelseed

Signature :

ABSTRACT

PROBABILISTIC MODELING OF FAILURE IN ROCK SLOPES

Fadlelmula F., Mohamed M.

M.Sc., Mining Engineering Department

Supervisor: Prof. Dr. Celal Karpuz

Co-Supervisor: Assoc. Prof. Dr. H. Ş. Düzgün

July 2007, 134 Pages

This study presents the results of probabilistic modeling of plane and wedge types of slope failures, based on the "Advance First Order Second Moment (AFOSM)" reliability method. In both of those failure types, two different failure criteria namely, Coulomb linear and Barton Bandis non-linear failure criteria are utilized in the development of the probabilistic models.

Due to the iterative nature of the AFOSM method, analyzing spreadsheets have been developed in order to carry out the computations. The developed spreadsheets are called "Plane Slope Analyzer (PSA)" and "Wedge Slope Analyzer (WSA)".

The developed probabilistic models and their spreadsheets are verified by investigating the affect of rock and slope parameters such as, ground water level, slope height, cohesion, friction angle, and joint wall compressive strength (JCS) and

their distribution types on the reliability index (β), and probability of slope failure (P_F).

In this study, different probability distributions are used and the inverse transformation formulas of their non-normal variates to their equivalent normal ones are developed as well.

In addition, the wedge failure case is also modeled by using system reliability approach and then the results of conventional probability of failure and the system reliability approach are compared.

Keywords: Plane Failure, Wedge Failure, Advance First Order Second Moment (AFOSM) Method, Reliability Index, Probability of Slope Failure, System Reliability.

ÖZ

KAYA ŞEV YENİLMELERİNİN OLASILIKSAL MODELLEMESİ

Fadlelmula F., Mohamed M.

Y. Lisans, Maden Mühendisliği Bölümü

Danışman: Prof. Dr. Celal Karpuz

Yardımcı Danışman: Doç. Dr. H. Ş. Düzgün

Temmuz 2007, 134 Sayfa

Bu çalışma, “Gelişmiş Birinci Derece İkinci Moment (GBDİM)” güvenilirlik yöntemine dayanarak, şevlerde düzlemsel ve kama tipi yenilmelerin olasılıksal modellemesine göre sonuçlarını sunmaktadır. Olasılıksal modelinin geliştirilmesinde, her iki yenilme tipinde de, doğrusal Coulomb ve doğrusal olmayan Barton-Bandis olmak üzere iki farklı yenilme yaklaşımı kullanılmıştır.

GBDİM metodunun tekrarlayıcı yapısından ötürü, hesaplamaları yapabilmek için analiz yapan hesap çizelgeleri geliştirilmiştir. Geliştirilen hesap çizelgeleri “Plane Slope Analyzer (PSA) ve “Wedge Slope Analyzer (WSA)” olarak adlandırılmıştır.

Geliştirilen olasılıksal modeller ve onların hesap çizelgeleri, yeraltı su seviyesi, şev yüksekliği, kohezyon, sürtünme açısı ve çatlak duvarı basma dayanım direnci (JCS) gibi kaya ve şev değişkenlerinin etkisi, bunların güvenilirlik indeksi üzerindeki dağılım tipleri ve şev yenilme olasılığı incelenerek doğrulanmıştır.

Bu alıřmada, deęiřik olasılık daęılımları kullanılmıř ve bunların normal olmayan deęiřkenlerinin eřdeęer normal olanlara ters dnüşüm formülleri de geliştirilmiřtir.

Buna ek olarak, kama tipi yenilme yaklaşımı durumu da sistem güvenilirlik yaklaşımı ile modellenmiř ve sonra geleneksel řev yenilme olasılıęı ile karşılaştırılmıřtır.

Anahtar Kelimeler: Düzlemsel Yenilme, Kama Tipi Yenilme, Geliřmiř Birinci Derece İkinci Moment (GBDİM) Yöntemi, Güvenilirlik İndeksi, řev Yenilme Olasılıęı, Sistem Güvenilirlięi.

To My Parents

ACKNOWLEDGEMENTS

I would like to express my sincere gratitude to my supervisor Prof. Dr. Celal Karpuz and co-supervisor Prof. Dr. H. Şebnem Düzgün for their guidance, advices, criticism, encouragements and insight throughout the study.

I am grateful also to my friend Swaleh Kavuma for his help in the application of Visual Basic.

I would like also to thank my friends Ebru Demir and Arman Koçal for their help with the Turkish translation of the Abstract.

Thanks also go to the examining committee members especially Dr. Nuray Demirel for their valuable comments and suggestions.

Additionally, I would like to thank my parents for their support, great patience and constant understanding at all time. Thanks also go to all members of my family for their endless understanding. Moreover, I would like to express my deepest gratitude to my best friend Fatma Kayan for her tremendous help, support and understanding at all time.

Finally, I would like to thank my friend Sabbil Mahmoud for his kindness and priceless help during the most important time of this thesis.

TABLE OF CONTENTS

	Page
ABSTRACT	iv
ÖZ.....	vi
ACKNOWLEDGEMENTS	iix
TABLE OF CONTENTS	x
LIST OF TABLES	xiv
LIST OF FIGURES.....	xix
LIST OF SYMBOLS.....	xxv
CHAPTER	
I. INTRODUCTION.....	1
1.1. Introduction	1
1.2. The Objectives of This Study	2
II. LITERATURE SURVEY	5
2.1. Introduction	5
2.2 Deterministic Analyses.....	5
2.3. Probabilistic Analyses	6
2.3.1. Monte Carlo Simulation Technique (MCST).....	6
2.3.2. Rosenblueth Point Estimate Method (RPEM).....	7
2.3.3. Reliability Index Methods	8
III. BASIC MECHANISMS OF PLANE AND WEDGE FAILURES	14
3.1. Introduction	14

3.2. Basic Mechanisms of Plane Failure	14
3.3. Basic Mechanisms of Wedge Failure	21
3.3.1. Biplane sliding.....	26
3.3.2. Sliding along plane 1 only	30
3.3.3. Sliding along plane 2 only	31
3.3.4. Floating failure	31
IV. ADVANCED FOSM APPROACH	32
4.1. Introduction	32
4.2. The Performance Function	33
4.3. Linear Performance Function	34
4.4. Nonlinear Performance Function	38
4.5. Non-normal Distributions.....	42
4.5.1. Uniform Distribution.....	43
4.5.2. Symmetric Triangular Distribution	44
4.5.3. Upper Triangular Distribution.....	46
4.5.4. Lower Triangular Distribution	47
4.5.5. Lognormal Distribution	48
V. DEVELOPED PROBABILISTIC MODELS	49
5.1. Introduction	49
5.2. Plane Failure.....	49
5.2.1. Coulomb Failure Criterion	49
5.2.2. Barton Bandis Failure Criterion	51
5.3. Wedge Failure	52
5.3.1. Coulomb Failure Criterion	52
5.3.1.1. Biplane Sliding	52
5.3.1.2. Sliding Along Plane 1 Only.....	54
5.3.1.3. Sliding Along Plane 2 Only.....	55
5.3.1.4. Floating Failure	56

5.3.2. Barton Bandis Failure Criterion	56
5.3.2.1. Biplane Sliding	57
5.3.2.2. Sliding Along Plane 1 Only.....	58
5.3.2.3. Sliding Along Plane 2 Only.....	58
5.3.2.4. Floating Failure	59
5.4. System Reliability	60
VI. DEVELOPMENT OF SLOPE ANALYZING SPREADSHEETS	62
6.1. Introduction	62
6.2. Plane Slope Analyzer (PSA)	63
6.2.1. Plane Slope Analyzer (Coulomb).....	63
6.2.1.1. Coding in Excel	64
6.2.1.2. Solver Optimization Tool.....	67
6.2.2. Plane Slope Analyzer (Barton Bandis).....	69
6.3. Wedge Slope Analyzer (WSA)	70
6.3.1. Wedge Slope Analyzer (Coulomb)	70
6.3.2. Wedge Slope Analyzer (Barton Bandis)	75
6.4. Defining and Enabling Macros.....	78
6.5. Verification of PSA and WSA Spreadsheets.....	81
6.5.1. Plane Slope Analyzers	81
6.5.1.1. Plane Slope Analyzer (Coulomb).....	82
6.5.1.2. Plane Slope Analyzer (Barton Bandis).....	86
6.5.2. System Reliability	89
6.5.3. Wedge Slope Analyzer	91
6.5.3.1. Wedge Slope Analyzer (Coulomb)	91
6.5.3.2. Wedge Slope Analyzer (Barton Bandis)	94
6.6. Sensitivity Analysis Based on Distribution Function for PSA.....	97
6.6.1 Sensitivity analysis for PSA (Coulomb).....	97
6.6.2 Sensitivity analysis for PSA (Barton Bandis)	99
6.7. Discussion.....	100

VII. CONCLUSIONS AND RECOMMENDATIONS	103
REFERENCES	105
APPENDICES	
A: PLANE SLOPE ANALYZER (COULOMB).....	111
B: THE USER DEFINED CODE IN THE DEVELOPED SPREADSHEETS.	113
C: PLANE SLOPE ANALYZER (BARTON BANDIS).....	116
D: WEDGE SLOPE ANALYZER (COULOMB)	118
E: WEDGE SLOPE ANALYZER (BARTON BANDIS)	123
F: TABLES OF RESULTS FOR PSA (COULOMB).....	127
G: TABLES OF RESULTS FOR PSA (BARTON BANDIS).....	131

LIST OF TABLES

	Page
Table 4.1 The Means and c.o.v.'s of various distributions (Ang and Tang, 1984)	42
Table 6.1 Summary of the basic variables and their statistical parameters for PSA (Coulomb)	82
Table 6.2 Constant parameters for PSA	82
Table 6.3 Values of H and Z used in the analysis	83
Table 6.4 Summary of the basic variables and their statistical parameters for PSA (Barton Bandis)	86
Table 6.5 Summary of the basic variables and their statistical parameters for WSA (Coulomb)	89
Table 6.6 Constant parameters for WSA	89
Table 6.7 Failure probability of single failure modes for the wedge slope considered	90
Table 6.8 Summary of the basic variables and their statistical parameters for WSA (Barton Bandis)	95
Table 6.9 Summary of the basic variables for PSA (Coulomb)	98

Table 6.10 Constant parameters for PSA	98
Table 6.11 Results of the Plane Slope Analyzer (Coulomb)	98
Table 6.12 Summary of the basic variables for PSA (Barton Bandis)	99
Table 6.13 Results of the Plane Slope Analyzer (Barton Bandis)	99
Table 6.14 Probability of failure, P_F , of a plane with cohesion of 15 (ton/m ²) for different slope heights at 10 m height of water table	101
Table 6.15 Probability of failure, P_F , of a wedge with cohesion of 30 (kPa) for different slope heights at 0.5 Normalized water pressure	101
Table F.1 Values of P_f for $H = 60$ m and at 0 m height of water table	128
Table F.2 Values of P_f for $H = 70$ m and at 0 m height of water table	128
Table F.3 Values of P_f for $H = 80$ m and at 0 m height of water table	128
Table F.4 Values of P_f for $H = 100$ m and at 0 m height of water table	129
Table F.5 Values of P_f for $H = 60$ m and at 10 m height of water table	129
Table F.6 Values of P_f for $H = 70$ m and at 10 m height of water table	129

Table F.7 Values of Pf for H = 80 m and at 10 m	
height of water table	129
Table F.8 Values of Pf for H = 100 m and at 10 m	
height of water table	129
Table F.9 Values of Pf for H = 60 m and at 0 m	
height of water table	130
Table F.10 Values of Pf for H = 70 m and at 0 m	
height of water table	130
Table F.11 Values of Pf for H = 80 m and at 0 m	
height of water table	130
Table F.12 Values of Pf for H = 100 m and at 0 m	
height of water table	130
Table F.13 Values of Pf for H = 60 m and at 10 m	
height of water table	130
Table F.14 Values of Pf for H = 70 m and at 10 m	
height of water table	131
Table F.15 Values of Pf for H = 80 m and at 10 m	
height of water table	131
Table F.16 Values of Pf for H = 100 m and at 10 m	
height of water table	131
Table G.1 Values of Pf for H = 60 m and at 0 m	
height of water table	132

Table G.2 Values of Pf for H = 70 m and at 0 m	
height of water table	132
Table G.3 Values of Pf for H = 80 m and at 0 m	
height of water table	132
Table G.4 Values of Pf for H = 100 m and at 0 m	
height of water table	133
Table G.5 Values of Pf for H = 60 m and at 10 m	
height of water table	133
Table G.6 Values of Pf for H = 70 m and at 10 m	
height of water table	133
Table G.7 Values of Pf for H = 80 m and at 10 m	
height of water table	133
Table G.8 Values of Pf for H = 100 m and at 10 m	
height of water table	133
Table G.9 Values of Pf for H = 60 m and at 0 m	
height of water table	134
Table G.10 Values of Pf for H = 70 m and at 0 m	
height of water table	134
Table G.11 Values of Pf for H = 80 m and at 0 m	
height of water table	134
Table G.12 Values of Pf for H = 100 m and at 0 m	
height of water table	134

Table G.13 Values of Pf for H = 60 m and at 10 m	
height of water table	134
Table G.14 Values of Pf for H = 70 m and at 10 m	
height of water table	135
Table G.15 Values of Pf for H = 80 m and at 10 m	
height of water table	135
Table G.16 Values of Pf for H = 100 m and at 10 m	
height of water table	135

LIST OF FIGURES

	Page
Figure 2.1 Illustration of the reliability index of the AFOSM method in plane (Low 1997)	10
Figure 3.1 Sliding condition in an inclined plane (Hoek and Bray, 1981)	15
Figure 3.2 Forces acting on a sliding mass	16
Figure 3.3 Geometry of a plane slope with a tension crack in its upper surface (Hoek and Bray, 1981)	18
Figure 3.4 Forces acting on a block on a failure plane of a slope with a tension crack in its upper surface (Hoek and Bray, 1981)	18
Figure 3.5 Geometry of a plane slope with a tension crack in its face (Hoek and Bray, 1981)	19
Figure 3.6 Forces acting on a block on a failure plane of a slope with a tension crack in its surface (Hoek and Bray, 1981)	19
Figure 3.7 Sliding condition for wedge slope	22
Figure 3.8 Wedge failure geometry (Hoek and Bray, 1981)	23
Figure 3.9 Forces acting on the wedge slope (Hoek and Bray, 1981)	24

Figure 3.10 Geometry of wedge used for stability analysis by Hoek et al. (1973)	25
Figure 3.11 Slope geometry in wedge failure (Low and Einstein, 1992)	27
Figure 4.1 Limit state surface in - space (Ang and Tang, 1984)	35
Figure 4.2 Tangent Plane to $g(x) = 0$ at x^* (Ang and Tang, 1984)	39
Figure 5.1 Series representation of the wedge failure	60
Figure 6.1 Converter tool	64
Figure 6.2 Equivalent mean value	65
Figure 6.3 Meaning of para1 and para2 according to their distribution type	65
Figure 6.4 Reliability index in the spreadsheet	66
Figure 6.5 Constraints of Plane Slope Analyzer (Coulomb)	68
Figure 6.6 Solver results window	68
Figure 6.7 Required parameters in PSA (Barton Bandis)	69
Figure 6.8 Constraints of PSA (Barton Bandis)	70
Figure 6.9 Constraints of Biplane failure WSA (Coulomb)	72
Figure 6.10 The Constraints of the failure along plane 1 WSA (Coulomb)	73

Figure 6.11 The Constraints of the failure along plane 2 WSA (Coulomb)	74
Figure 6.12 Constraints of the Floating failure WSA (Coulomb)	75
Figure 6.13 Constraints of the Biplane failure WSA (Barton Bandis)	76
Figure 6.14 Defining macros in Excel, step (1)	78
Figure 6.15 Defining macros in Excel, step (5)	79
Figure 6.16 Enabling macros, steps (1)	79
Figure 6.17 Enabling macros, steps (2).....	80
Figure 6.18 Excel warning window	80
Figure 6.19 Solver of PSA (Coulomb) after eliminating ψ_f and ψ_p	81
..	
Figure 6.20 Cohesion versus Beta values for different slope heights at dry condition	84
Figure 6.21 Cohesion versus Beta values for different slope heights at 10 m height of water table	84
Figure 6.22 Friction angle versus Beta values for different slope heights at dry condition	85
Figure 6.23 Friction angle versus Beta values for different slope heights at 10 m height of water table	85

Figure 6.24 JCS versus Beta values for different slope heights at 0 m height of water table	87
Figure 6.25 JCS versus Beta values for different slope heights at 10 m height of water table	87
Figure 6.26 Basic friction angle versus Beta values for different slope heights at 0 m height of water table	88
Figure 6.27 Basic friction angle versus Beta values for different slope heights at 10 m height of water table	88
Figure 6.28 Comparison of system reliability result with the results of single failure modes	91
Figure 6.29 Cohesion versus probability of slope failure for different slope heights at 0.25 Normalized water pressure	92
Figure 6.30 Cohesion versus probability of slope failure for different slope heights at 0.5 Normalized water pressure	93
Figure 6.31 Friction angle versus probability of slope failure for different slope heights at 0.25 Normalized water pressure	93
Figure 6.32 Friction angle versus probability of slope failure for different slope heights at 0.5 Normalized water pressure	94
Figure 6.33 JCS versus probability of slope failure for different slope heights at 0.25 Normalized water pressure	95
Figure 6.34 JCS versus probability of slope failure for different slope heights at 0.5 Normalized water pressure	96

Figure 6.35 Friction angle versus probability of slope failure for different slope heights at 0.25 Normalized water pressure	96
Figure 6.36 Friction angle versus probability of slope failure for different slope heights at 0.5 Normalized water pressure	97
Figure A.1 Plane Slope Analyzer (Coulomb) definitions and details worksheet (1)	112
Figure A.2 Plane Slope Analyzer (Coulomb) definitions and details worksheet (2)	113
Figure A.3 Plane Slope Analyzer (Coulomb) input & output worksheet	113
Figure C.1 Plane Slope Analyzer (Barton Bandis) definitions and details worksheet (1)	117
Figure C.2 Plane Slope Analyzer (Barton Bandis) definitions and details worksheet (2)	118
Figure C.3 Plane Slope Analyzer (Barton Bandis) input & output worksheet	118
Figure D.1 Wedge Slope Analyzer (Coulomb) definitions and details worksheet (1)	119
Figure D.2 Wedge Slope Analyzer (Coulomb) definitions and details worksheet (2)	120
Figure D.3 Wedge Slope Analyzer (Coulomb) input & output worksheet	120

Figure D.4 Wedge Slope Analyzer (Coulomb) Biplane failure worksheet	121
Figure D.5 Wedge Slope Analyzer (Coulomb) Plane 1 failure worksheet	121
Figure D.6 Wedge Slope Analyzer (Coulomb) Plane 2 failure worksheet	122
Figure D.7 Wedge Slope Analyzer (Coulomb) Floats worksheet	122
Figure D.8 Wedge Slope Analyzer (Coulomb) summary worksheet	123
Figure E.1 Wedge Slope Analyzer (Barton Bandis) definitions and details worksheet	124
Figure E.2 Wedge Slope Analyzer (Barton Bandis) input & output worksheet	125
Figure E.3 Wedge Slope Analyzer (Barton Bandis) Biplane failure worksheet	125
Figure E.4 Wedge Slope Analyzer (Barton Bandis) Plane 1 failure worksheet	126
Figure E.5 Wedge Slope Analyzer (Barton Bandis) Plane 2 failure worksheet	126
Figure E.6 Wedge Slope Analyzer (Barton Bandis) Floats worksheet	127
Figure E.7 Wedge Slope Analyzer (Barton Bandis) summary worksheet	127

LIST OF SYMBOLS

A : Base area of the sliding block

a_1, a_2, b_1, b_2 : Parameters that depend on the geometry of slope

C : Cohesion of joint

D_f : Driving forces

$F_{x_i}(x_i^*)$: Original CDF of x_i evaluated at x_i^*

F_S : Factor of safety

F_i : Failure modes

G_{w1} and G_{w2} : Normalized water pressure parameters

$g(x_i)$: Performance function

H : Slope height

M : Very large positive number

P_F : Probability of Failure

$P(F_i)$: Probability of failure modes

P_S : Probability of survival

R_f : The total resisting force

$R(x_i)$: Strength (capacity) of slope

R_A : Normal reactions provided by planes A

R_B : Normal reactions provided by planes B

$S(x_i)$: Load (demand) acting on the slope

S_γ : Specific density of rock

U: Uplift force due to pressure on the sliding surface

u_1 and u_2 : Average water pressures

V: Force due to water pressure in the tension crack

W: Weight of sliding block

x_i : Basic variables

x'_i : Reduced (standardized) variables

X, Y, A and B : Dimensionless factors that depend upon the geometry of wedge slope

Z: Height of the tension crack from the upper surface of the slope

Z_w : Height of water in tension crack (Height of water table)

α_i : Direction cosines of the variable x_i

β : Reliability index

$\delta_1, \delta_2, \beta_1, \beta_2$, and ε : Angles defining wedge slope

Ω : Inclination of the upper ground surface (wedge slope)

α : Inclination of wedge slope face

$\Phi()$: CDF of the standard normal distribution

$\phi()$: PDF of the standard normal distribution

ϕ : Friction angle

ϕ_r : Residual friction angle

γ : Unit weight of rock

γ_w : Unit weight of water

μ_i : Mean value of i^{th} variable

μ_{xi}^N : Mean value of equivalent normal distribution for the variable x_i

ψ_f : Dip of slope face

ψ_p : Dip of discontinuity plane

ψ_{fi} : Inclination of the slope face, measured in view at right angle to the line of intersection of discontinuities

ψ_i : Dip of the line of intersection

σ_n : Normal stress

σ_i : Standard deviation of the i^{th} variable

σ_{xi}^N : Standard deviation of equivalent normal distribution for the variable x_i

τ : Shear stress causing failure

λ : Mean of $(\ln x)$ and a parameter of the lognormal distribution

ξ : Standard deviation of $(\ln x)$ and a parameter of the lognormal distribution

c.o.v: Coefficient of variation

AFOSM: Advanced First Order Second Moment

FOSM: First Order Second Moment

CDF: Cumulative distribution function

JCS: Joint wall compressive strength

JRC: Joint roughness coefficient

PSA: Plane Slope Analyzer

PDF: Probability density function

WSA: Wedge Slope Analyzer

CHAPTER I

INTRODUCTION

1.1. Introduction

Numerous numbers of lives and properties were lost all over the world due to slope failures although stability analyses are carried out. Most of these analyses are based on the deterministic methods which do not consider the effect of uncertainty associated with certain parameters like ground water pressure, rock mass, and discontinuities' shear strength. Such uncertainties cause variation in failure probability of slopes that have the same factor of safety. As a result, the use of probabilistic analysis techniques that take into account such kind of uncertainties became more common in recent years. Some of the most widely used probabilistic methods are Monte Carlo simulation technique, Rosenblueth point estimate method, and reliability index methods. Among these the "Advanced First Order Second Moment (AFOSM)" reliability method proposed by Hasofer and Lind (1974) is an outstanding one as it considers the uncertainty and variability of the parameters involved as well as their correlation structure.

Many researchers have tried to generate formulas in order to calculate safety factor of plane and wedge failure cases. As an example, Hoek and Bray (1977; 1981) have formulated equations to calculate the safety factor of such cases. They

also calculated safety factor of the wedge failure depending on a stereoplot. However, Low (1979) obtained an alternative method for that method, which does not require any stereographic plot. Thus, the calculation mechanism was eased. Low assumed that the upper ground surface is horizontal. However, Low and Einstein (1992) generalized this method to include cases with inclined upper ground surface, which dips in the same direction as the considered slope face. Low (1997) calculated the safety factor for a wedge slope utilizing AFOSM. In addition, utilizing Excel spreadsheet he calculated the reliability index and probability of failure for that slope. Low (1997) used Coulomb linear failure criterion and he assumed that all the parameters are normally distributed. However, some researchers have stated that although the Coulomb criterion is widely used, it is not particularly satisfactory in considering peak strength criterion for rock material. As a result, other peak shear strength criteria are preferred for the analysis of shear failure on rock discontinuities. Barton Bandis shear failure criterion is an example of these criteria.

1.2. The Objectives of This Study

There are two main objectives of this study. The first one is to develop probabilistic models of plane and wedge failure cases utilizing AFOSM reliability method by both Coulomb linear and Barton Bandis non-linear failure criteria. The second objective is to investigate the affect these criteria on the results of slope stability analyses. The developed plane failure models are based on the methodology proposed by Hoek and Bray (1981), whereas, wedge failure models are based on the methodology proposed by Low and Einstein (1992). Moreover, the developed model does not consider only normally distributed variables, but also it considers variables having lognormal, uniform, and triangular (symmetric, upper, lower) distributions.

The developed probabilistic models are coded in spreadsheets to ease the calculations involved, which are very excessive and time consuming due to the

iterative nature of AFOSM method. The developed spreadsheets are named as “Plane Slope Analyzer (PSA)” and “Wedge Slope Analyzer (WSA)”. Each one of these analyzers has two types corresponding to the linear and non-linear failure criteria. The verifications of these analyzers are made by investigating the effect of slope height, ground water level, cohesion, friction angle, and joint wall compressive strength (JCS) on reliability index (β) and probability of slope failure (P_F).

After the verification of the developed spreadsheets, two analyses are carried out. The first analysis is investigating the affect of Coulomb linear and Barton Bandis non-linear failure criteria on probability of slope failure. The second one is a sensitivity analysis in which, the affect of distribution function of parameters on the reliability index and probability of failure is investigated. In order to perform such analyses the equivalent normal moments of non-normal distributions are needed. Thus, transformation formulas are derived.

Beside that, evaluating the safety of wedge slope is carried out by two methods. The first one is the conventional method depending on the failure probability of single modes. The second one is the system reliability approach proposed by Ang and Tang (1984).

The present study is divided into seven chapters. Chapter I covers a brief introduction of the thesis together with its aim. In Chapter II, a literature review of previous probabilistic studies on stability of rock slopes is elucidated. Chapter III covers the basic mechanisms of plane and wedge failures. Next, in Chapter IV brief information about AFOSM method as well as the inverse transformation techniques developed to evaluate the equivalent normal variates of the non-normal ones are considered. Chapter V gives the details of the probabilistic models developed in for cases of plane and wedge failures based on linear and non-linear failure criteria.

Moreover, this chapter covers the explanation of the system reliability approach, which is used in the evaluation of the failure probability for wedge slopes.

In Chapter VI the developed analyzing spreadsheets are explained in details. In other words, the fifth chapter explicates the techniques followed in the coding of the models explained in Chapter VI using Excel software. Additionally, this chapter considers some applications of these spreadsheets as well as the discussion of the results. After that, in Chapter VII the major conclusions of this thesis and the main recommendations are specified. Finally, the macro defined and illustrating figures of the developed spreadsheets are presented in Appendices A, B, C, and D.

CHAPTER II

LITERATURE SURVEY

2.1. Introduction

In rock engineering, slope stability analysis is a two stage procedure. In the first stage the motion of rock blocks without reference to the forces causing it is the main concern and called kinematic analysis. In the second stage (kinetic analysis) the forces acting on the questioned rock block are considered. Thus, it is more detailed, and provides engineers with more reliable outcomes than the kinematic analysis. As a result of that many kinetic analyses have been developed. The kinematic and kinetic analyses can be performed either deterministic or probabilistic.

2.2 Deterministic Analyses

These types of analyses are based on the calculation of a safety factor that is defined as the ratio of the forces resisting the slide of a rock block over the forces causing the slide. The factor of safety calculated by the deterministic methods is not reliable since it does not take in to consideration the uncertainty associated with the utilized parameters. In other words, the deterministic methods use single values that are normally the mean values of the considered parameters. However, in nature

these parameters are random variables, which contain considerable amount of uncertainty (Duzgun, 1994).

2.3. Probabilistic Analyses

These types of analyses were first developed to overcome the limitation of the deterministic analysis methods. In other words, these types of analyses consider the uncertainties and randomness associated with the stability parameters. Probabilistic analysis was first introduced to rock slope stability by McMahon (1971). After that many researchers have utilized this type of analyses. An example of that is the study of Gokceoglu et al. (2000). Some of the most widely used Probabilistic methods of analysis are the Monte Carlo simulation technique, the Rosenblueth point estimate method, and the reliability indexes method.

2.3.1. Monte Carlo Simulation Technique (MCST)

This method was first introduced during World War II in order to develop the atomic bomb. The simulation involves the construction of the sample space for the considered random variables repeating the analysis over and over using these random variables which are driven from the distribution of the variables using a random number generator (Feng, 1997). The technique got the name Monte Carlo because of the “roulette” method that has been used to generate the random variables before the computers were introduced (Giani, 1992).

The MCST generate a large quantity of random numbers varying between 0 and 1. These numbers are used to generate the variables of the examined problem in a way that fits the assumed probability distribution curves. Such curves can also be histograms that are drawn according to some experimental data results. This

simulation can be carried out to determine the probability density distribution of a safety factor or a safety margin (resisting forces – driving forces). The MCST is applied to the problems that are very difficult to solve with the analytical methods (Giani, 1992).

The usage of MCST in stability analyses of planes and three dimensional wedges have been described by Kim et al. (1978) and Major et al. (1978). Following these authors many others have used the MCST in rock engineering. Some of these authors are Priest and Brown (1983), and Morris and stoter (1983), Esterhuizen (1990), Muralha and Trunk (1993), and Duzgun et al. (2005).

It is also one of the most used probabilistic methods in rock engineering. The reason for that is its avoidance for the complexity of the failure functions that are very difficult to analyze analytically. Despite its wide usage, the MCST has some limitations and drawbacks. One of these is that MCST may not achieve solutions in some cases, especially when complex limit state functions are used or when dealing with problems of low probability of failure (Jimenez-Rodriguez et al., 2006). Beside this one Duzgun (1994) has cited that Mostyn and Li (1993) stated another major drawback of MCST. They reported that the rock properties in this method are modeled as spatially perfectly correlated random variables in order to make the procedure simple, which make the result doubtful.

2.3.2. Rosenblueth Point Estimate Method (RPEM)

As the previous method i.e. MCST, this method is also based on a deterministic procedure. Giani (1992) cited that the method was first given by Rosenblueth (1975) and later modified by the same author (1981). He also cited that the first person who applied the point estimate method to geomechanical problems was Harr (1981). As cited by Duzgun. (1994), Kimmance and Howe (1991)

presented an application of RPEM in slope stability analysis. She also cited that Nguyen and Chowdhury (1985) proved that RPEM is more computationally efficient than MCST.

This method permits the one to use several correlated random variables given by their two or three first statistical moments (mean, standard deviation and skewness). By doing so we can get results that are expressed in terms of the first statistical moments of the examined parameters (Giani, 1992). The principles and the complete procedures of the RPEM are discussed in details by Bolle et al. (1987).

The RPEM becomes impractical when the numbers of random variables involved are large. Such a case is encountered in slope stability analysis as the numbers of random variables considered are generally large (Duzgun, 1994).

2.3.3. Reliability Index Methods

This method differs from all the already mentioned methods of analysis in that the safety of a given slope is formulated by a reliability index (β) rather than the conventional safety factor. In order to find this reliability index, we should first formulate the performance function of slope, which in general expressed as (Ang and Tang, 1984):

$$g(x_1, x_2, x_3, \dots, x_n) = g(x_i) \quad (2.1)$$

Where x_i are the basic variables (i.e. the random input parameters). The importance of this function is that it represents the stability situation of a given slope as follows:

If $g(x_i) < 0$ “failure state” and,

If $g(x_i) > 0$ “safe state”

However, if $g(x_i) = 0$ then the slope is said to be in the “limit state” and “ $g(x_i) = 0$ ” is called the limit state equation.

The performance function for a slope is in general defined as (Duzgun, 1994):

$$g(x_i) = R(x_i) - S(x_i) \quad (2.2)$$

Where,

$R(x_i)$ = Strength (capacity) of the slope

$S(x_i)$ = Load (demand) acting on the slope

Ang and Tang (1984) and Duzgun (1994) stated that there are two reliability methods which are generally used. The first is the First Order Second Moment (FOSM) method. In this method, if the limit state function is nonlinear then the approximation is obtained by utilizing Taylor series expansion around the mean values (Cornell, 1969). As Duzgun (1994) and Low (2003) reported this is one of the main basic drawbacks of the FOSM method. That is because when the performance function is linearized at the mean values of the basic variable, significant errors will appear especially for the nonlinear functions at increasing distance from the linearizing point. Another drawback of this method as they reported is the lack of invariance for nonlinear performance function.

The second method is the Advanced First Order Second Moment (AFOSM) method proposed by Hasofer and Lind (1974). This method overcame the drawbacks of the traditional FOSM method and thus, it is a better alternative (USACE, 1999). The basic principle and structure of the AFOSM method is given in details by Ang

and Tang (1984). Beside these authors Low (1996) as well has given the meaning and the definition of the reliability index (β) of the AFOSM method (Figure 2.1).

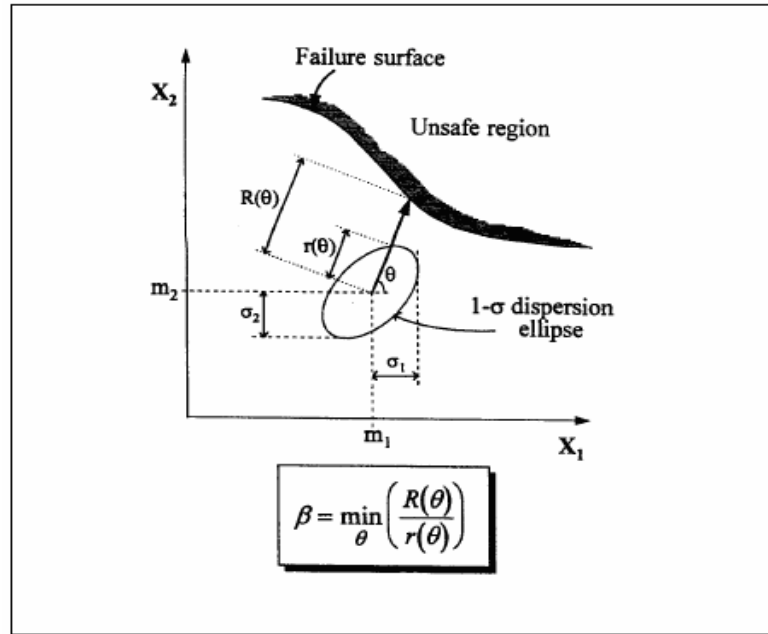


Figure 2.1 Illustration of the reliability index of the AFOSM method in plane
(Low 1997)

In this Figure m_1 , σ_1 , m_2 , and σ_2 are the mean values and standard deviations of the parameters X_1 and X_2 . The index β may be regarded as the distance from the boundary of the failure region, in units of directional standard deviation. Ditlevsen (1981) has given the following formulation for Hasofer and Lind (1974) index (or the index of AFOSM method) as follows:

$$\beta_{HL} = \min \sqrt{(x-m)^T C^{-1} (x-m)} \quad (2.3)$$

and, $x \in F$

Where x is a vector representing the set of random variables, C is the covariance matrix of the random variables, and F is the failure region.

One of the procedures that are widely used for the computation of β is the one in which the failure surface is transformed into the space of reduced variates, where the shortest distance between the transformed failure surface and the origin of the reduced variates is the reliability index (β). In other words, the Hasofer and Lind (1974) index can be calculated by minimizing the quadratic form (an ellipsoid) subject to the constraint that the ellipsoid just touches the surface of the failure region (Figure 2.1).

Many authors have used this method and stated its advantages over the probabilistic, numerical and analytical analysis methods. For example, Duzgun et al. applied AFOSM to wedge slope failure (1994; 1995). Moreover, Duzgun et al. applied this method to plane slope failure (2003). In addition, Hassan and Wolff (1999) utilized the method in the stability analysis of Connon Dam. Beside these authors, Low applied the AFOSM method to analyze the stability of, rock wedges (1997), anchored retaining wall (2002), and embankment on soft ground (2003).

Low (1979) developed a compact closed-form equation for the calculation of the factor of safety for two-joint tetrahedral wedges. This equation is an alternative for equation (2.1), but no stereographic projection is required in utilizing it. He assumed that the upper ground surface is horizontal. However, Low and Einstein (1992) generalized this method to include cases with inclined upper ground surface that dips in the same direction as the considered slope face.

Low and Einstein (1992) calculated the factors of safety for different modes of failures. These modes are:

1. Sliding along the line of intersection of both planes forming the block (Biplane sliding)
2. Sliding along plane 1 only
3. Sliding along plane 2 only
4. Floating failure (due to high water pressure or high in-situ stresses)

Low (1997) proposed a new computational method that eases the utilization of the AFOSM method. He implemented the AFOSM method using the solver tool available in the Excel spreadsheet to analysis rock slope stability. In that analysis Low used Coulomb failure criterion and assumed that the parameters are normally distributed.

Giani (1992) however, cited that although the Coulomb criterion is widely used, it is not particularly satisfactory in considering peak strength criterion for rock material. The reasons for that were given by Brady and Brown (1985) as:

1. The Coulomb criterion implies that a major shear fracture exists at peak strength. However, that was proven not to be the general case (Wawersik and Fairhurst, 1970).
2. It also implies a direction of the shear failure which is not always in a good agreement with experimental observations.
3. As the experimental peak strength envelopes are generally non-linear, they can consider only a limited range of σ_n or σ_3 .

As a result of these reasons other peak shear strength criteria are preferred for the analysis of shear failure on rock discontinuities. Barton Bandis shear failure criterion, which is given in equation 2.33, is among the most widely used non-linear shear strength criteria.

Barton Bandis criterion (1990):

$$\tau = \sigma_n \tan \left[JRC \log_{10} \left(\frac{JCS}{\sigma_n} \right) + \phi_r \right] \quad (2.4)$$

Where,

τ = Shear stress causing failure

JRC = Joint roughness coefficient

JCS = Joint compressive strength

σ_n = Normal stress

ϕ_r = Residual friction angle

CHAPTER III

BASIC MECHANISMS OF PLANE AND WEDGE FAILURES

3.1. Introduction

In rock engineering many researchers have studied plane and wedge slope failures. The plane failure occurs rarely if compared with wedge failure that is the more common case in rock slopes. Therefore, many engineers treat the plane failure as a special case of wedge failure.

The basic mechanisms of these types of slope failure have been studied by many engineers and in many different ways. However, the most widely used approaches are the ones proposed by Hoek et al. (1973). Hoek and Bray (1981) used Coulomb linear criteria in developing these approaches. Besides they expressed the water forces due to water pressure on the sliding surface and in tension crack as uplift forces.

3.2. Basic Mechanisms of Plane Failure

Hoek and Bray (1981) stated the general condition of a Plane failure to take place is:

$$\psi_f > \psi_p > \phi \quad (3.1)$$

Where,

ψ_f = Inclination of the slope face

ψ_p = Dip of the failure plane

ϕ = Friction angle

This case can be seen clearly in Figure (3.1).

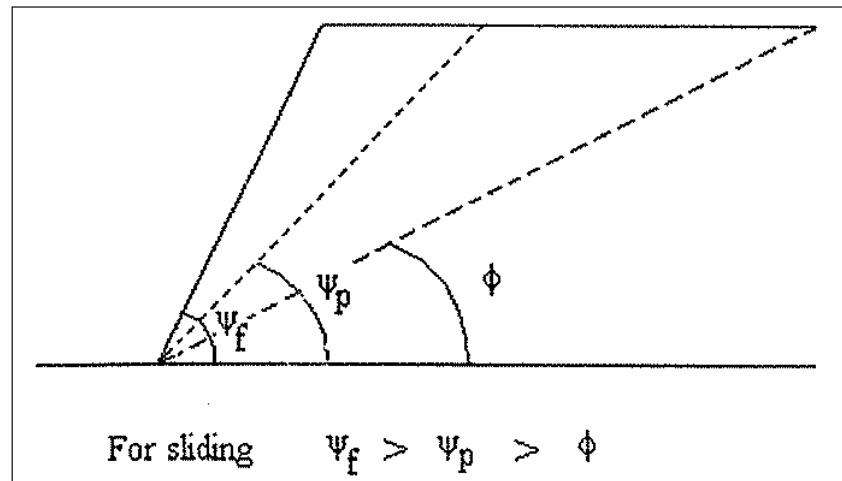


Figure 3.1 Sliding condition in an inclined plane (Hoek and Bray, 1981)

Beside that the plane on which sliding takes place must strike parallel or nearly parallel to the slope face. In other words, this plane must strike within $\pm 20^\circ$ to the slope face.

Plane failure has the same basic mechanisms of a sliding block along an inclined surface due to gravitational loading. Figure (3.2) shows such block, where,

W = Weight of the block

ψ = Inclination of the sliding surface from the horizontal

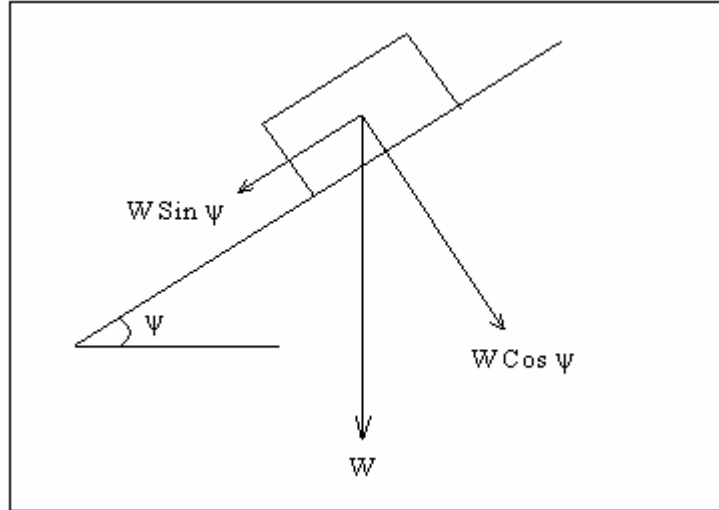


Figure 3.2 Forces acting on a sliding mass

In this case the force ($W \sin \psi$) is tending to cause the sliding, while the force $W \cos \psi$ is contributing to the total resistance to the sliding. So, the normal stress σ which is acting on the sliding surface is (Hoek and Bray, 1981):

$$\sigma = \frac{W \cos \psi}{A} \quad (3.2)$$

Where,

A = Base area of the sliding block

Now, substituting the value of σ in Coulomb failure criterion which is:

$$\tau = c + \sigma \tan \phi \quad (3.3)$$

The following is found:

$$\tau = c + \frac{W \cos \psi}{A} \tan \phi \quad (3.4)$$

Where,

τ = Shear stress causing the slide

ϕ = Friction angle

c = Cohesion

Then if equation (3.4) is multiplied by the base area of the block:

$$\tau A = cA + W \cos \psi \tan \phi \quad (3.5)$$

Where, τA is the shear force that resists the sliding and which is equal to the driving force $W \sin \psi$. This force is equal to the resisting force $W \cos \psi$ at the limit state.

That is, at the limit state:

$$W \sin \psi = cA + W \cos \psi \tan \phi \quad (3.6)$$

The geometries of the plane slopes considered in this thesis work are defined in Figures 3.3 through 3.6.

Where,

H = Slope height (m)

W = Weight of the sliding block (kN/m)

V = Force due to water pressure in the tension crack (kN/m)

U = Uplift force due to pressure on the sliding surface (kN/m)

ψ_f = Dip of slope face

ψ_p = Dip of discontinuity plane

Z = Height of the tension crack from the upper surface of the slope (m)

Z_w = Height of water in tension crack (m)

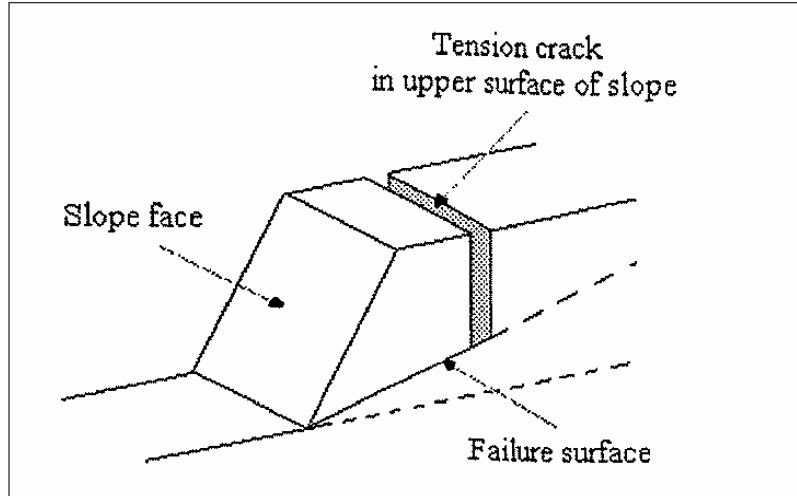


Figure 3.3 Geometry of a plane slope with a tension crack in its upper surface
(Hoek and Bray, 1981)

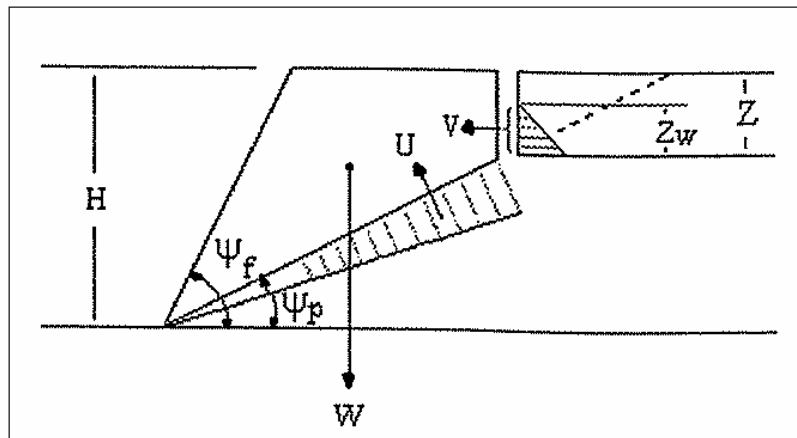


Figure 3.4 Forces acting on a block on a failure plane of a slope with a tension crack in its upper surface (Hoek and Bray, 1981)

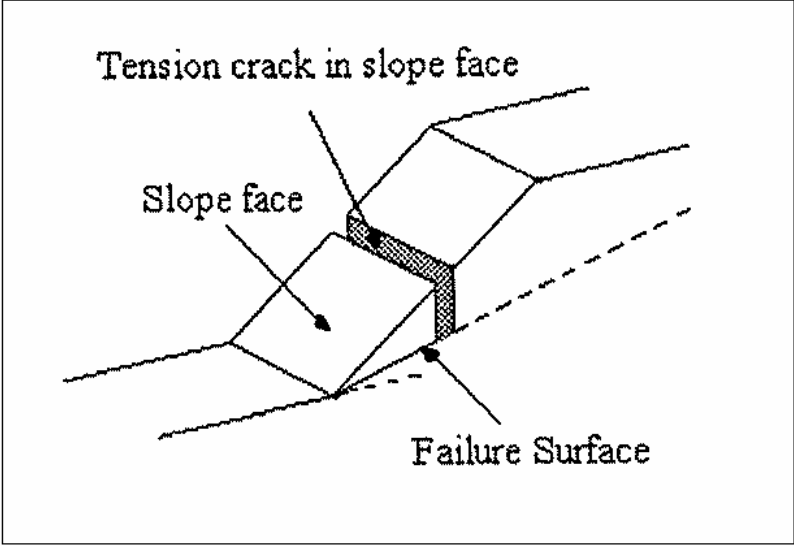


Figure 3.5 Geometry of a plane slope with a tension crack in its face (Hoek and Bray, 1981)

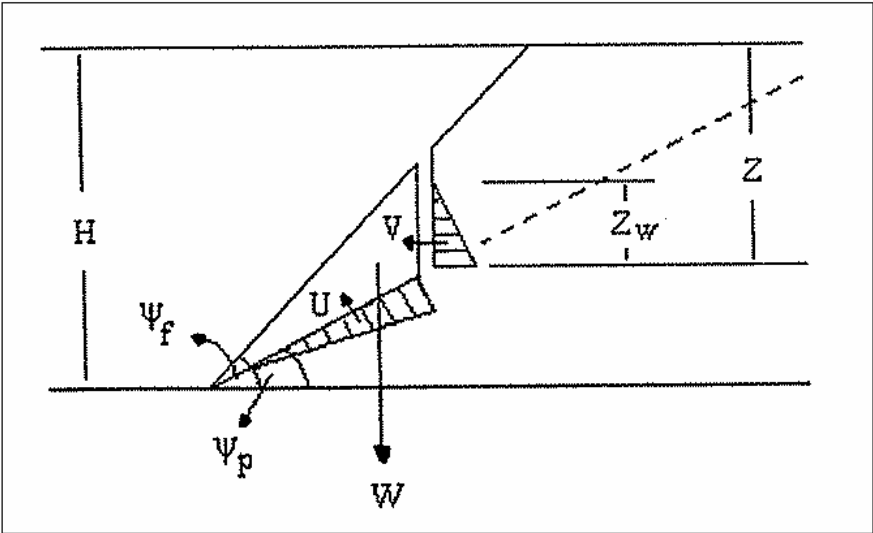


Figure 3.6 Forces acting on a block on a failure plane of a slope with a tension crack in its surface (Hoek and Bray, 1981)

In these slopes the affect of water pressure in the block is also taken into consideration. Observably, two cases are considered, namely:

1. A slope having a tension crack in its upper surface.
2. A slope with a tension crack in its face.

Hoek and Bray (1981) formulated the two cases as:

$$A = (H - Z) \cdot \text{Cosec} \psi_p \quad (3.7)$$

$$U = \frac{1}{2} \gamma_w \cdot Z_w (H - Z) \text{Cosec} \psi_p \quad (3.8)$$

$$V = \frac{1}{2} \gamma_w \cdot Z_w^2 \quad (3.9)$$

The area and the water forces' equations are the same for both cases. However, the weight of the sliding block is calculated by different equation each cases. That is due to the position change of the tension crack. So, when the tension crack is situated in the upper surface of the slope, the weight is calculated by the following equation:

$$W = \frac{1}{2} \gamma H^2 \left[\left(1 - \left(\frac{Z}{H} \right)^2 \right) \cdot \text{Cot} \psi_p - \text{Cot} \psi_f \right] \quad (3.10)$$

However, when the tension crack is situated in the slope face, the weight is:

$$W = \frac{1}{2} \gamma H^2 \left[\left(1 - \frac{Z}{H} \right)^2 \cdot \text{Cot} \psi_p \cdot (\text{Cot} \psi_p \cdot \text{Tan} \psi_f - 1) \right] \quad (3.11)$$

Where,

A = Base area of the sliding block (m²/m)

- H = Slope height (m)
 W = Weight of the sliding block (ton/m)
 V = Force due to water pressure in the tension crack (ton/m)
 U = Uplift force due to pressure on the sliding surface (ton/m)
 ψ_f = Dip of slope face (radian)
 ψ_p = Dip of discontinuity plane (radian)
 Z = Height of the tension crack from the upper surface of the slope (m)
 Z_w = Height of water in tension crack (m)
 γ_w = Unit weight of water (ton/m³)
 γ = Unit weight of rock (ton/m³)

Finally, and by considering the equations (3.6 - 3.11) Hoek and Bray (1981) gave the factor of safety of a plane slope for the two cases mentioned earlier in this chapter as:

$$F_s = \frac{cA + (W \cdot \cos \psi_p - U - V \cdot \sin \psi_p) \cdot \tan \phi}{W \cdot \sin \psi_p + V \cdot \cos \psi_p} \quad (3.12)$$

3.3. Basic Mechanisms of Wedge Failure

When two discontinuities strike obliquely across the slope face and their line of intersection daylights in the slope face, the wedge of rock resting on these discontinuities will slide down the line of intersection, provided that the inclination of this line is significantly greater than the angle of friction. In other words, and as Hoek and Bray (1981) stated the general condition of a wedge failure to take place is:

$$\psi_{f_i} > \psi_i > \phi \quad (3.13)$$

Where,

ψ_{f_i} = Inclination of the slope face, measured in the view at right angle to the line of intersection of the discontinuities

ψ_i = Dip of the line of intersection

ϕ = Friction angle

This case can be seen clearly in Figure (3.7).

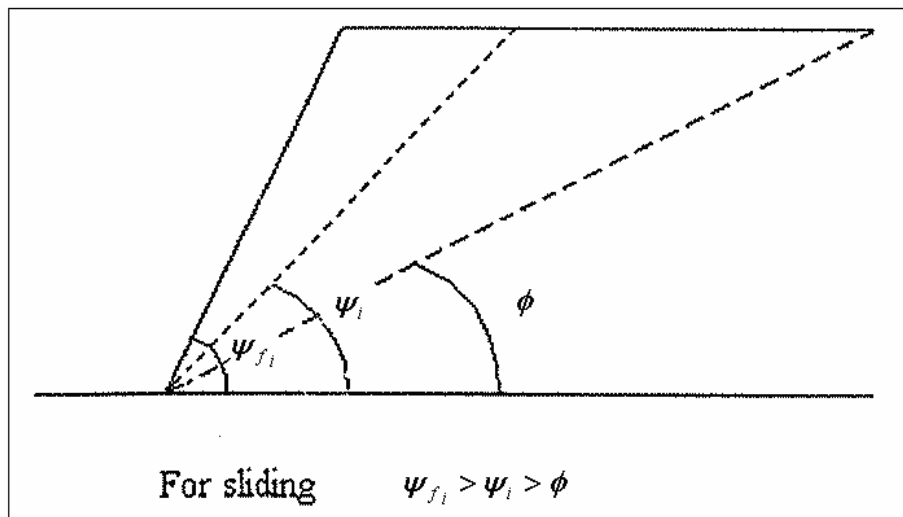


Figure 3.7 Sliding condition for wedge slope

Noting that ψ_{f_i} would be the same as ψ_f , the true dip of the slope face, only if the dip direction of the line of intersection was the same as the dip direction of the slope face.

For the wedge shown in Figure (3.8) Hoek and Bray (1981) stated that, if the sliding is resisted by friction only and if the friction angle (ϕ) is the same for both planes then the factor of safety for that wedge is given by:

$$F_s = \frac{(R_A + R_B) \cdot \tan \phi}{W \cdot \sin \psi_i} \quad (3.14)$$

Where, W is the weight of the wedge block, while R_A and R_B are as illustrated in Figure (3.9) the normal reactions provided by planes A and B, respectively.

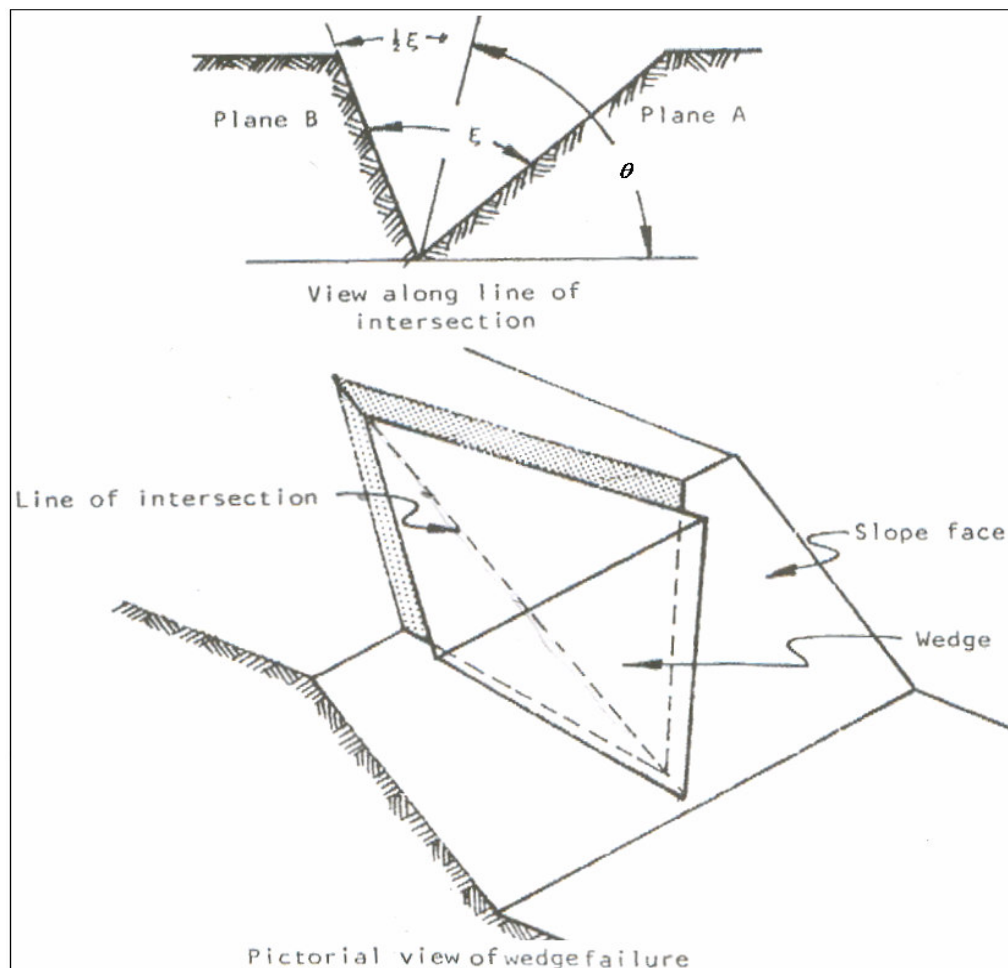


Figure 3.8 Wedge failure geometry (Hoek and Bray, 1981)

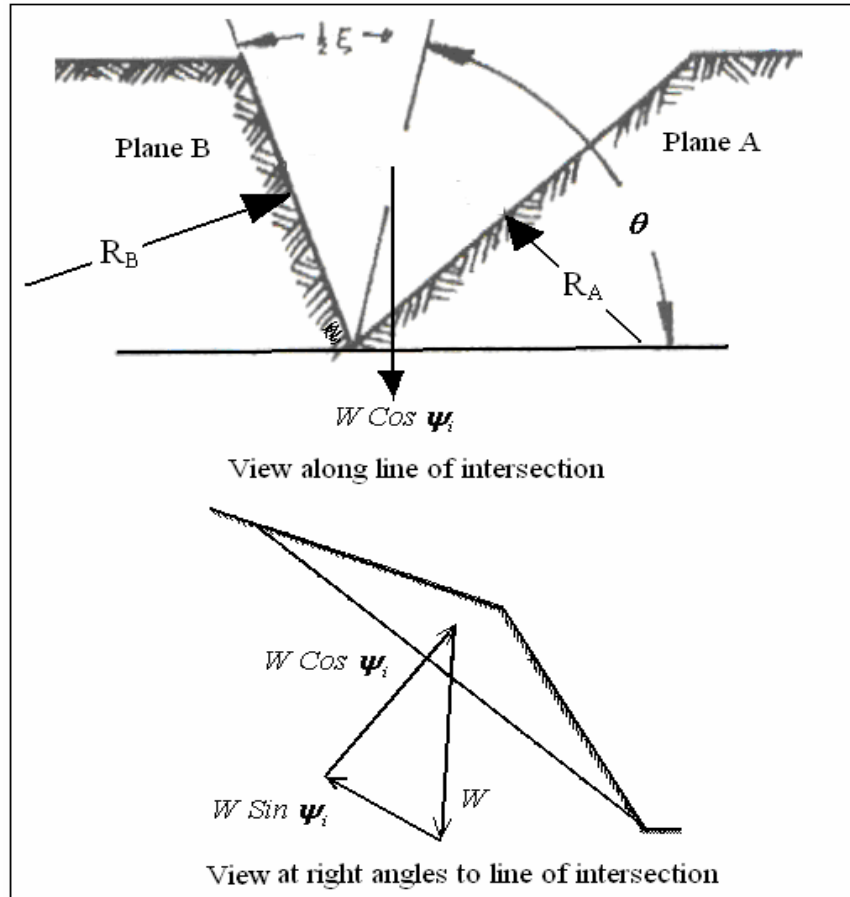


Figure 3.9 Forces acting on the wedge slope (Hoek and Bray, 1981)

The value of $R_A + R_B$ is found by resolving the forces into their horizontal and vertical components then adding:

$$R_A + R_B = \frac{W \cdot \cos \psi_i \cdot \sin \theta}{\sin \frac{1}{2} \xi} \quad (3.15)$$

By substituting the value of $R_A + R_B$ from equation (3.15) into equation (3.14) then:

$$F_S = \frac{\sin \theta \cdot \tan \phi}{\sin \frac{1}{2} \xi \cdot \tan \psi_i} \quad (3.16)$$

Hoek et al. (1973) accomplished a detailed analysis for the wedge slope failure shown in Figure 3.10. First of all, they assumed that the sliding of that wedge always occurs along the line of intersection (line 5 in Figure 3.10).

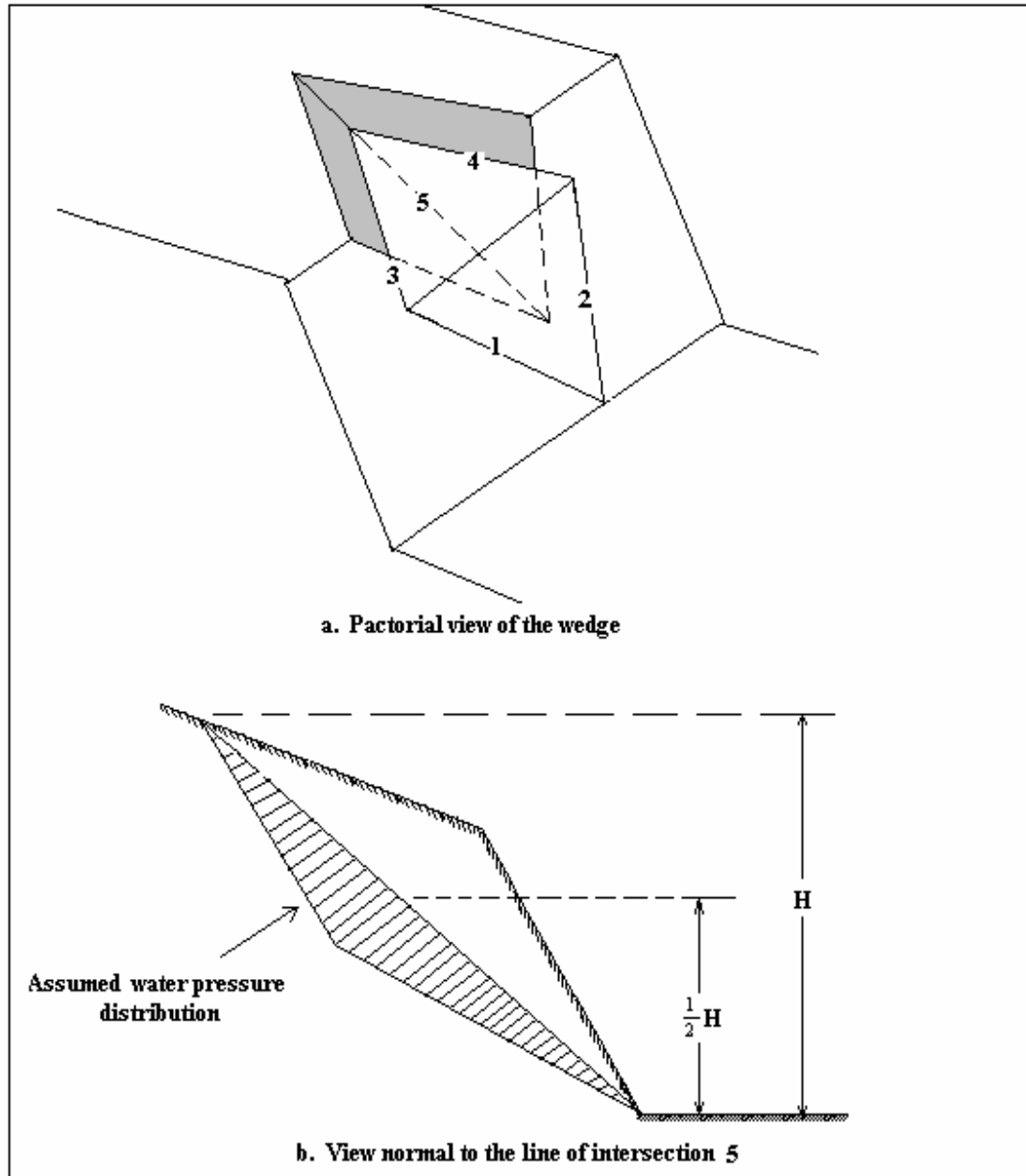


Figure 3.10 Geometry of wedge used for stability analysis by Hoek et al. (1973)

Then, they derived the safety factor of that slope depending on a stereoplot of the data that defines the geometry of the wedge as well as the slope.

Low (1979) developed a compact closed-form equation for the calculation of the factor of safety for two-joint tetrahedral wedges. This equation is an alternative for the one developed by Hoek et al. (1973), but no stereographic projection is required in utilizing it. Low (1979) assumed that the upper ground surface is horizontal. However, Low and Einstein (1992) generalized this method to include cases with inclined upper ground surface that dips in the same direction as the considered slope face.

Low and Einstein (1992) calculated the factors of safety for all the possible modes of failures namely, Biplane failure, failure along plane 1 only, failure along plane 2 only, and Floating failure. These modes of failure also considered separately in the following subsections.

3.3.1. Biplane sliding

For this mode of failure the factor of safety is:

$$Fs = \left(a_1 - \frac{b_1 G_{w1}}{S_y} \right) \times \tan \phi_1 + \left(a_2 - \frac{b_2 G_{w2}}{S_y} \right) \times \tan \phi_2 + 3b_1 \frac{c_1}{yh} + 3b_2 \frac{c_2}{yh} \quad (3.17)$$

This equation is valid only when there is contact on both planes that is:

$$\left(a_1 - \frac{b_1 G_{w1}}{S_y} \right) > 0 \quad (3.18)$$

And

$$\left(a_2 - \frac{b_2 G_{w2}}{S_y} \right) > 0 \quad (3.19)$$

Where a_1, a_2, b_1, b_2 are parameters that depend on the geometry of the slope which is defined with the angles ($\delta_1, \delta_2, \beta_1, \beta_2, \alpha, \Omega$ and ϵ) as shown in Figure (3.11).

G_{w1} and G_{w2} = Normalized water pressure parameters (dimensionless)

c_1 and c_2 = Cohesive strengths of planes 1 and 2 (kPa)

ϕ_1 and ϕ_2 = Angles of friction on Planes A and B (radians)

$S_\gamma = \frac{\gamma}{\gamma_w}$ = Specific density of rock (dimensionless)

γ = Unit weight of rock (kN/m³)

γ_w = Unit weight of water (kN/m³)

h = Height of the wedge (m)

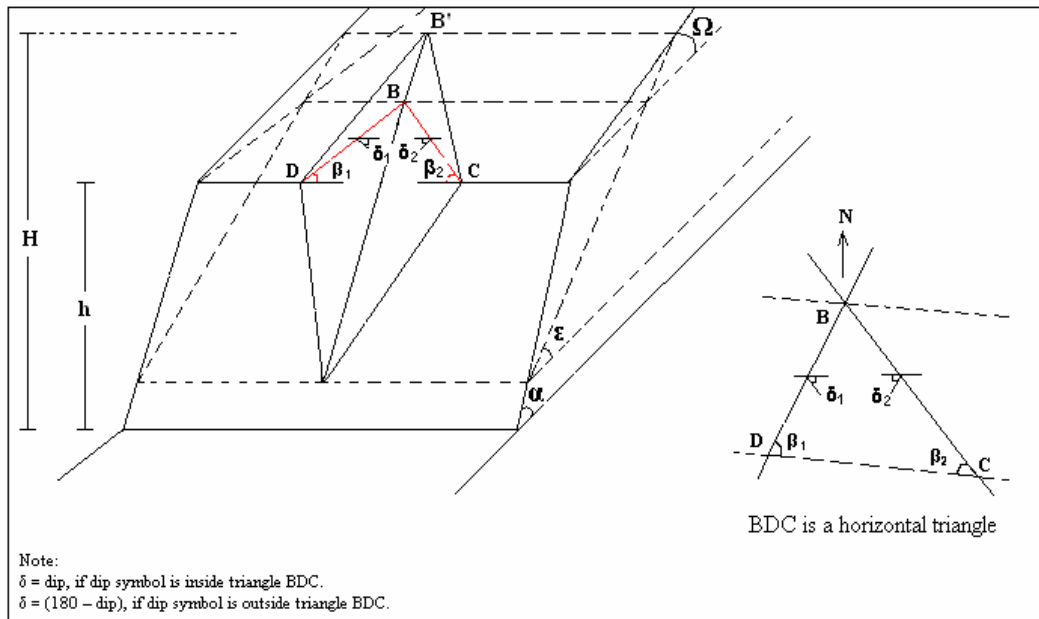


Figure 3.11 Slope geometry in wedge failure (Low and Einstein, 1992)

The parameters of Low's formulas (1997) are calculated by equations (3.20 through 2.29).

$$a_1 = \frac{[\text{Sin} \delta_2 \cdot \text{Cot} \delta_1 - \text{Cos} \delta_2 \cdot \text{Cos}(\beta_1 + \beta_2)]}{\text{Sin} \psi \cdot \text{Sin}(\beta_1 + \beta_2)} \quad (3.20)$$

$$a_2 = \frac{[\text{Sin} \delta_1 \cdot \text{Cot} \delta_2 - \text{Cos} \delta_1 \cdot \text{Cos}(\beta_1 + \beta_2)]}{\text{Sin} \psi \cdot \text{Sin}(\beta_1 + \beta_2)} \quad (3.21)$$

$$b_1 = a_0 \cdot \text{Sin} \beta_2 \cdot \text{Sin} \delta_2 \quad (3.22)$$

$$b_2 = a_0 \cdot \text{Sin} \beta_1 \cdot \text{Sin} \delta_1 \quad (3.23)$$

In equations (3.20) and (3.21), $\text{Sin} \psi$ is defined as in equation (3.24).

$$\text{Sin} \psi = \sqrt{1 - \left[\text{Sin} \delta_1 \cdot \text{Sin} \delta_2 \cdot \text{Cos}(\beta_1 + \beta_2) + \text{Cos} \delta_1 \cdot \text{Cos} \delta_2 \right]^2} \quad (3.24)$$

$$a_0 = \frac{\text{Sin} \psi}{[\text{Sin}(\beta_1 + \beta_2) \cdot \text{Sin} \delta_1 \cdot \text{Sin} \delta_2]^2 \cdot (\text{Cot} \varepsilon - \text{Cot} \alpha)} \quad (3.25)$$

$$\tan \varepsilon = \frac{\text{Sin}(\beta_1 + \beta_2)}{\text{Sin} \beta_1 \cdot \text{Cot} \delta_2 + \text{Sin} \beta_2 \cdot \text{Cot} \delta_1} \quad (3.26)$$

$$G_{w1} = G_{w2} = 0.5 \kappa \quad (3.27)$$

$$\kappa = \frac{H}{h} = \left(1 - \frac{\tan \Omega}{\tan \alpha} \right) / \left(1 - \frac{\tan \Omega}{\tan \varepsilon} \right) \quad (3.28)$$

Where Ω is inclination of the upper ground surface, and α is inclination of the slope face. Note the difference between H and h from Figure (3.11). From Figure (3.11) h is obtained if only the length of DC is known:

$$h = \frac{DC}{(\text{Cot}\varepsilon - \text{Cot}\alpha) \cdot (\text{Cot}\beta_1 + \text{Cot}\beta_2)} \quad (3.29)$$

Here the dimensionless parameters G_{w1} and G_{w2} are based on pyramidal water pressure conditions. Another alternative is that assigning the average water pressures u_1 and u_2 that act on planes B'DO and B'CO, respectively. In this case the values of G_{w1} and G_{w2} in equation (3.17) should be substituted with the values of the corresponding average water pressures, that is:

$$G_1 = \frac{3u_1}{\gamma_w \cdot h} \quad (3.30)$$

$$G_2 = \frac{3u_2}{\gamma_w \cdot h} \quad (3.31)$$

For the case represented by equation (3.27), the corresponding value of average water pressures u_1 and u_2 is:

$$u_1 = u_2 = \frac{\gamma_w \cdot h \cdot \kappa}{6} \quad (3.32)$$

3.3.2. Sliding along plane 1 only

When sliding along plane 1 only occurs, the normal force on plane 2 is an uplift force, which can be resolved into two components. One of these components is perpendicular to plane 1 and the other is tangential to it. The former is superimposed on the net normal force on plane 1. However, the latter is added vectorially to the driving force along the line of intersection of the two joint planes, and thus, deviating the resultant driving force from the line of intersection. As a result of these changes, the factor of safety is obtained by the dimensionless equation (3.33).

$$F_s = \frac{\left[\left(a_1 - \frac{b_1 G_{w1}}{S_\gamma} \right) - \left(\frac{b_2 G_{w2}}{S_\gamma} - a_2 \right) \cdot Z \right] \cdot \tan \phi_1 + 3b_1 \frac{c_1}{\gamma h}}{\sqrt{1 + \left[\left(\frac{b_2 G_{w2}}{S_\gamma} - a_2 \right) \cdot \sin \psi \right]^2}} \quad (3.33)$$

In equation (3.33),

$$Z = \cos \delta_1 \cdot \cos \delta_2 + \sin \delta_1 \cdot \sin \delta_2 \cdot \cos(\beta_1 + \beta_2) \quad (3.34)$$

This situation, that is, the sliding along plane 1 only is valid when:

$$\left(a_2 - \frac{b_2 G_{w2}}{S_\gamma} \right) < 0 \quad (3.35)$$

And

$$\left[\left(a_1 - \frac{b_1 G_{w1}}{S_\gamma} \right) - \left(\frac{b_2 G_{w2}}{S_\gamma} - a_2 \right) \cdot Z \right] > 0 \quad (3.36)$$

3.3.3. Sliding along plane 2 only

In this case, the change in the equation of the factor of safety is following the same scenario as the one in the sliding along plane 1 only. The factor of safety for this case is obtained by:

$$F_s = \frac{\left[\left(a_2 - \frac{b_2 G_{w2}}{S_\gamma} \right) - \left(\frac{b_1 G_{w1}}{S_\gamma} - a_1 \right) \cdot Z \right] \cdot \tan \phi_2 + 3b_2 \frac{c_2}{\gamma h}}{\sqrt{1 + \left[\left(\frac{b_1 G_{w1}}{S_\gamma} - a_1 \right) \cdot \sin \psi \right]^2}} \quad (3.37)$$

This case is valid only when:

$$\left(a_1 - \frac{b_1 G_{w1}}{S_\gamma} \right) < 0 \quad (3.38)$$

And

$$\left[\left(a_2 - \frac{b_2 G_{w2}}{S_\gamma} \right) - \left(\frac{b_1 G_{w1}}{S_\gamma} - a_1 \right) \cdot Z \right] > 0 \quad (3.39)$$

3.3.4. Floating failure

In this case, the contact is lost on both planes, in other words, the wedge floats as a result of the water pressures that are acting on both planes. Thus, the factor of safety falls to zero in this case, and it is valid when:

$$\left[\left(a_1 - \frac{b_1 G_{w1}}{S_\gamma} \right) - \left(\frac{b_2 G_{w2}}{S_\gamma} - a_2 \right) \cdot Z \right] < 0 \quad (3.40)$$

And

$$\left[\left(a_2 - \frac{b_2 G_{w2}}{S_\gamma} \right) - \left(\frac{b_1 G_{w1}}{S_\gamma} - a_1 \right) \cdot Z \right] < 0 \quad (3.41)$$

CHAPTER IV

ADVANCED FOSM APPROACH

4.1. Introduction

In engineering the reliability of a problem is normally originated as a comparison of the demand and supply in order to meet certain demand requirements. In rock engineering the demand refers to the applied load while the supply refers to the strength of the rock (Duzgun et al., 2003). In order to calculate safe state or failure probabilities of a rock slope, a good knowledge about the distributions of the strength and the load applied are required. Yet, if the distributions are known, an accurate estimation of the probabilities is impractical as a result of the numerical integrations involved.

Normally, the data obtained are only enough to calculate the first and second moments of the random variables under consideration. That is, the information is sufficient only to calculate the means and standard deviations of those random variables. Thus, the reliability evaluation of a problem is restricted to the utilizations of these two moments. As a result of that, implementation of the reliability concepts is limited to the method proposed by Cornell in 1969, namely, the First Order Second Moment method (Ang and Tang, 1984). However, due to the drawbacks of

this method, as mentioned earlier in Chapter II, the need for a better alternative came up.

The Advanced First Order Second Moment method (AFOSM), proposed by Hasofer and Lind (1974), overcame the drawbacks of the traditional FOSM method and therefore, it is a better alternative (USACE, 1999). As a result of that, the AFOSM became the most widely used method for the reliability evaluation. At this point, it is essential to call attention to that the AFOSM approach is consistent with the equivalent normal representation of non-normal distributions as well as the normal ones (Ang and Tang, 1984). In other words, if sufficient information is available about the distribution types of the random variables under consideration, then it is possible to calculate the probability of the system on based on the equivalent normal distributions.

4.2. The Performance Function

The reliability of a system in engineering is defined as the probability of that system in performing its intended task or assignment. So, the level of performance of a system will clearly depend on its properties. Thus, the performance function should be generalized in order to fit all possible engineering systems.

Such a general performance function is defined as:

$$g(x_1, x_2, x_3, \dots, x_n) = g(x_i) \quad (4.1)$$

Where, $x_i = (x_1, x_2, x_3, \dots, x_n)$ is a vector of the basic variables of a system, in other words, x_i are the properties of that system. While, $g(x_i)$ is the performance function of that system.

Then, $g(x_i) = 0$ is called the limit-state of the system and therefore,

If $g(x_i) < 0$ is the “failure state” and,

If $g(x_i) > 0$ is the “safe state”

In rock engineering, the performance function of a slope is generally defined as (Duzgun, 1994):

$$g(x_i) = R(x_i) - S(x_i) \quad (4.2)$$

Where,

$R(x_i)$ = Strength (capacity) of the slope

$S(x_i)$ = Load (demand) acting on the slope

4.3. Linear Performance Function

A linear performance function may be represented as:

$$g(x_i) = a_0 + \sum_i a_i \cdot x_i \quad (4.3)$$

Where a_0 and a_i 's are constants and x_i are the basic variables. Therefore, the corresponding limit-state is:

$$a_0 + \sum_i a_i \cdot x_i = 0 \quad (4.4)$$

Then if equation (4.4) is expressed in terms of reduced variates, it yields:

$$a_0 + \sum_i a_i (\sigma_{x_i} \cdot x_i' + \mu_{x_i}) = 0 \quad (4.5)$$

Where,

x'_i : Reduced (standardized) variables

σ_{x_i} and μ_{x_i} : Standard deviations and mean values of the basic variables x_i , respectively.

Equation (4.5) in three dimensions for example is written as:

$$a_0 + a_1(\sigma_{x_1} \cdot x'_1 + \mu_{x_1}) + a_2(\sigma_{x_2} \cdot x'_2 + \mu_{x_2}) + a_3(\sigma_{x_3} \cdot x'_3 + \mu_{x_3}) = 0 \quad (4.6)$$

Which is a plane surface in x'_1, x'_2, x'_3 space as shown in Figure (4.1).

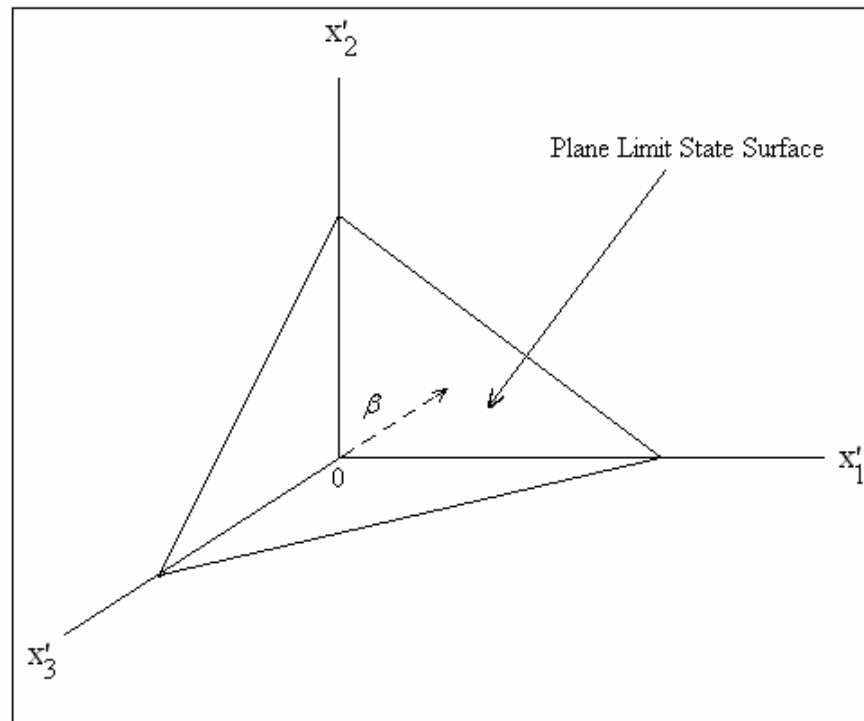


Figure 4.1 Limit state surface in x'_1, x'_2, x'_3 - space (Ang and Tang, 1984)

If the random variables are uncorrelated and normally distributed variates, then failure point can be expressed in term of the direction cosines (α_i) and reliability index (β) as follows:

$$x_i^* = \sigma_{xi} \cdot x_i^* + \mu_{xi} = \mu_{xi} - \alpha_i \cdot \beta \cdot \sigma_{xi} \quad (4.7)$$

Where,

$$\alpha_i = \frac{a_i}{\sqrt{\sum_{i=1}^n a_i^2}} \quad (4.8)$$

$$\beta = \frac{a_0 + \sum_i a_i \cdot \mu_{xi}}{\sqrt{\sum_i (a_i \cdot \sigma_{xi})^2}} \quad (4.9)$$

Then the probability of the safe state is obtained by:

$$P_s = \Phi(\beta) \quad (4.10)$$

Thus, the probability of failure is:

$$P_f = 1 - \Phi(\beta) \quad (4.11)$$

If the probability distributions of the random variables x_1, x_2, \dots, x_n are not normal, it is still possible to calculate P_s and P_f . That is done by utilizing the equivalent normal distributions of the non-normal variates. They are obtained in a way that their cumulative probabilities as well as their probability density ordinates are equal to the corresponding non-normal distributions at appropriate point x_i^* on the failure surface (Ang and Tang, 1984). So, at that point:

$$\Phi\left(\frac{x_i^* - \mu_{xi}^N}{\sigma_{xi}^N}\right) = F_{xi}(x_i^*) \quad (4.12)$$

Where,

$\mu_{xi}^N, \sigma_{xi}^N$ = The mean value and the standard deviation, respectively, of the equivalent normal distribution for x_i

$F_{xi}(x_i^*)$ = The original cumulative density function (CDF) of x_i evaluated at x_i^*

$\Phi()$ = The CDF of the standard normal distribution

By rearranging the terms in equation (4.12), the following is obtained:

$$\mu_{xi}^N = x_i^* - \sigma_{xi}^N \cdot \Phi^{-1}[F_{xi}(x_i^*)] \quad (4.13)$$

Now, equating the corresponding probability density functions at point x_i^* yields:

$$\frac{1}{\sigma_{xi}^N} \cdot \phi\left(\frac{x_i^* - \mu_{xi}^N}{\sigma_{xi}^N}\right) = f_{xi}(x_i^*) \quad (4.14)$$

Where, $\phi()$ is the probability density function (PDF) of the standard normal variable.

From equations (4.13 – 4.14) it is obtained that:

$$\sigma_{xi}^N = \frac{\phi\{\Phi^{-1}[F_{xi}(x_i^*)]\}}{f_{xi}(x_i^*)} \quad (4.15)$$

Then the failure point of x_i is (Ang and Tang, 1984):

$$x_i^* = \sigma_{xi}^N \cdot x_i^* + \mu_{xi}^N = \mu_{xi}^N - \alpha_i \cdot \beta \cdot \sigma_{xi}^N \quad (4.16)$$

Following that, the reliability index is found as:

$$\beta = \sqrt{\sum_i \frac{(x_i^* - \mu_{xi}^N)^2}{(\sigma_{xi}^N)^2}} \quad (4.17)$$

So, by substituting the result of equation (4.17) for β in equations (4.10) and (4.11) the probability of the safe state and the failure state are obtained, respectively.

Obviously, if an actual distribution is replaced with an equivalent normal distribution, then the actual mean and standard deviation should also be replaced with their equivalent normal distributions (Ang and Tang, 1984).

4.4. Nonlinear Performance Function

For the nonlinear performance function $g(x_i)$, the evaluation of the exact probability of safety or failure is normally possible. However, for practical proposes, it is necessary to approximation the exact probability. Beside that, the nonlinear case is unlike the linear case since there is no unique distance from the failure surface to the origin of the reduced variates.

Clearly, Figure (4.2) illustrate that the point $(x_1'^*, x_2'^*)$ on the failure surface with the minimum distance to the origin of the reduced variates is the most probable

failure point (Shinozuka, 1983). The tangent plane to the failure surface at $(x_1'^*, x_2'^*)$ may then be used to approximate the actual failure surface. Then the required reliability index, the probability of safety, and the probability of failure may be evaluated as in the linear case mentioned earlier in this chapter. Of course this approximation will be on the safe side or unsafe side, respectively, depending on whether the exact nonlinear failure surface is convex or concave toward the origin. That is seen clearly from Figure (4.2).

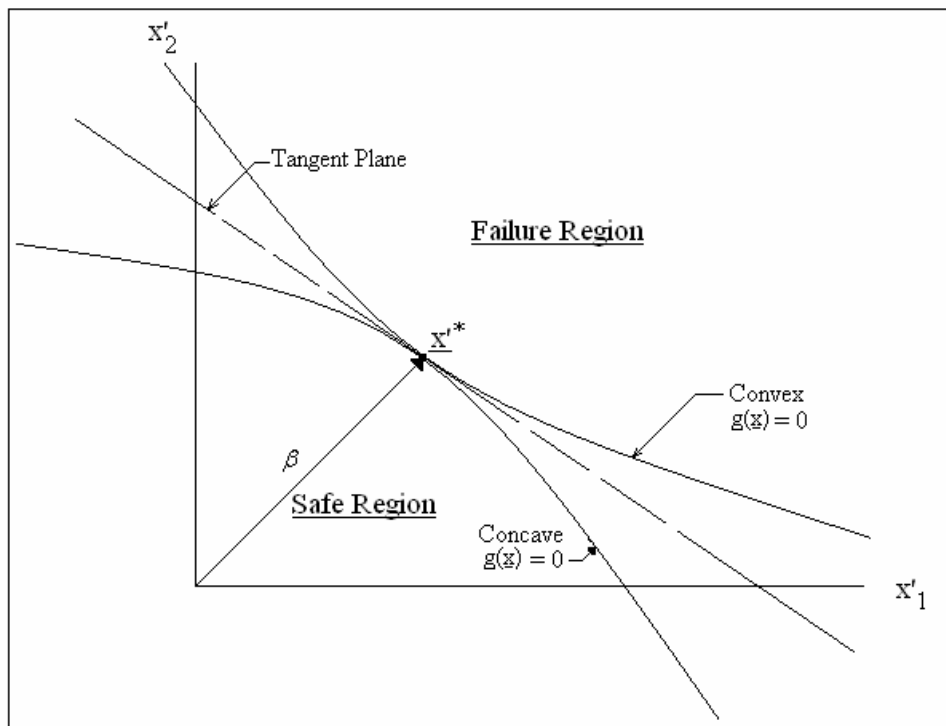


Figure 4.2 Tangent Plane to $g(\underline{x}) = 0$ at \underline{x}'^* (Ang and Tang, 1984)

In general, the pertinent tangent plane at $\underline{x}'^* = (x_1'^*, x_2'^*, \dots, x_n'^*)$ is (Ang and Tang, 1984):

$$\sum_{i=1}^n \left(x_i' - x_i'^* \right) \cdot \left(\frac{\partial g}{\partial x_i'} \right)_* = 0 \quad (4.18)$$

Where, the partial derivatives $\left(\frac{\partial g}{\partial x_i'} \right)_*$ are evaluated at the point $\left(x_1'^*, x_2'^*, \dots, x_n'^* \right)$.

Based on the approximation discussed, the minimum distance from the tangent plane calculated by equation (4.18) to the origin of the reduced variates is the appropriate reliability index. This index is used to represent the reliability of the considered situation.

In the case of nonlinear performance function, the determination of the required reliability index is not as simple as in the linear case. However, the linear approximation is used in this case in order to ease the calculation. It is very important at this stage to emphasize that the outcome of such approximation is yet yielding reliable results.

So, the solution of the limit-state equation (4.19) below yields the reliability index:

$$g(x_1^*, x_2^*, x_3^*, \dots, x_n^*) = 0 \quad (4.19)$$

Then, the most probable failure point in this case is given by equation (4.16). Thereafter, if the variables are uncorrelated with non-normal distributions, the reliability index is given by equation (4.17). Yet again, by substituting the result of equation (4.17) for β in equations (4.10) and (4.11) the probability of the safe state and the failure state are obtained, respectively.

Ang and Tang (1984) summarized the procedure of the iterative algorithm that is used to calculate the reliability index as follows:

1. Define the appropriate limit-state function.
2. Make an initial guess for the reliability index
3. Start with $x_i^* = \mu_i$ for all $i = 1, 2, \dots, n$.
4. Calculate the equivalent normal mean and the standard deviation for the non-normally distributed variables.
5. Find reduced variates as:

$$x_i^* = \frac{x_i^* - \mu_i}{\sigma_i} \quad (4.20)$$

6. Calculate $\left(\frac{\partial g}{\partial x_i^*}\right)_*$ at point x_i^* .
7. Evaluate the direction cosines:


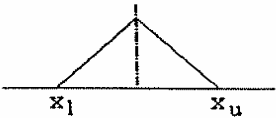
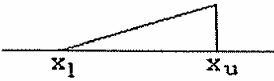
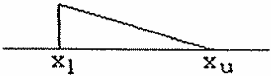
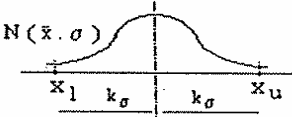
$$\alpha_i = \frac{\left(\frac{\partial g}{\partial x_i^*}\right)_*}{\sqrt{\sum_{i=1}^n \left(\frac{\partial g}{\partial x_i^*}\right)_*^2}} \quad (4.21)$$

8. Calculate the new values of x_i^* by equation (4.7).
9. Substitute the value of x_i^* found in step 8 into $g\left(x_1^*, x_2^*, \dots, x_n^*\right) = 0$ and solve for β .
10. Using the value of β obtained in step 9, resolve equation (4.7).
11. Keep repeating steps 5 through 10 until convergence is reached.

4.5. Non-normal Distributions

When the basic variables have non-normal distributions, their moments have to be transformed into equivalent normal distributions. In this thesis the equivalent normal moments of the uniform, symmetric triangular, upper triangular, lower triangular, and the lognormal distributions are evaluated and coded in spreadsheets. The mean and the coefficient of variation of a variable x having these distributions are given in Table (4.1) (Ang and Tang, 1984). These distributions and the detailed calculation of the equivalent normal for each of them are explained in the subsections 4.5.1 through 4.5.5.

Table 4.1 The Means and c.o.v.'s of various distributions (Ang and Tang, 1984)

P.D.F.	Mean Value, \bar{X}	C.O.V. δx or Δx
	$1/2 (x_l + x_u)$	$\frac{1}{\sqrt{3}} \left(\frac{x_u - x_l}{x_u + x_l} \right)$
	$1/2 (x_l + x_u)$	$\frac{1}{\sqrt{6}} \left(\frac{x_u - x_l}{x_u + x_l} \right)$
	$1/3 (x_l + 2x_u)$	$\frac{1}{\sqrt{2}} \left(\frac{x_u - x_l}{2x_u + x_l} \right)$
	$1/3 (2x_l + x_u)$	$\frac{1}{\sqrt{2}} \left(\frac{x_u - x_l}{x_u + 2x_l} \right)$
	$1/2 (x_l + x_u)$	$\frac{1}{k} \left(\frac{x_u - x_l}{x_u + x_l} \right)$

4.5.1. Uniform Distribution

Ang and Tang (1984) stated that:

$$c.o.v = \frac{\sigma}{\mu} \quad (4.22)$$

Where,

$c.o.v$ = Coefficient of variation

σ = Standard deviation

μ = Mean value

So, from equation (4.22) and Table (4.1), the standard deviation of the uniform distribution is given by:

$$\sigma = \frac{b-a}{2\sqrt{3}} \quad (4.23)$$

The probability density function (PDF) and cumulative distribution function (CDF) for a continuous uniform distribution on the interval $[a, b]$ are (Weisstein, 2004):

$$PDF = f(x) = \begin{cases} 0 & \text{for } x \leq a \\ \frac{1}{b-a} & \text{for } a < x < b \\ 0 & \text{for } x \geq b \end{cases} \quad (4.24)$$

Where a and b are the minimum and maximum values of the variable under consideration, respectively.

$$CDF = F(x) = \begin{cases} 0 & \text{for } x \leq a \\ \frac{x-a}{b-a} & \text{for } a < x < b \\ 1 & \text{for } x \geq b \end{cases} \quad (4.25)$$

Based on these functions equations (4.26) and (4.27) are derived:

$$\sigma_{xi}^N = \frac{\frac{1}{\sqrt{2\pi}} \exp \left[-\frac{1}{2} \left\{ \Phi^{-1} \left(\frac{x-a}{b-a} \right) \right\}^2 \right]}{\left[\frac{1}{b-a} \right]} \quad (4.26)$$

$$\mu_{xi}^N = x_i^* - \sigma_{xi}^N \cdot \Phi^{-1} \left[\frac{x-a}{b-a} \right] \quad \text{for } a < x < b \quad (4.27)$$

4.5.2. Symmetric Triangular Distribution

From equation (4.22) and Table (4.1), the standard deviation of the symmetric triangular distribution is given by:

$$\sigma = \frac{b-a}{2\sqrt{6}} \quad (4.28)$$

Then PDF and CDF for this distribution on the interval $[a, b]$ are (Weisstein, 2005):

$$PDF = f(x) = \begin{cases} 0 & \text{for } x < a \\ \frac{4(x-a)}{(b-a)^2} & \text{for } a \leq x \leq \mu \\ \frac{4(b-x)}{(b-a)^2} & \text{for } \mu < x \leq b \\ 0 & \text{for } x > b \end{cases} \quad (4.29)$$

$$CDF = F(x) = \begin{cases} 0 & \text{for } x < a \\ \frac{2(x-a)^2}{(b-a)^2} & \text{for } a \leq x \leq \mu \\ 1 - \frac{2(b-x)^2}{(b-a)^2} & \text{for } \mu < x \leq b \\ 0 & \text{for } x > b \end{cases} \quad (4.30)$$

Equations (4.31) and (4.32) are derived based on equations (4.26) and (4.27):

$$\sigma_{xi}^N = \begin{cases} \frac{\frac{1}{\sqrt{2\pi}} \exp \left[-\frac{1}{2} \left\{ \Phi^{-1} \left[\frac{2(x-a)^2}{(b-a)^2} \right] \right\}^2 \right]}{4(x-a)/(b-a)^2} & \text{for } a \leq x \leq \mu \\ \frac{\frac{1}{\sqrt{2\pi}} \exp \left[-\frac{1}{2} \left\{ \Phi^{-1} \left[1 - \frac{2(b-x)^2}{(b-a)^2} \right] \right\}^2 \right]}{4(b-x)/(b-a)^2} & \text{for } \mu < x \leq b \end{cases} \quad (4.31)$$

$$\mu_{xi}^N = \begin{cases} x_i^* - \sigma_{xi}^N \cdot \Phi^{-1} \left[\frac{2(x-a)^2}{(b-a)^2} \right] & \text{for } a \leq x \leq \mu \\ x_i^* - \sigma_{xi}^N \cdot \Phi^{-1} \left[1 - \frac{2(x-a)^2}{(b-a)^2} \right] & \text{for } \mu < x \leq b \end{cases} \quad (4.32)$$

4.5.3. Upper Triangular Distribution

From equation (4.22) and Table (4.1), the standard deviation of this distribution is given by:

$$\sigma = \frac{b-a}{3\sqrt{2}} \quad (4.33)$$

Then PDF and CDF for this distribution on the interval $[a, b]$ are (Weisstein, 2005):

$$PDF = f(x) = \begin{cases} 0 & \text{for } x < a \\ \frac{2(x-a)}{(b-a)^2} & \text{for } a \leq x \leq b \\ 0 & \text{for } x > b \end{cases} \quad (4.34)$$

$$CDF = F(x) = \begin{cases} 0 & \text{for } x < a \\ \frac{(x-a)^2}{(b-a)^2} & \text{for } a \leq x \leq b \\ 1 & \text{for } x > b \end{cases} \quad (4.35)$$

Based on these functions equations (4.36) and (4.37) are derived:

$$\sigma_{xi}^N = \frac{\frac{1}{\sqrt{2\pi}} \exp \left[-\frac{1}{2} \left\{ \Phi^{-1} \left[\frac{(x-a)^2}{(b-a)^2} \right] \right\}^2 \right]}{2(x-a)/(b-a)^2} \quad \text{for } a \leq x \leq b \quad (4.36)$$

$$\mu_{xi}^N = x_i^* - \sigma_{xi}^N \cdot \Phi^{-1} \left[\frac{(x-a)^2}{(b-a)^2} \right] \quad \text{for } a \leq x \leq b \quad (4.37)$$

4.5.4. Lower Triangular Distribution

The standard deviation of this distribution is given by equation (4.33). Then PDF and CDF for this distribution on the interval $[a, b]$ are (Weisstein, 2005):

$$PDF = f(x) = \begin{cases} 0 & \text{for } x < a \\ \frac{2(b-x)}{(b-a)^2} & \text{for } a \leq x \leq b \\ 0 & \text{for } x > b \end{cases} \quad (4.38)$$

$$CDF = F(x) = \begin{cases} 1 & \text{for } x < a \\ 1 - \frac{(b-x)^2}{(b-a)^2} & \text{for } a \leq x \leq b \\ 0 & \text{for } x > b \end{cases} \quad (4.39)$$

Equations (4.40) and (4.41) are derived based on (4.35) and (4.36):

$$\sigma_{xi}^N = \frac{\frac{1}{\sqrt{2\pi}} \exp\left[-\frac{1}{2}\left\{\Phi^{-1}\left[1-\frac{(b-x)^2}{(b-a)^2}\right]\right\}^2\right]}{2(b-x)/(b-a)^2} \quad \text{for } a \leq x \leq b \quad (4.40)$$

$$\mu_{xi}^N = x_i^* - \sigma_{xi}^N \cdot \Phi^{-1}\left[1-\frac{(b-x)^2}{(b-a)^2}\right] \quad \text{for } a \leq x \leq b \quad (4.41)$$

4.5.5. Lognormal Distribution

Rosenblatt transformation is used to calculate the equivalent normal distributions of variables that have lognormal distribution (Ang and Tang, 1984).

$$\xi^2 = \ln\left(1 + \frac{\sigma^2}{\mu^2}\right) \quad (4.42)$$

$$\lambda = \ln \mu - \frac{1}{2}\xi^2 = \ln \mu - \ln\left(1 + \frac{\sigma^2}{\mu^2}\right) \quad (4.23)$$

Where, λ and ξ are, respectively, the mean and the standard deviation of $(\ln x)$, and are the parameters of the distribution.

$$\sigma_{xi}^N = x_i^* \cdot \left[\ln\left(1 + \frac{\sigma^2}{\mu^2}\right)\right]^{\frac{1}{2}} \quad (4.44)$$

$$\Rightarrow \sigma_{xi}^N = x_i^* \cdot \xi \quad (4.45)$$

$$\mu_{xi}^N = x_i^* \cdot (1 - \ln x_i^* + \lambda) \quad (4.46)$$

CHAPTER V

DEVELOPED PROBABILISTIC MODELS

5.1. Introduction

In this chapter the probabilistic models developed in order to analyze cases of plane and wedge failure are given in details. Each slope has two models corresponding to the linear and non-linear failure criteria. These criteria are Coulomb criterion and Barton Bandis criterion, respectively.

5.2. Plane Failure

In the development probabilistic models of plane failure case are based on the methodology proposed by Hoek and Bray (1981). This methodology is given in Chapter III (equations 3.6 through 3.12).

5.2.1. Coulomb Failure Criterion

Based on equations (3.6) through (3.12) the performance function of this model is:

$$g(x) = cA + (W \cdot \cos\psi_p - U - V \cdot \sin\psi_p) \cdot \tan\phi - W \cdot \sin\psi_p - V \cdot \cos\psi_p \quad (5.1)$$

Where,

W = Weight of the sliding block (ton/m)

V = Force due to water pressure in the tension crack (ton/m)

U = Uplift force due to pressure on the sliding surface (ton/m)

ψ_f = Dip of slope face (radians)

ψ_p = Dip of discontinuity plane (radians)

A = Base area of the sliding block (m²/m)

c = Cohesion (ton/m²)

ϕ = Friction angle (radians)

This is identical to (Duzgun, 1994):

$$g(x) = R_f - D_f \quad (5.2)$$

Where,

R_f = The total resisting force

D_f = The total driving force which tends to cause the slide

Then the limit-state equation becomes:

$$cA + (W \cdot \cos\psi_p - U - V \cdot \sin\psi_p) \cdot \tan\phi - W \cdot \sin\psi_p - V \cdot \cos\psi_p = 0 \quad (5.3)$$

This equation can be written as:

$$\frac{cA + (W \cdot \cos\psi_p - U - V \cdot \sin\psi_p) \cdot \tan\phi}{W \cdot \sin\psi_p + V \cdot \cos\psi_p} = 1 \quad (5.4)$$

In this limit state equation the basic variables are ψ_f , ψ_p , c , $\tan \phi$ and Z_w which will change U and V . While the constant are H , γ , and Z .

When analyzing a specific slope ψ_f and ψ_p can be taken as constant parameters.

5.2.2. Barton Bandis Failure Criterion

Based on equation (2.4) the performance function of this model is:

$$g(x) = \sigma_n \cdot \tan \left[JRC \cdot \log \left(\frac{JCS}{\sigma_n} \right) + \phi_r \right] - \tau \quad (5.5)$$

Then the limit-state equation becomes:

$$\sigma_n \cdot \tan \left[JRC \cdot \log \left(\frac{JCS}{\sigma_n} \right) + \phi_r \right] - \tau = 0 \quad (5.6)$$

This can be written as:

$$\frac{\sigma_n \cdot \tan \left[JRC \cdot \log \left(\frac{JCS}{\sigma_n} \right) + \phi_r \right]}{\tau} = 1 \quad (5.7)$$

In which,

$$\sigma_n = (W \cdot \cos \psi_p - U - V \cdot \sin \psi_p) / A \quad (5.8)$$

$$\tau = (W \cdot \sin \psi_p + V \cdot \cos \psi) / A \quad (5.9)$$

Where,

σ_n = Normal stress (ton/m²)

JRC = Joint roughness coefficient (dimensionless)

JCS = Joint compressive strength (ton/m²)

ϕ_r = Residual friction angle (radians)

While A , V , U , W , ψ_p , and ψ_f are as defined in connection with equation (5.1).

The basic variables in this case are JRC , JCS , Z_w , ψ_p , ψ_f and ϕ_r . Whereas, the constant are H , γ , and Z .

5.3. Wedge Failure

The technique of wedge failure analysis proposed by Low (1997) in equations (3.17) through (2.41) is used in the probabilistic stability analysis of the wedge slope in this thesis work. For wedge slopes every mode of failure is having its own performance function and therefore it has its own reliability index and probability of failure. First these reliability indices and failure probabilities are calculated. Then, the total failure probability of the slope is obtained by utilizing the system reliability approach proposed by Ang and Tang (1984).

5.3.1. Coulomb Failure Criterion

5.3.1.1. Biplane Sliding

Based on equation (3.17) the following formula is developed:

$$F_S = \frac{yh(a_1S_y - b_1G_{w1}) \cdot \tan\phi_1 + yh(a_2S_y - b_2G_{w2}) \cdot \tan\phi_2 + 3S_y(b_1c_1 + b_2c_2)}{S_y \cdot y \cdot h} \quad (5.10)$$

Where a_1, a_2, b_1, b_2 are parameters that depend on the geometry of the slope which is defined with the angles ($\delta_1, \delta_2, \beta_1, \beta_2, \alpha, \Omega$ and ε) as shown in Figure (3.11).

G_{w1} and G_{w2} = Normalized water pressure parameters (dimensionless)

c_1 and c_2 = Cohesive strengths of planes 1 and 2 (kPa)

ϕ_1 and ϕ_2 = Angles of friction on Planes A and B (radians)

$S_\gamma = \frac{\gamma}{\gamma_w}$ = Specific density of rock (dimensionless)

γ = Unit weight of rock (kN/m³)

γ_w = Unit weight of water (kN/m³)

h = Height of the wedge (m)

This equation is identical to (Hoek and Bray, 1981):

$$F_S = \frac{C + \sigma_n \cdot \tan\phi}{\tau} \quad (5.11)$$

In which,

$$\sigma_{n1} = yh(a_1S_y - b_1G_{w1}) \quad (5.12)$$

$$\sigma_{n2} = yh(a_2S_y - b_2G_{w2}) \quad (5.13)$$

$$C = 3S_y(b_1c_1 + b_2c_2) \quad (5.14)$$

$$\tau = S_y \cdot y \cdot h \quad (5.15)$$

The limit-state equation of this case is:

$$\frac{\gamma h(a_1 S_y - b_1 G_{w1}) \cdot \tan \phi_1 + \gamma h(a_2 S_y - b_2 G_{w2}) \cdot \tan \phi_2 + 3S_y(b_1 c_1 + b_2 c_2)}{S_y \cdot \gamma \cdot h} = 1 \quad (5.16)$$

The basic variables of the limit-states for all the failure modes of a wedge slope, which is being analyzed by the same failure criterion, are the same. That is also valid for the constants of these limit-states.

The basic variables are β_1 , β_2 , δ_1 , δ_2 , $\tan \phi_1$, $\tan \phi_2$, G_{w1} , G_{w2} , c_1 , and c_2 . While, the constants are α , Ω , h , γ , and S_γ .

5.3.1.2. Sliding Along Plane 1 Only

Based on equation (3.33) the following formula is developed:

$$F_s = \frac{\gamma \cdot h \cdot \left[\left(a_1 - \frac{b_1 G_{w1}}{S_\gamma} \right) - \left(\frac{b_2 G_{w2}}{S_\gamma} - a_2 \right) \cdot Z \right] \cdot \tan \phi_1 + 3b_1 c_1}{\gamma \cdot h \cdot \sqrt{1 + \left[\left(\frac{b_2 G_{w2}}{S_\gamma} - a_2 \right) \cdot \sin \psi \right]^2}} \quad (5.17)$$

So, limit-state equation of this case is:

$$\frac{\gamma \cdot h \cdot \left[\left(a_1 - \frac{b_1 G_{w1}}{S_\gamma} \right) - \left(\frac{b_2 G_{w2}}{S_\gamma} - a_2 \right) \cdot Z \right] \cdot \tan \phi_1 + 3b_1 c_1}{\gamma \cdot h \cdot \sqrt{1 + \left[\left(\frac{b_2 G_{w2}}{S_\gamma} - a_2 \right) \cdot \sin \psi \right]^2}} = 1 \quad (5.18)$$

That is once more identical to equation (5.11), in which,

$$\sigma_n = \gamma \cdot h \cdot \left[\left(a_1 - \frac{b_1 G_{w1}}{S_\gamma} \right) - \left(\frac{b_2 G_{w2}}{S_\gamma} - a_2 \right) \cdot Z \right] \quad (5.19)$$

$$C = 3b_1c_1 \quad (5.20)$$

$$\tau = \gamma \cdot h \cdot \sqrt{1 + \left[\left(\frac{b_2 G_{w2}}{S_\gamma} - a_2 \right) \cdot \text{Sin} \psi \right]^2} \quad (5.21)$$

Where, all the symbols are as defined in connection with equation (5.10).

5.3.1.3. Sliding Along Plane 2 Only

Based on equation (3.37) the following formula is developed:

$$F_S = \frac{\gamma \cdot h \cdot \left[\left(a_2 - \frac{b_2 G_{w2}}{S_\gamma} \right) - \left(\frac{b_1 G_{w1}}{S_\gamma} - a_1 \right) \cdot Z \right] \cdot \tan \phi_2 + 3b_2c_2}{\gamma \cdot h \cdot \sqrt{1 + \left[\left(\frac{b_1 G_{w1}}{S_\gamma} - a_1 \right) \cdot \text{Sin} \psi \right]^2}} \quad (5.22)$$

Then, the limit-state equation becomes:

$$\frac{\gamma \cdot h \cdot \left[\left(a_2 - \frac{b_2 G_{w2}}{S_\gamma} \right) - \left(\frac{b_1 G_{w1}}{S_\gamma} - a_1 \right) \cdot Z \right] \cdot \tan \phi_2 + 3b_2c_2}{\gamma \cdot h \cdot \sqrt{1 + \left[\left(\frac{b_1 G_{w1}}{S_\gamma} - a_1 \right) \cdot \text{Sin} \psi \right]^2}} = 1 \quad (5.23)$$

That is again identical to equation (5.11), where,

$$\sigma_n = \gamma \cdot h \cdot \left[\left(a_2 - \frac{b_2 G_{w2}}{S_\gamma} \right) - \left(\frac{b_1 G_{w1}}{S_\gamma} - a_1 \right) \cdot Z \right] \quad (5.24)$$

$$C = 3b_2c_2 \quad (5.25)$$

$$\tau = \gamma \cdot h \cdot \sqrt{1 + \left[\left(\frac{b_1 G_{w1}}{S_\gamma} - a_1 \right) \cdot \sin \psi \right]^2} \quad (5.26)$$

Where, all the symbols are as defined in connection with equation (5.10).

5.3.1.4. Floating Failure

The factor of safety falls to zero in this case as the contact is lost on both planes. That is, the wedge floats due to the water pressures that are acting on both planes.

So, limit-state equation of this case is:

$$\frac{yh(a_1S_y - b_1G_{w1}) \cdot \tan\phi_1 + yh(a_2S_y - b_2G_{w2}) \cdot \tan\phi_2 + 3S_y(b_1c_1 + b_2c_2)}{S_y \cdot y \cdot h} = 0 \quad (5.27)$$

Where, all the symbols are as defined in connection with equation (5.10).

5.3.2. Barton Bandis Failure Criterion

The basic variables of the limit-states for all the failure modes of a wedge slope, which is being analyzed by this failure criterion, are the same. That is also valid for the constants of these limit-states. The basic variables in case are *JRC*,

JCS , β_1 , β_2 , δ_1 , δ_2 , ϕ_1 , ϕ_2 , G_{w1} , and G_{w2} . While, the constants are α , Ω , h , γ , and S_γ .

5.3.2.1. Biplane Sliding

Based on equation (3.17) the following formula is developed:

$$F_s = \frac{\sigma_{n1} \tan \left[JRC \cdot \log \left(\frac{JCS}{\sigma_{n1}} \right) + \phi_1 \right] + \sigma_{n2} \tan \left[JRC \cdot \log \left(\frac{JCS}{\sigma_{n2}} \right) + \phi_2 \right]}{S_y \cdot y \cdot h} \quad (5.28)$$

This is identical to equation (2.4), in which:

$$\sigma_{n1} = yh(a_1 S_y - b_1 G_{w1}) \quad (5.29)$$

$$\sigma_{n2} = yh(a_2 S_y - b_2 G_{w2}) \quad (5.30)$$

Where,

σ_{n1} and σ_{n2} are the normal stresses on plane 1 and 2, respectively, and all the other symbols are as defined in connection with equation (5.7).

Then, the limit-state equation is written as:

$$\frac{\sigma_{n1} \tan \left[JRC \cdot \log \left(\frac{JCS}{\sigma_{n1}} \right) + \phi_1 \right] + \sigma_{n2} \tan \left[JRC \cdot \log \left(\frac{JCS}{\sigma_{n2}} \right) + \phi_2 \right]}{S_y \cdot y \cdot h} = 1 \quad (5.31)$$

All the symbols in equation (5.31) are as defined in connection with equation (5.7).

5.3.2.2. Sliding Along Plane 1 Only

Based on equation (3.33) the following formula is developed:

$$F_S = \frac{\sigma_{n1} \cdot \tan \left[JRC \cdot \log \left(\frac{JCS}{\sigma_{n1}} \right) + \phi_1 \right]}{\tau} \quad (5.32)$$

In which,

$$\sigma_{n1} = yh \left[\left(a_1 - \frac{b_1 G_{w1}}{S_\gamma} \right) - \left(\frac{b_2 G_{w2}}{S_\gamma} - a_2 \right) \cdot Z \right] \quad (5.33)$$

$$\tau = y \cdot h \cdot \sqrt{1 + \left[\left(\frac{b_2 G_{w2}}{S_\gamma} - a_2 \right) \cdot \sin \psi \right]^2} \quad (5.34)$$

So, limit-state equation of this case becomes:

$$\frac{yh \left[\left(a_1 - \frac{b_1 G_{w1}}{S_\gamma} \right) - \left(\frac{b_2 G_{w2}}{S_\gamma} - a_2 \right) \cdot Z \right] \cdot \tan \left[JRC \cdot \log \left(\frac{JCS}{\sigma_{n1}} \right) + \phi_1 \right]}{y \cdot h \cdot \sqrt{1 + \left[\left(\frac{b_2 G_{w2}}{S_\gamma} - a_2 \right) \cdot \sin \psi \right]^2}} = 1 \quad (5.35)$$

All the symbols in equation (5.35) are as defined in connection with equation (5.7).

5.3.2.3. Sliding Along Plane 2 Only

Based on equation (3.37) the author developed the following formulation:

$$F_s = \frac{\sigma_{n2} \cdot \tan \left[JRC \cdot \log \left(\frac{JCS}{\sigma_{n2}} \right) + \phi_2 \right]}{\tau} \quad (5.36)$$

In which,

$$\sigma_{n2} = yh \left[\left(a_2 - \frac{b_2 G_{w2}}{S_\gamma} \right) - \left(\frac{b_1 G_{w1}}{S_\gamma} - a_1 \right) \cdot Z \right] \quad (5.37)$$

$$\tau = y \cdot h \cdot \sqrt{1 + \left[\left(\frac{b_1 G_{w1}}{S_\gamma} - a_1 \right) \cdot \sin \psi \right]^2} \quad (5.38)$$

Then the limit-state equation is:

$$\frac{yh \left[\left(a_2 - \frac{b_2 G_{w2}}{S_\gamma} \right) - \left(\frac{b_1 G_{w1}}{S_\gamma} - a_1 \right) \cdot Z \right] \cdot \tan \left[JRC \cdot \log \left(\frac{JCS}{\sigma_{n2}} \right) + \phi_2 \right]}{y \cdot h \cdot \sqrt{1 + \left[\left(\frac{b_1 G_{w1}}{S_\gamma} - a_1 \right) \cdot \sin \psi \right]^2}} = 1 \quad (5.39)$$

All the symbols in equation (5.39) are as defined in connection with equation (5.7).

5.3.2.4. Floating Failure

The factor of safety falls to zero in Floating failure case as the contact is lost on both planes due to the water pressures that are acting on these planes.

So, limit-state equation of this case is:

$$\frac{\sigma_{n1} \tan \left[JRC \cdot \log \left(\frac{JCS}{\sigma_{n1}} \right) + \phi_1 \right] + \sigma_{n2} \tan \left[JRC \cdot \log \left(\frac{JCS}{\sigma_{n2}} \right) + \phi_2 \right]}{S_y \cdot y \cdot h} = 0 \quad (5.40)$$

Where σ_{n1} and σ_{n2} are defined as in connection to equation (5.28), while, all the other symbols are as defined in connection with equation (5.7).

5.4. System Reliability

The failure probability of the wedge slope depends on the reliability indices of the four possible failure modes mentioned above. So, in order to find the probability of such a wedge, it should be treated as a system composed of these four components. The occurrence of one or more of these components or failures constitutes the failure of the whole system. In other words, the reliability of this system requires that none of the components fail. Thus, it is treated as a series-connected system. Such a system is represented by the diagram shown in Figure (5.1). Then, the failure probability of this system or slope is calculated by the system reliability method.

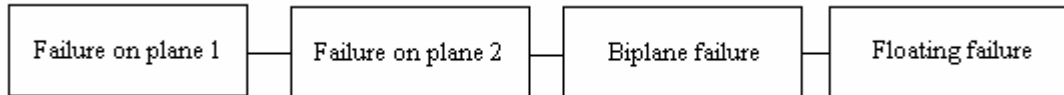


Figure 5.1 Series representation of the wedge failure

The first-order series bounds for all the failure modes are used as these events are positively correlated (Low, 1997). So, the probability of such a system is given by the range (Ang and Tang, 1984):

$$\max[P(F_i)] \leq P(Failure) \leq 1 - \prod_{i=1}^k [1 - P(F_i)] \quad (5.41)$$

Where,

F_i = The failure modes

$P(F_i)$ = The failure probability for the modes of failure

Then, the probability of failure in for a wedge slope is given by:

$$\max[P(F_1), P(F_2), P(F_3), P(F_4)] \leq P(Failure) \leq 1 - \left[\begin{array}{l} (1 - [1 - \Phi(\beta_1)]) \cdot \\ (1 - [1 - \Phi(\beta_2)]) \cdot \\ (1 - [1 - \Phi(\beta_3)]) \cdot \\ (1 - [1 - \Phi(\beta_4)]) \end{array} \right] \quad (5.42)$$

In equation (5.42) $\beta_1, \beta_2, \beta_3, \beta_4$ are the reliability indices of Biplane sliding, sliding along plane 1 only, sliding along plane 2 only, and Floating failure, respectively.

CHAPTER VI

DEVELOPMENT OF SLOPE ANALYZING SPREADSHEETS

6.1. Introduction

The AFOSM approach used in the calculation of the reliability index is an iterative approach, in other words, it is a time consuming method. As a result of that, the need for software application is essential. Such a computational method has been proposed by Low (1997). He implemented the AFOSM method using the solver tool available in Excel spreadsheet to the stability analysis of rock wedge slopes. In that study Low used the Coulomb linear failure criterion and it was assumed the parameters were normally distributed.

The author developed spreadsheets similar to the one proposed by Low (1997), but with broader applications. The developed spreadsheets are called Plane Slope Analyzer (PSA) and Wedge Slope Analyzer (WSA). Each one of them has two spreadsheets that correspond to the failure criteria, namely, Coulomb and Barton Bandis criteria. The PSA is divided into two sub-analyzers. These analyzers are corresponding to the possible positions of tension crack, that is, the slope face and the upper slope surface.

6.2. Plane Slope Analyzer (PSA)

As mentioned above, this analyzer has two sub-analyzers. The sub-analyzers are called Plane Slope Analyzer 1 (PSA1) and Plane Slope Analyzer 2 (PSA2). If the tension crack is in the upper surface of the slope then PAS1 is used. On the other hand, PSA2 is used when the tension crack is located in the slope face. The only difference between PSA1 and PSA2 is the weight calculation method for the sliding block (equations 3.10 and 3.11).

6.2.1. Plane Slope Analyzer (Coulomb)

Plane Slope Analyzer has two worksheets, namely, *definitions and details*, and *Inputs & Outputs* (Appendix A, Figures A.1 and A.3). The former gives the user information about the type of the slope to be analyzed, the input and output parameters (Figure A.1), the assumptions, and the application instructions (Figure A.2). Whereas, the latter is the calculation worksheet, in which the user will input the required parameters and their distributions (Figure A.3). Then, by following the instruction given in Figure (A.2), the reliability index and the probability of failure are calculated. It is important to emphasize that the angles must be in radian rather than in degrees. That is because the Excel software performs angle calculation in radians instead of degrees. For this reason converter tool is added to the spreadsheet in order to ease the user's work. In this converter the right cell contains the formula given in equation (6.1) (Figure 6.1):

$$F27 = \text{RADIANS} (E27) \quad (6.1)$$

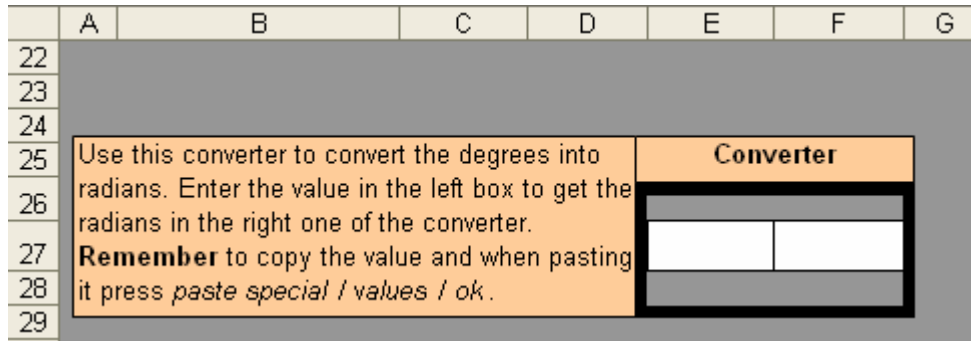


Figure 6.1 Converter tool

The required parameters for this analyzer are ψ_p , ψ_f , C , ϕ_r , H , γ , γ_w , Z_w and Z .

6.2.1.1. Coding in Excel

In order to calculate the equivalent normal mean and standard deviation, a code is defined utilizing the visual basic language based on the code written by Low and Tang (2004). This code is given in Appendix (B).

In the *Inputs & Outputs* the equivalent mean value is given by the formula in Figure (6.2). In this formula the function **EquivalentNormal ()** is called from the user defined code mentioned above. This function asks for some values in order to calculate the required mean value. In fact it is written as **EquivalentNormal (DistributionName, paralist, x, code)**. So, first of all it asks for the distribution type of the variable. Then, it asks for the parameters' values, that is, para1 and para2, which will change according to the type of distribution (Figure 6.3). Next, the function will ask for the initial value of the parameter, which is the mean value calculated automatically in column I. That is the column labeled **xi initial values**. Finally, the function asks for a code, which is either 1 or 2. These codes correspond to the equivalent normal mean value and the equivalent normal standard deviation,

respectively. In other words, if the user is intended to calculate the equivalent normal standard deviation, he will use the same function except for the code which is replaced by 2.

	A	B	C	D	E	K	L	M
1	INPUTS					OUTPUTS		
2								
3		Distribution	Symbol	para1	para2	x	μ^N	σ^N
4			Ψ_f			=EquivalentNormal(B4,D4:E4,K4,1)		
5			Ψ_p					
6			C					
7			tan θ					
8			Zw					

Figure 6.2 Equivalent mean value

	A	B	C	D	E
1	INPUTS				
2					
3		Distribution	Symbol	para1	para2
4		Normal	Ψ_f		
5		Normal	Ψ_p		
6		Symmetric Triangular	C		
7		Upper Triangular	tan θ		
8		Lower Triangular	Zw		
9					
10		Check the box below to know what you need to input as para1 and para2 for each distribution			
11					
12		H	y	y _w	Z
13					
14					
15			Para 1	Para 2	
16		Normal distribution	Mean	StDev	
17		Lognorma distribution	Mean	StDev	
18		Uniform distribution	Min	Max	
19		Triangular distribution	Min	Max	

Figure 6.3 Meaning of para1 and para2 according to their distribution type

As mentioned in Chapter IV, the reliability index is calculated by:

$$\beta = \sqrt{\sum_i \frac{(x_i^* - \mu_{xi}^N)^2}{(\sigma_{xi}^N)^2}} \quad (6.1)$$

In the analyzer, the symbol \mathcal{K}^2 is:

$$(\mathcal{K})^2 = \frac{(x_i^* - \mu_{xi}^N)^2}{(\sigma_{xi}^N)^2} \quad (6.2)$$

Then, the reliability index is coded as (Figure 6.4):

$$\beta = \text{SQRT}(\text{SUM}(N4 : N8)) \quad (6.3)$$

	I	J	K	L	M	N
1	OUTPUTS					
2						
3	x_i initial values		x	μ^N	σ^N	$(\mathcal{K})^2$
4						
5						
6						
7						
8						
9						
10						

Figure 6.4 Reliability index in the spreadsheet

The failure probability of the slope is calculated at the end as:

$$P_F = 1 - \Phi(\beta) \quad (6.4)$$

This is coded in the spreadsheet as:

$$P_F = 1 - \text{NORMSDIST}(M17) \quad (6.5)$$

Where, M17 is the cell containing the value of the reliability index.

All the other formulas used in the calculation of β and P_F are coded as shown in Figure (A.3).

6.2.1.2. Solver Optimization Tool

The Solver tool can be accessed from the Tool list in the toolbar. However, if it is not there, it must be added to the Tool list. That can be done as follows:

1. In the toolbar click Add-Ins function
2. Select Solver Add-in
3. Click ok
4. Now the Solver function has been added to the Tool list

The Solver tool is used to calculate the minimum reliability index. When the Solver is invoked, set the cell of the reliability index to minimum. *By changing* the values of the x column (Figure 6.5), that is K4:K5 cells. Then it is advised to add constraints that will define the range within which the changing cells can vary. For this case, the Plane Slope Analyzer (Coulomb), the constraints are (Figure 6.6):

1. $\$K\$4 : \$K\$5 \leq 1.57$ which means ψ_f and $\psi_p \leq 90^\circ$
2. $\$K\$4 : \$K\$8 \geq 0$ which means $\psi_f, \psi_p, c, \tan \phi$ and Z_w must be ≥ 0
3. $\$M\$16 = 1$ which means $F_s = 1$

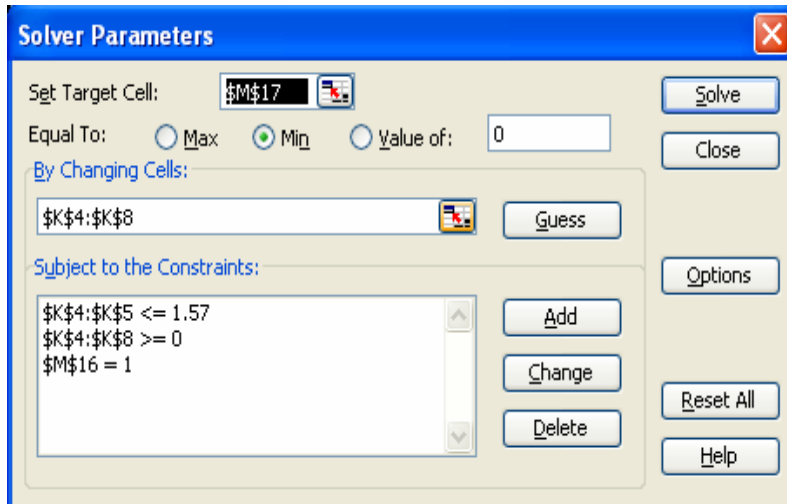


Figure 6.5 Constraints of Plane Slope Analyzer (Coulomb)

After adding the constraints, press the solve button. After solving the spreadsheet will open a new window (Figure 6.7)

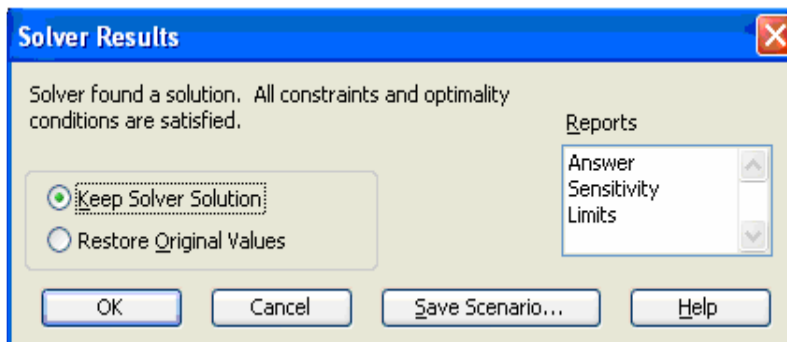


Figure 6.6 Solver results window

If needed the user may get the answer, sensitivity, and limits reports of the solution.

6.2.2. Plane Slope Analyzer (Barton Bandis)

1. This analyzer is similar to the Plane Slope Analyzer (Coulomb) except for two differences (Appendix C, Figures C.1 through C.3). The first difference is the required parameters, and therefore, the constraints. Whereas, the second is the addition of two new outputs, namely, the normal stress σ_n and $\tan \theta$. Where, θ is the term between the parentheses in equation (5.7) (Figure C.3). The required parameters for this analyzer are JRC , JCS , Z_w , ψ_p , ψ_f , ϕ_r , H , γ , and Z (Figure 6.7).

	A	B	C	D	E
1	INPUTS				
2					
3		Distribution	Symbol	para1	para2
4			ψ_f		
5			ψ_p		
6			ϕ		
7			Z_w		
8			JRC		
9			JCS		
10					
11					
12		H	y	y_w	Z
13					
14					

Figure 6.7 Required parameters in PSA (Barton Bandis)

While, the constraints are (Figure 6.8):

1. $\psi_f, \psi_p \leq 1.57$ which means ψ_f and $\psi_p \leq 90^\circ$
2. $\psi_f, \psi_p, \phi, Z_w, JRC$ and JCS must be ≥ 0
3. $JRC \leq 20$ which means $JRC \leq 20$
4. $F_s = 1$ which means $F_s = 1$

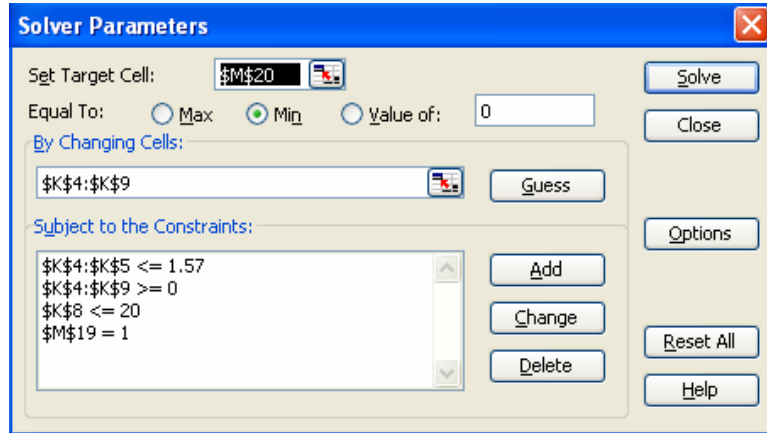


Figure 6.8 Constraints of PSA (Barton Bandis)

All the other formulas used in the calculation of β and P_F are coded as shown in Figure (C.3).

6.3. Wedge Slope Analyzer (WSA)

This analyzer is more complicated than the PSA. That is because of the four failure modes involved in the analysis. The probability of each single mode of failure is calculated after that the reliability of the slope is evaluated based on the system reliability approach introduced earlier in Chapter 4.

6.3.1. Wedge Slope Analyzer (Coulomb)

This analyzer has seven worksheets, namely, *definitions and details*, *Inputs & Outputs*, *BiPlane Failure*, *Plane 1 Failure*, *Plane 2 Failure*, *Floats*, and *Summary* (Appendix D, Figures D.1 through D.8). The first one gives the user information about the type of the slope to be analyzed, the input and output parameters, the assumptions, and the application instructions (Figure D.1 and D.2). The second is

the general calculation worksheet, in which the user will input the required parameters and their distributions (Figure D.3). The worksheets from the third till the sixth are related to the failure modes as their names imply. Each one of these worksheets calculates the reliability and the failure probability for the mode of its name. The seventh and the last worksheet provide the user with the summary of the calculation involved as its name implies. This summary includes the failure probability of the single modes as well as the system reliability (Figure D.8). Once more this system reliability is based on equation (5.42).

The required parameters in this case are $\beta_1, \beta_2, \delta_1, \delta_2, \tan \phi_1, \tan \phi_2, G_{w1}, G_{w2}, C_1, C_2, \alpha, \Omega, h, \gamma,$ and S_γ . These parameters are as defined in connection with equations (2.8) through (2.20). For simplicity it was assumed that $G_{w2} = G_{w1}, \tan \phi_2 = \tan \phi_1,$ and $C_2 = C_1$.

On the other hand, the constraints of each mode of failure are different than those of the others. For example, constraints of Biplane failure are (Figure 6.9):

1. $\beta_1, \beta_2, \delta_1, \delta_2 \leq 180^\circ$
2. $\beta_1, \beta_2, \delta_1, \delta_2, \tan \phi_1, G_{w1},$ and C_1 are all ≥ 0
3. $F_s \leq 1$ that means $F_s \leq 1$. The reason why this constraint was set rather than $F_s = 1$ is that the latter misleads to a bigger value of the reliability index (Low, 1997).
4. abG_1 and abG_2 are ≥ 0

Where,

$$abG_1 = \left(a_1 - \frac{b_1 G_{w1}}{S_y} \right) \quad (6.6)$$

And

$$abG_2 = \left(a_2 - \frac{b_2 G_{w2}}{S_y} \right) \quad (6.7)$$

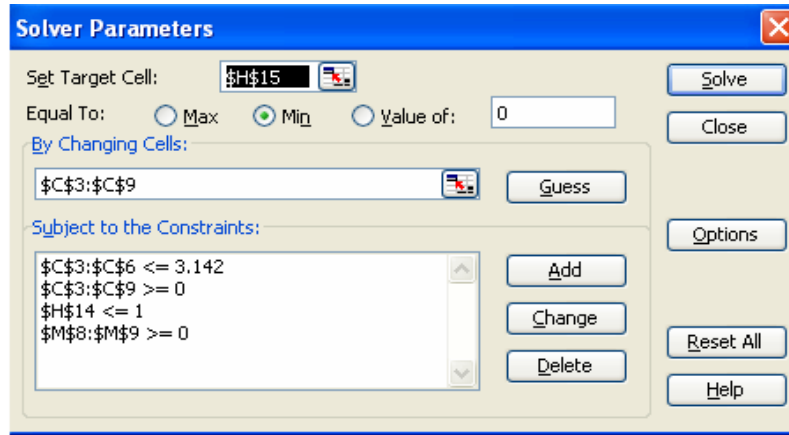


Figure 6.9 Constraints of Biplane failure WSA (Coulomb)

The Constraints of the failure along plane 1 are (Figure 6.10):

1. \$C\$3:\$C\$6 ≤ 3.142 that means $\beta_1, \beta_2, \delta_1, \delta_2 \leq 180^\circ$
2. \$C\$3:\$C\$9 ≥ 0 that means $\beta_1, \beta_2, \delta_1, \delta_2, \tan \phi_1, G_{w1}$, and C_1 are all ≥ 0
3. \$H\$14 ≤ 1 that means $F_s \leq 1$
4. \$M\$9 ≥ 0 that means $abGZ_1 \geq 0$

Where,

$$abGZ_1 = \left[\left(a_1 - \frac{b_1 G_{w1}}{S_\gamma} \right) - \left(\frac{b_2 G_{w2}}{S_\gamma} - a_2 \right) \cdot Z \right] \quad (6.8)$$

In which Z is given by equation (2.25)

5. $\$M\$10 \leq 0$ that means $abG_2 \leq 0$, where abG_2 is defined by equation (6.7)

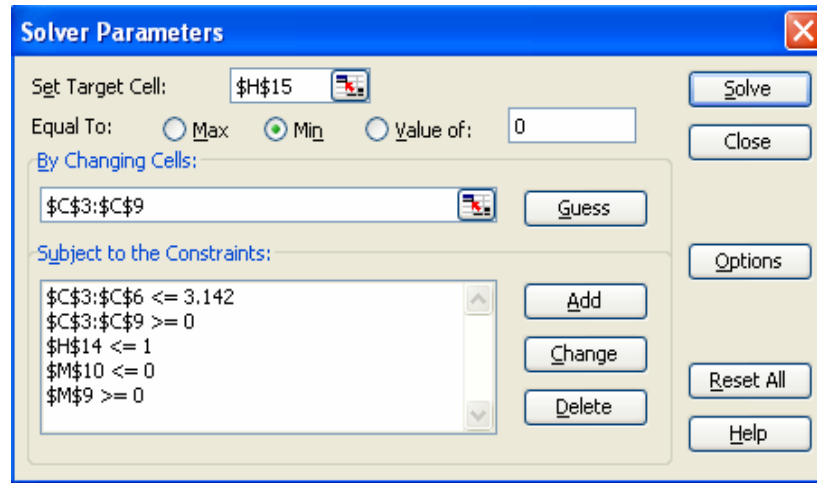


Figure 6.10 The Constraints of the failure along plane 1 WSA (Coulomb)

The Constraints of the failure along plane 2 are (Figure 6.11):

1. $\$C\$3 : \$C\$6 \leq 3.142$ that means $\beta_1, \beta_2, \delta_1, \delta_2 \leq 180^\circ$
2. $\$C\$3 : \$C\$9 \geq 0$ that means $\beta_1, \beta_2, \delta_1, \delta_2, \tan \phi_1, G_{w1}$, and C_1 are all ≥ 0
3. $\$H\$14 \leq 1$ that means $F_s \leq 1$
4. $\$M\$9 \leq 0$ that means $abG_1 \leq 0$, where abG_1 is defined by equation (6.6)
5. $\$M\$10 \geq 0$ that means $abGZ_2 \geq 0$

Where,

$$abGZ_2 = \left[\left(a_2 - \frac{b_2 G_{w2}}{S_\gamma} \right) - \left(\frac{b_1 G_{w1}}{S_\gamma} - a_1 \right) \cdot Z \right] \quad (6.9)$$

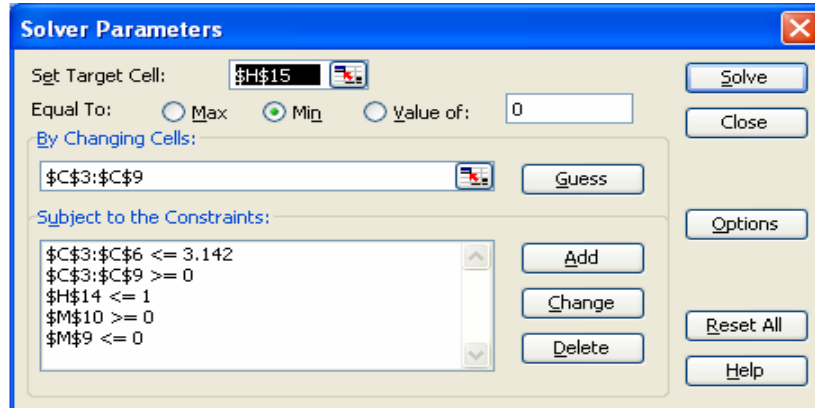


Figure 6.11 The Constraints of the failure along plane 2 WSA (Coulomb)

Constraints of the Floating failure (Floats) (Figure 6.12):

1. $\$C\$3:\$C\$6 \leq 3.142$ that means $\beta_1, \beta_2, \delta_1, \delta_2 \leq 180^\circ$
2. $\$C\$3:\$C\$9 \geq 0$ that means $\beta_1, \beta_2, \delta_1, \delta_2, \tan \phi_1, G_{w1}$, and C_1 are all ≥ 0
3. $\$H\$14 \leq 1$ that means $F_s \leq 1$
4. $\$M\$9:\$M\$10 \leq 0$ that means $abGZ_1$ and $abGZ_2$ are ≤ 0 , where $abGZ_1$ and $abGZ_2$ are defined by equations (6.8) and (6.9), respectively.

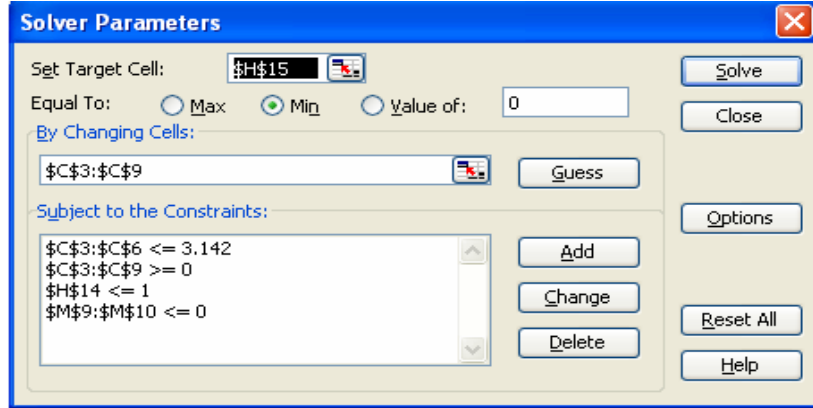


Figure 6.12 Constraints of the Floating failure WSA (Coulomb)

6.3.2. Wedge Slope Analyzer (Barton Bandis)

This analyzer is similar to the Wedge Slope Analyzer (Coulomb) except for two differences (Appendix E, Figures E.1 through E.7). The first is the required parameters, and therefore, the constraints. The second is the addition of new outputs, that is, σ_{n1} , σ_{n2} , $\tan \theta_1$, and $\tan \theta_2$. Where, θ_1 and θ_2 are:

$$\theta_1 = \left[JRC \cdot \log \left(\frac{JCS}{\sigma_{n1}} \right) + \phi_1 \right] \quad (6.10)$$

$$\theta_2 = \left[JRC \cdot \log \left(\frac{JCS}{\sigma_{n2}} \right) + \phi_2 \right] \quad (6.11)$$

While σ_{n1} , σ_{n2} are given by equations (5.29) and (5.30), respectively.

The required parameters are β_1 , β_2 , δ_1 , δ_2 , ϕ_1 , G_{w1} , JRC , JCS , α , Ω , h , γ , and S_γ . For simplicity again it was assumed that $G_{w2} = G_{w1}$, and $\phi_2 = \phi_1$.

Yet again, the constraints of each mode of failure are different than those of the others.

Constraints of the Biplane failure are (Figure 6.13):

1. $\$C\$3:\$C\$10 \geq 0$ that means $\beta_1, \beta_2, \delta_1, \delta_2, \phi_1, G_{w1}, JRC$, and JCS are all ≥ 0
2. $\$C\$3:\$C\$6 \leq 3.142$ that means $\beta_1, \beta_2, \delta_1, \delta_2 \leq 180^\circ$
3. $\$C\$7 \leq 1.57$ that means $\phi_1 \leq 90^\circ$
4. $\$C\$9 \leq 20$ which means $JRC \leq 20$
5. $\$H\$14 = 1$ that means $F_s = 1$. The reason why this constraint was set in this way is that the $F_s \leq 1$ constraint in some situations yields undefined values of F_s . That is due to the formulation of Barton Bandis failure criterion.
6. $\$L\$8:\$L\$9 \geq 0$ that means abG_1 and abG_2 are ≥ 0 .

Where, abG_1 and abG_2 are given by equations (6.6) and (6.7), respectively.

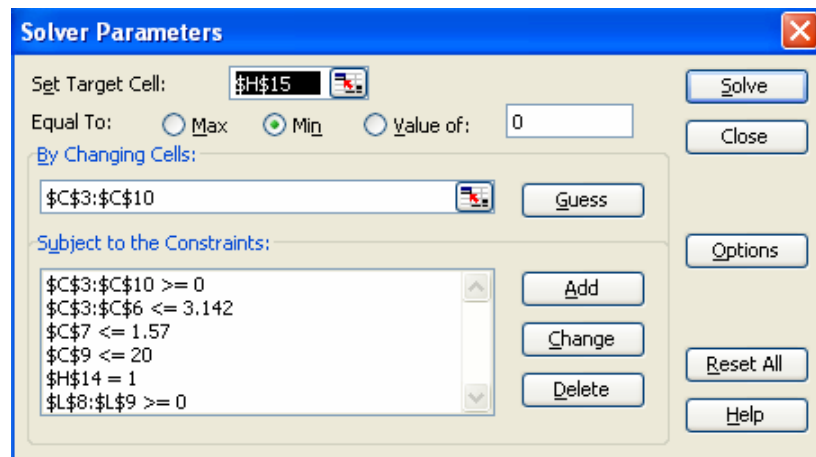


Figure 6.13 Constraints of the Biplane failure WSA (Barton Bandis)

The Constraints of the failure along plane 1 are:

The first five constraints of this mode of failure are the same as those of the Biplane failure mentioned above, whereas, the others are:

6. $\$L\$9 \geq 0$ that means $abGZ_1 \geq 0$.
7. $\$L\$10 \leq 0$ that means and $abG_2 \leq 0$

Where, $abGZ_1$ and abG_2 are given by equations (6.8) and (6.7), respectively.

The Constraints of the failure along plane 2:

The first five constraints of this mode of failure are again similar to those of the Biplane failure. While, the others are:

6. $\$L\$9 \leq 0$ that means $abG_1 \leq 0$.
7. $\$L\$10 \geq 0$ that means and $abGZ_2 \geq 0$

Where, abG_1 and $abGZ_2$ are given by equations (6.6) and (6.9), respectively.

Constraints of the Floating failure (Floats):

Once more the first five constraints are similar to those of the Biplane failure. Whereas, the others are:

6. $\$L\$9 \leq 0$ that means $abGZ_1 \leq 0$
7. $\$L\$10 \leq 0$ that means and $abGZ_2 \leq 0$

Where, $abGZ_1$ and $abGZ_2$ are given by equations (6.8) and (6.9), respectively.

6.4. Defining and Enabling Macros

In order to add a user defined macro to an Excel worksheet, the user need to follow the procedure given below (Figures 6.14-6.15):

1. Tools/Macros/Visual Basic Editor
2. Insert/Module
3. Define the new macro
4. Save
5. File/Close and Return to Microsoft Excel

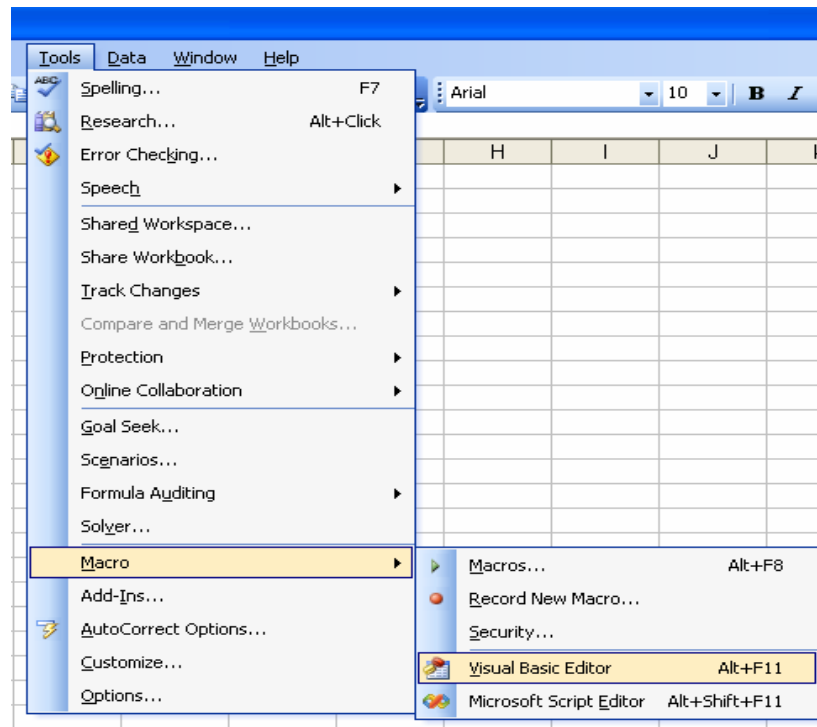


Figure 6.14 Defining macros in Excel, step (1)

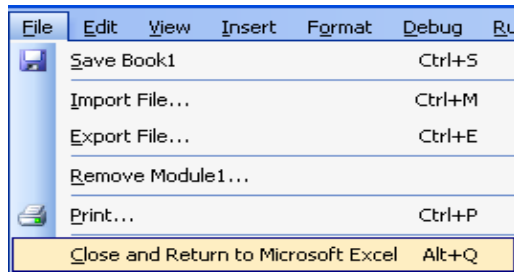


Figure 6.15 Defining macros in Excel, step (5)

Since the user defined macro does not work unless the macros are enabled, it is essential enable the macros when utilizing Excel spreadsheets. In order to enable such macros the user need to set the macro security level to medium. That is done by following the list below (Figures 6.16-6.17):

1. Tools/Macros/Security
2. Security level / *“Medium”* / *“Ok”*

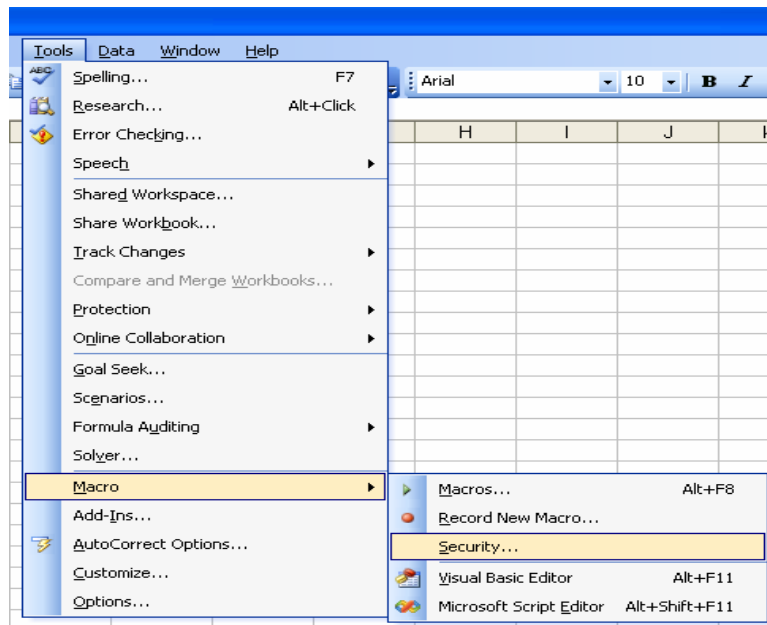


Figure 6.16 Enabling macros, steps (1)

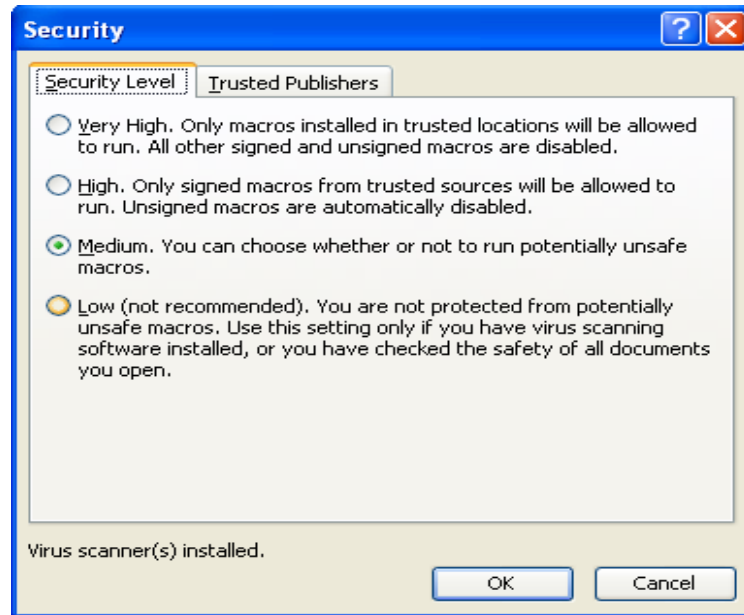


Figure 6.17 Enabling macros, steps (2)

After that, the user needs to close and re-open the Excel software. Before opening the analyzer, a warning window will show up (Figure 6.18). “*Enable Macros*” button should be selected in order to open the analyzer and make use of the user defined macro.

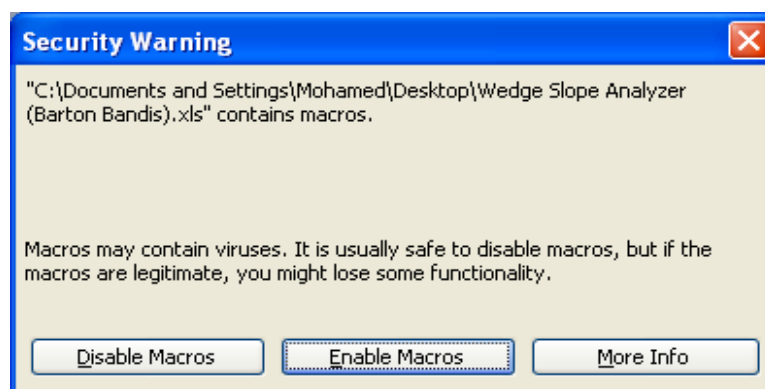


Figure 6.18 Excel warning window

6.5. Verification of PSA and WSA Spreadsheets

In this section the verifications of the developed spreadsheets are carried out. These verifications were accomplished by studying the affect of height of slope, height of water table, cohesion, friction angle, and JCS on the values of the reliability index, and failure probability of given plane and wedge slopes based on Coulomb and Barton Bandis failure criteria. The parameters were assumed to be normally distributed for simplicity.

6.5.1. Plane Slope Analyzers

In order to analyze the effect of the factors mentioned above on the stability of a specific plane slope, there was a need for changing the number of cells that are being changed during the solution in the solver tool so that it will represent the same slope in all cases. This adjustment was made by eliminating the cells containing the dip of slope surface (ψ_f) as well as the dip of discontinuity plane (ψ_p) from the cells under 'By Changing Cells' option. For example, after making such adjustment to PSA (Coulomb) the solver tool of Figure 6.5 will appear as shown in Figure 6.19.

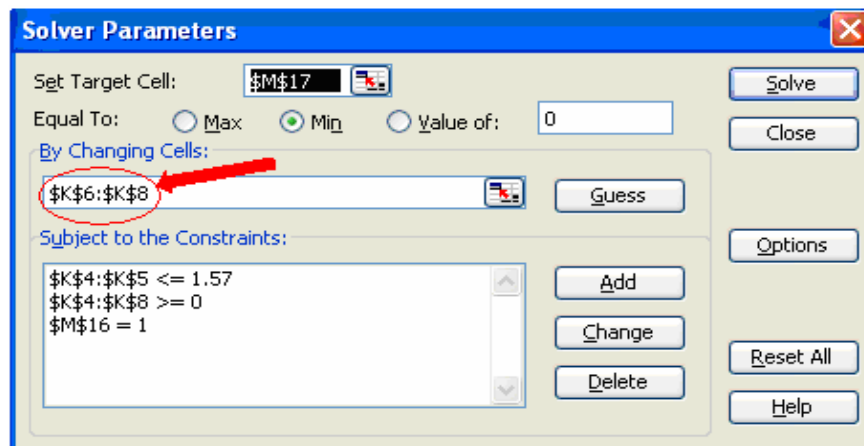


Figure 6.19 Solver of PSA (Coulomb) after eliminating ψ_f and ψ_p

6.5.1.1. Plane Slope Analyzer (Coulomb)

In order to verify the Plane Slope Analyzer (Coulomb) the affect of slope height, height of water table, cohesion and friction angle on *Beta value* (reliability index) and *probability of failure* is investigated. For this reason a plane slope with the basic variables and their statistical parameters as given in Table 6.1 is considered.

Table 6.1 Summary of the basic variables and their statistical parameters for PSA (Coulomb)

Variable Name	Dip of slope surface (ψ_f , rad)	Dip of discontinuity plane (ψ_p , rad.)	Cohesion of the joint (C, ton/m ²)	Tangent of the friction angle of the joint ($\tan\theta$, rad.)	Height of water in tension crack (Zw, m)
Mean	1.396	0.541	15.000	0.700	10.000
Standard deviation	0.070	0.125	3.001	0.150	0.100
c.o.v.	0.050	0.232	0.200	0.214	0.010

On the other hand, the constant parameters of the slope under consideration are shown in Table 6.2.

Table 6.2 Constant parameters for PSA

Slope height (H, m)	Unit weight of rock (y, ton/m ³)	Unit weight of water in (yw, ton/m ³)	Tension crack depth from the crest (Z, m)
60.00	2.70	1.00	40.00

In this study different slope heights are considered. However, the area of the considered plane had to be constant in order to make the results comparable. Thus, the difference between the height of the slope (H) and the height of the tension crack (Z) is kept constant. The values of the slope heights considered in this study are shown in Table 6.3.

Table 6.3 Values of H and Z used in the analysis

Height of the slope (H, m)	60	70	80	100
Height of tension crack (Z, m)	40	50	60	80

The effects of slope height, height of water table, cohesion and friction angle on the value of the reliability index (*Beta*) is shown in Figures 6.20 through 6.23, whereas, the effects of the same parameters on the *probability of failure* are given in Appendix F (Tables F.1 through F.16).

As seen form Figures 6.20 and 6.21, the value of Beta is directly proportion with the value of cohesion, but inversely proportional with slope height. On the other hand, the relation is linear when the slope is dry, but not linear when the height of water table increases to 10 meters.

From Figures 6.22 and 6.23, it is clear that Beta is directly proportion with the friction angle, but inversely proportional with the slope height. The increase is linear and highly sharp until 34.99 degrees angle. However, it is not the same for friction angles bigger than 34.99 degrees, as the increase is not linear and not as sharp as before it.

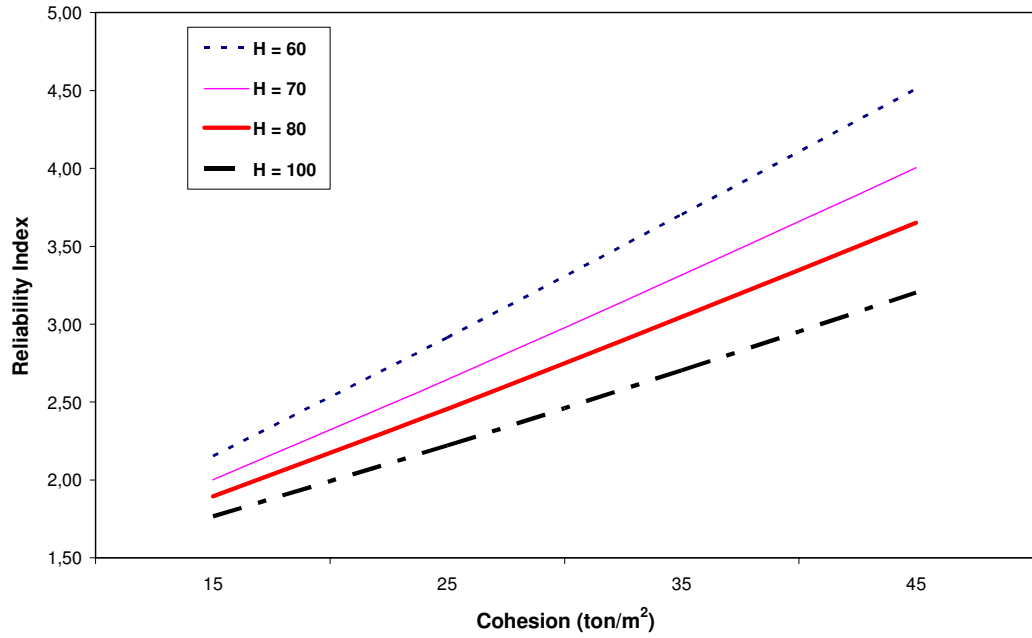


Figure 6.20 Cohesion versus Beta values for different slope heights at dry condition

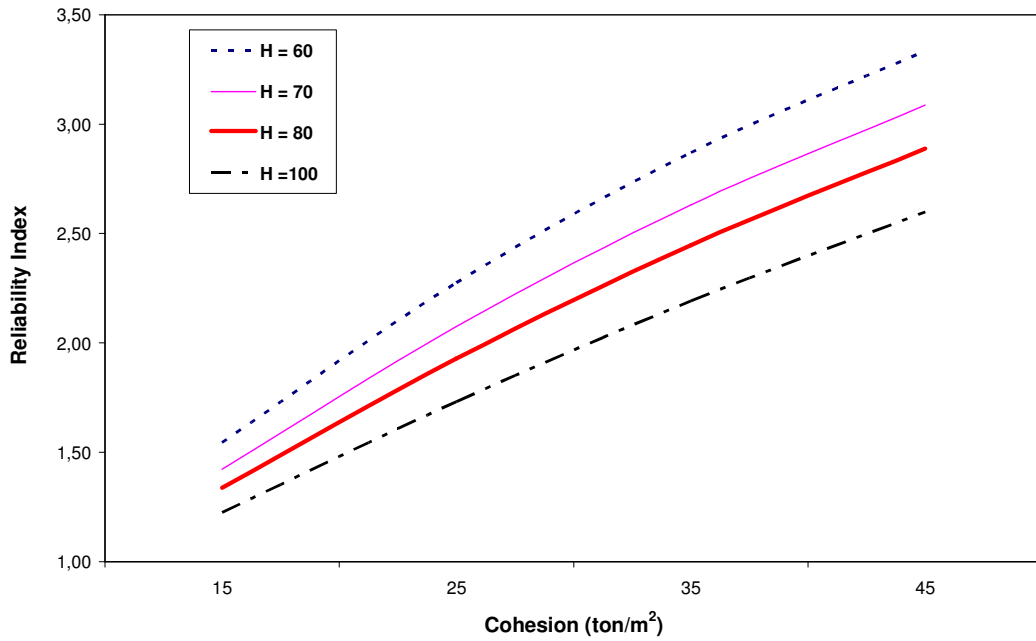


Figure 6.21 Cohesion versus Beta values for different slope heights at 10 m height of water table

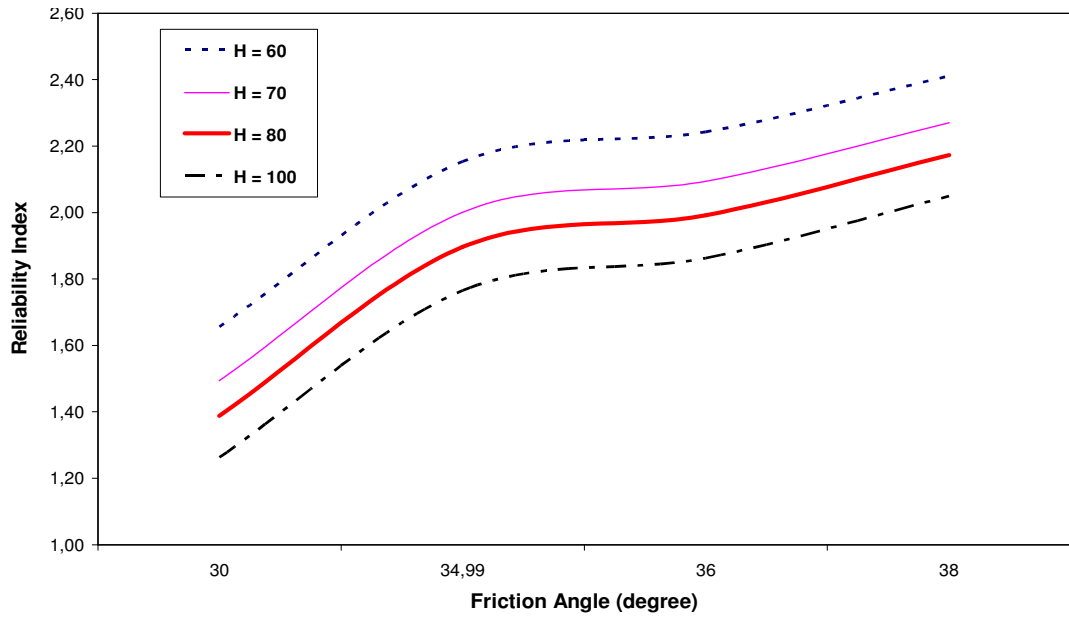


Figure 6.22 Friction angle versus Beta values for different slope heights at dry condition

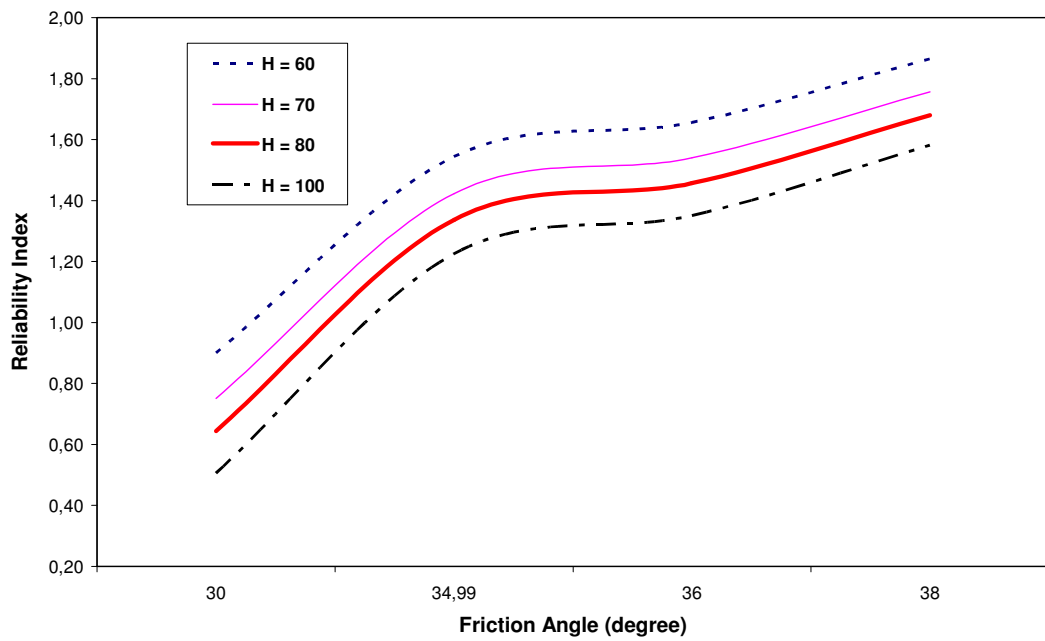


Figure 6.23 Friction angle versus Beta values for different slope heights at 10 m height of water table

6.5.1.2. Plane Slope Analyzer (Barton Bandis)

In order to verify the Plane Slope Analyzer (Barton Bandis) the affect of slope height, height of water table, JCS and friction angle on *Beta value* and *probability of failure* is investigated. For this reason a plane slope with the basic variables and their statistical parameters as given in Table 6.4 is considered.

Table 6.4 Summary of the basic variables and their statistical parameters for PSA
(Barton Bandis)

Variable Name	Dip of slope surface (ψ_b , rad)	Dip of discontinuity plane (ψ_p , rad.)	Friction angle of the joint (ϕ , rad.)	Joint wall compressive strength (JCS, ton/m ²)	Height of water in tension crack (Zw, m)	Joint roughness coefficient (JRC)
Mean	1.396	0.541	0.611	55682.957	10.000	10.000
Standard deviation	0.070	0.125	0.131	11136.591	0.100	0.100
c.o.v.	0.050	0.232	0.214	0.200	0.010	0.010

The constant parameters of this slope are as shown in Table 6.2.

The effects of slope height, height of water table, JCS and friction angle on *Beta value* is shown in Figures 6.24 through 6.27, whereas the effects of the same parameters on the *probability of failure* are given in Appendix G (Tables G.1 through G.16).

As can be seen form Figures 6.24 through 6.27, the value of Beta is directly proportion with the value of JCS and friction angle, but inversely proportional with slope height. In all the Figures it is very clear that the relation between Beta and JCS or friction angle is linear for Beta values less than 4.500.

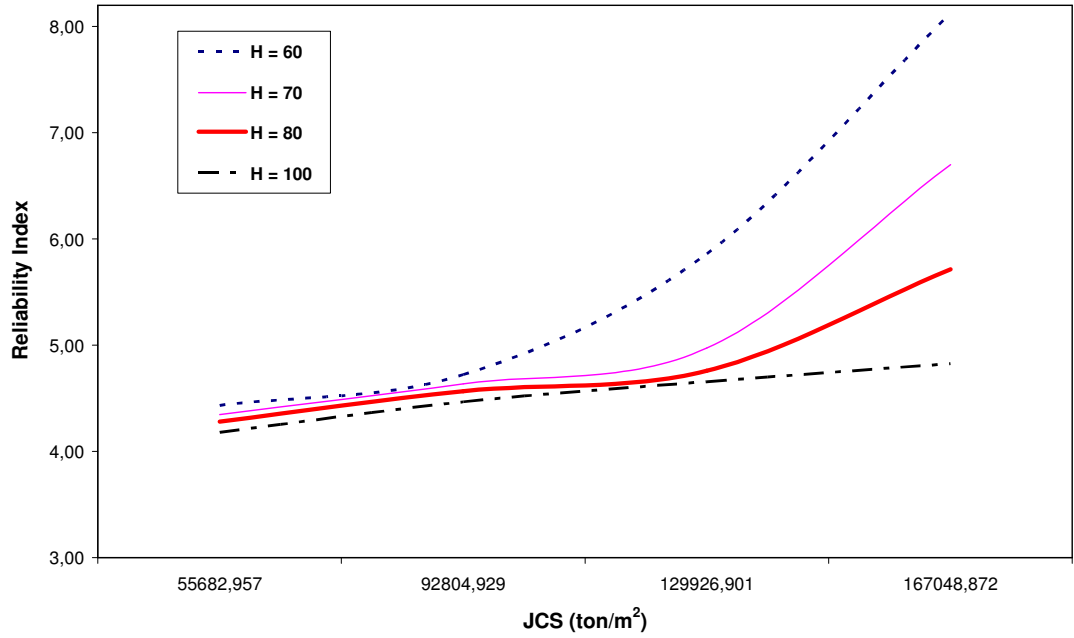


Figure 6.24 JCS versus Beta values for different slope heights at 0 m height of water table

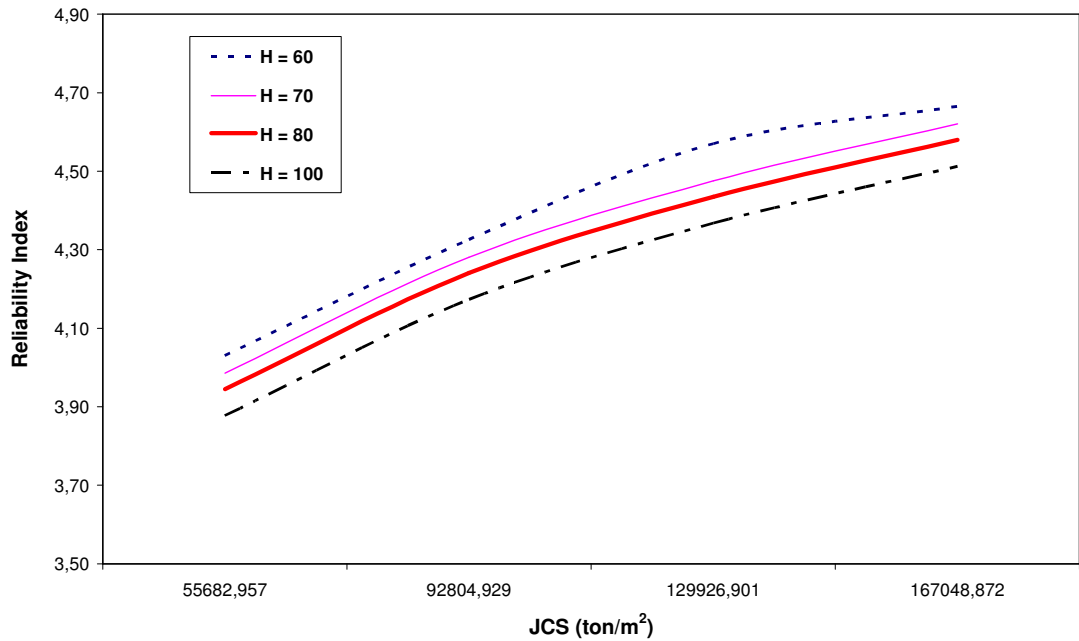


Figure 6.25 JCS versus Beta values for different slope heights at 10 m height of water table

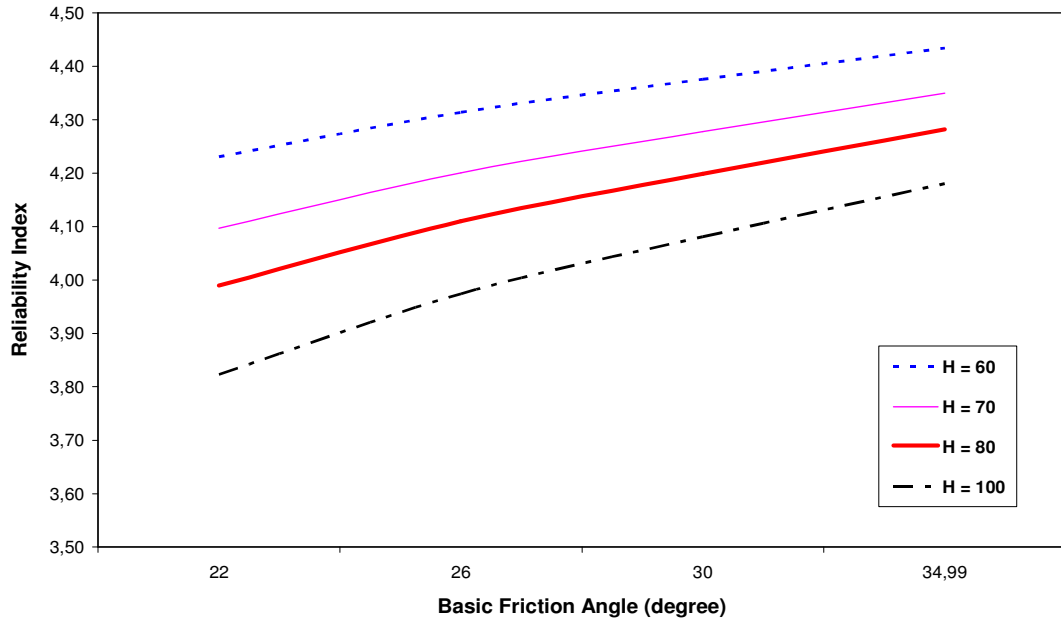


Figure 6.26 Basic friction angle versus Beta values for different slope heights at 0 m height of water table

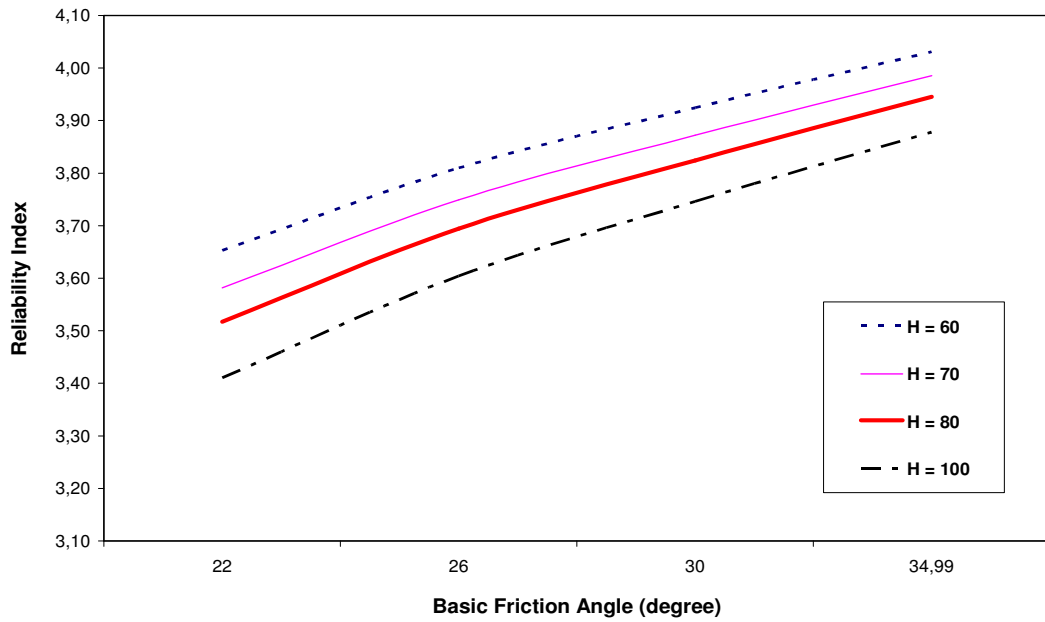


Figure 6.27 Basic friction angle versus Beta values for different slope heights at 10 m height of water table

6.5.2. System Reliability

For wedge failure case two methods are used the calculation of P_F . these methods are the system reliability method and the conventional method that depends on the values of P_F corresponding to single modes of failure. Then the results of these methods are compared to reveal the advantage of system reliability approach over the conventional one. For this reason a wedge slope with the basic variables and their statistical parameters as given in Tables 6.5 is considered (Low, 1997). These parameters are as defined in connection with equation (3.17)

Table 6.5 Summary of the basic variables and their statistical parameters for WSA (Coulomb)

	Mean	Standard deviation	c.o.v.
β_1 (radian)	1.082	0.052	0.048
δ_1 (radian)	0.873	0.035	0.040
β_2 (radian)	0.349	0.052	0.150
δ_2 (radian)	0.838	0.035	0.042
$\tan \phi_1$ (radian)	0.700	0.150	0.214
Gw_1	0.500	0.120	0.240
c_1 (kPa)	41.600	8.320	0.200

The constant parameters of this slope are given in Table 6.6.

Table 6.6 Constant parameters for WSA

α (degree)	Ω (degree)	h (m)	γ (kN/m ³)	S_y (dimensionless)
70	0	16	26	2.6

Once the failure probability of single failure modes is calculated (Table 6.7), the one may accept P_F of Mode 1 as the failure probability of the whole slope, but before doing so let us consider the result of the system reliability approach as well.

Table 6.7 Failure probability of single failure modes for the wedge slope considered

Failure Mode	Mode 1 (Plane 1)	Mode 2 (Plane 2)	Mode 3 (BiPlane)	Mode 4 (Floating)
Probability of Failure (P_F)	0.070	1.1×10^{-9}	0.041	6.9×10^{-6}

In order to evaluate the failure probability of a wedge slope by the system reliability approach, it should be treated as a system that composes of four components, that is, the four modes of failure. The occurrence of one or more of these components constitutes the failure of the whole system. In other words, the reliability of this system requires the stability of all the components. Such components are said to be positively correlated (Ang and Tang, 1984). For a system with such kind of components, Low (1997) suggested the utilization of the first-order series bounds. The application of such bounds to the wedge under consideration is given by equation (5.42). Clearly, the result is in a form of a range with two bounds namely, the upper and the lower bounds.

$$0.070 \leq P_t(\text{Failure}) \leq 0.092 \quad (6.1)$$

In equation (6.1) $P_t(\text{Failure})$ is total failure probability of the considered wedge slope.

Inequality (6.1) indicates that the failure probability of this slope is ranging between 0.092 and 0.070. So, depending on the failure probability of single failure modes

would miss lead to the lowest value of the probability range (Figure 6.28). Thus, the system reliability approach is more appropriate in the estimation of failure probability of wedge slopes.

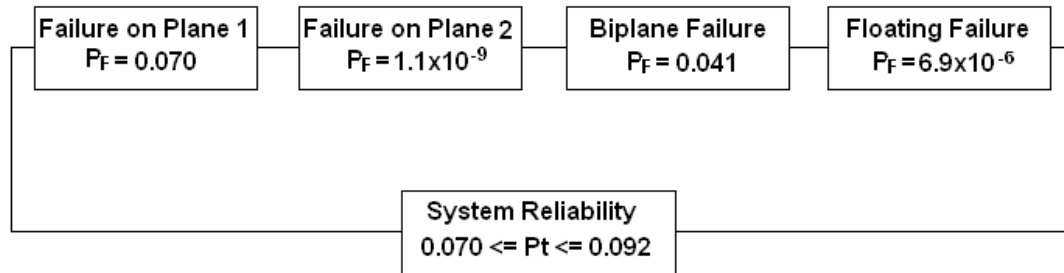


Figure 6.28 Comparison of system reliability result with the results of single failure modes

6.5.3. Wedge Slope Analyzer

In this section, the effect of slope height, height of water table, cohesion, friction angle, and JCS on the failure probability of wedge slope (P_t) is investigated. P_t is used instead of Beta value since it is the only outcome of system reliability approach, which gives the result as a range having a maximum and a minimum values. However, in this study only the maximum value of this failure probability range was considered as the failure probability of the whole wedge slope in order to simplify it.

6.5.3.1. Wedge Slope Analyzer (Coulomb)

In order to verify this spreadsheet a wedge slope having the same parameters as those listed in Tables 6.5 and 6.6 is considered. The results of this analysis are given by Figures 6.29 through 6.32.

As can be seen from Figures 6.29 through 6.32, the value P_F is inversely proportional with the value of cohesion and friction angle, but directly proportional with slope height. It is clear from the same figures that the relation between P_F and cohesion or friction angle is nonlinear. From the same figures, it is obvious that the decrease in P_F is sharper when the water pressure increases as expected.

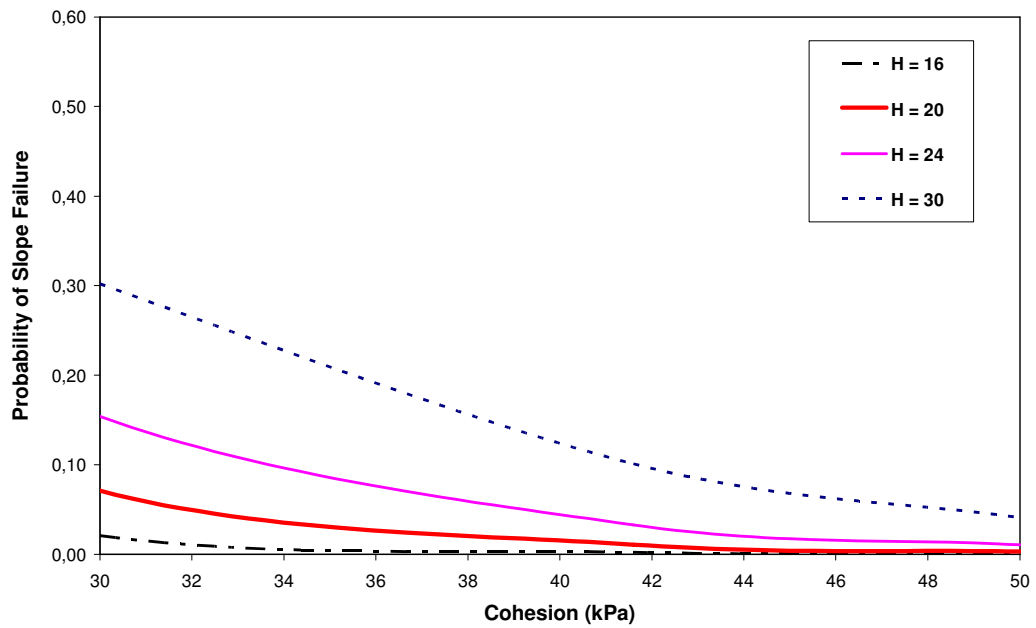


Figure 6.29 Cohesion versus probability of slope failure for different slope heights at 0.25 Normalized water pressure

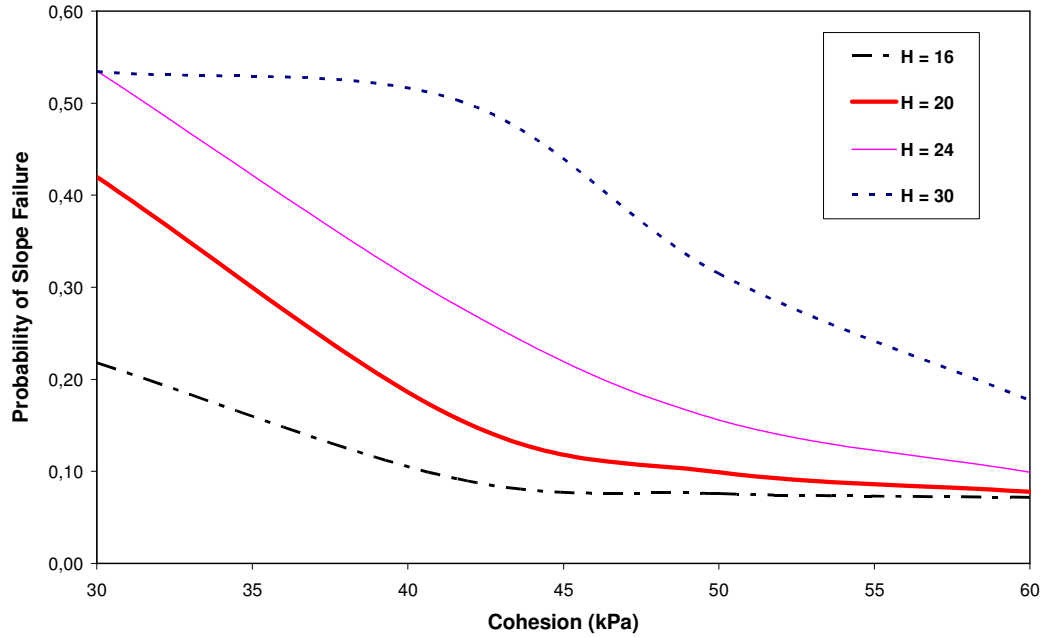


Figure 6.30 Cohesion versus probability of slope failure for different slope heights at 0.5 Normalized water pressure

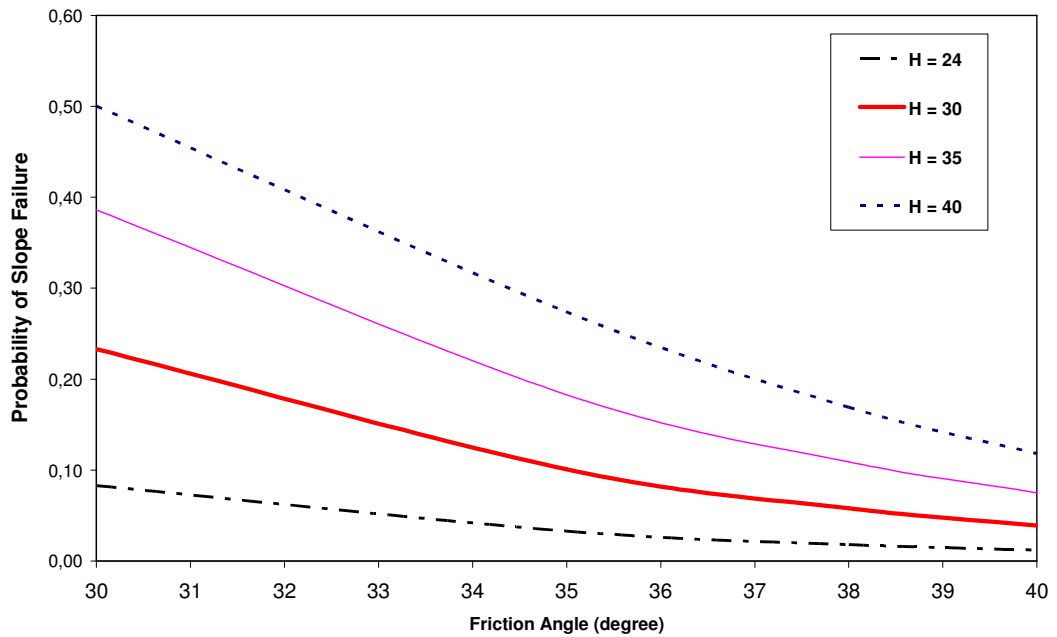


Figure 6.31 Friction angle versus probability of slope failure for different slope heights at 0.25 Normalized water pressure

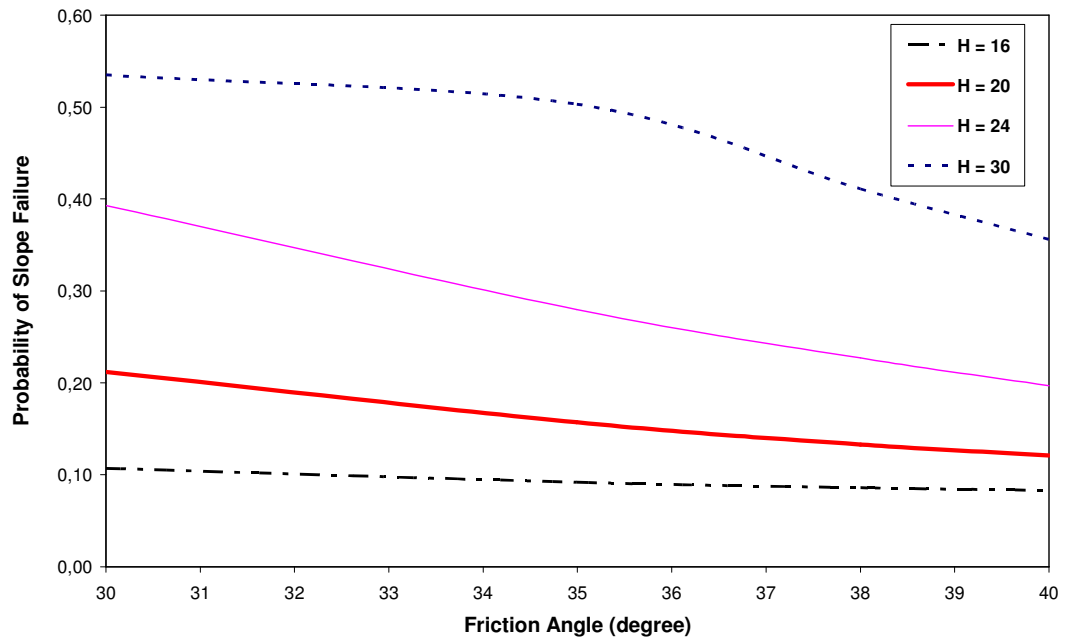


Figure 6.32 Friction angle versus probability of slope failure for different slope heights at 0.5 Normalized water pressure

6.5.3.2. Wedge Slope Analyzer (Barton Bandis)

In order to verify this spreadsheet a wedge slope with the basic variables and their statistical parameters as given in Table 6.6 and 6.8 are considered, while the . These parameters are as defined in connection with equation (3.17).

Table 6.8 Summary of the basic variables and their statistical parameters for WSA
(Barton Bandis)

	Mean	Standard deviation	c.o.v.
β_1 (radian)	1.082	0.052	0.048
δ_1 (radian)	0.873	0.035	0.040
β_2 (radian)	0.349	0.052	0.150
δ_2 (radian)	0.838	0.035	0.042
ϕ_1 (radian)	0.611	0.131	0.214
Gw_1 (dimensionless)	0.500	0.120	0.240
JRC (dimensionless)	11.930	4.180	0.350
JCS (kPa)	154427.402	87368.685	0.566

The constant parameters of this slope are as shown in Table 6.6, and the results of this analysis are given by Figures 6.33 through 6.36. These figures illustrate that the expected results are achieved, which prove the accuracy of this spreadsheet.

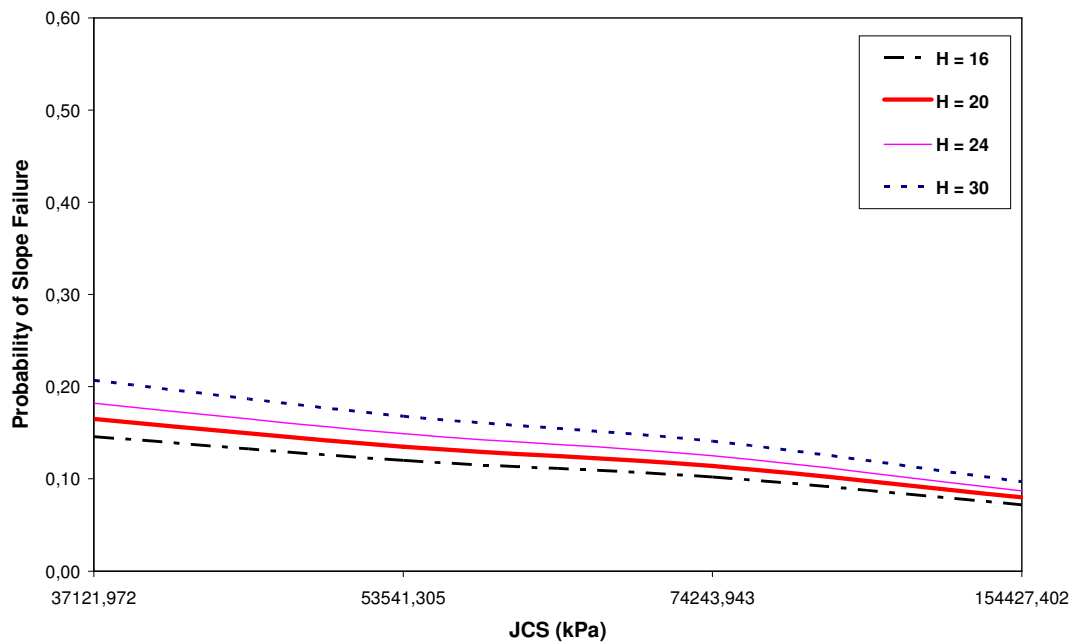


Figure 6.33 JCS versus probability of slope failure for different slope heights at 0.25
Normalized water pressure

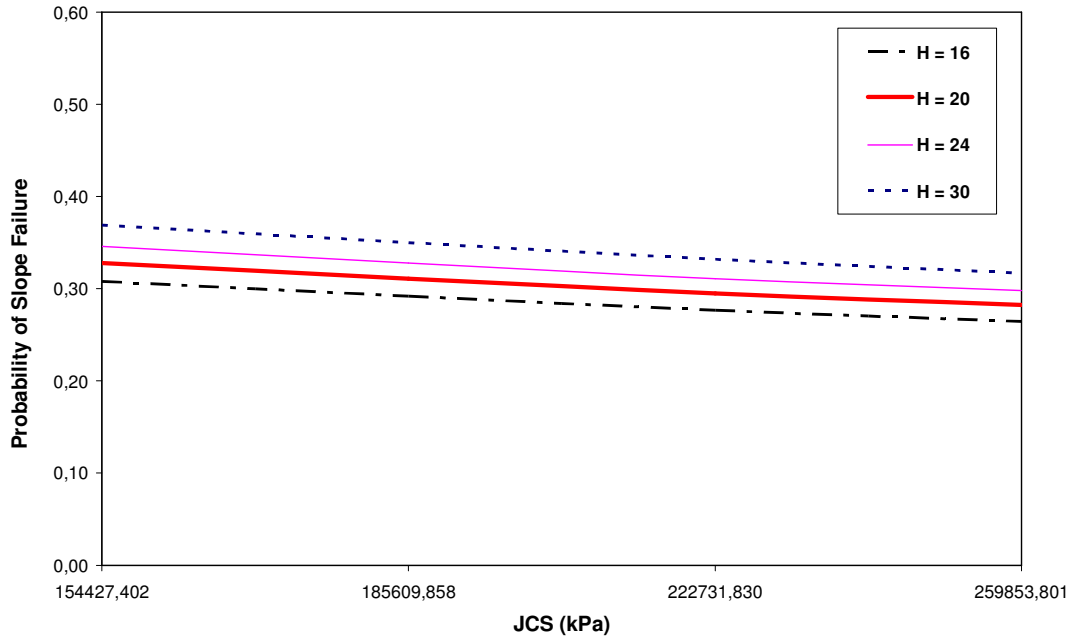


Figure 6.34 JCS versus probability of slope failure for different slope heights at 0.5 Normalized water pressure

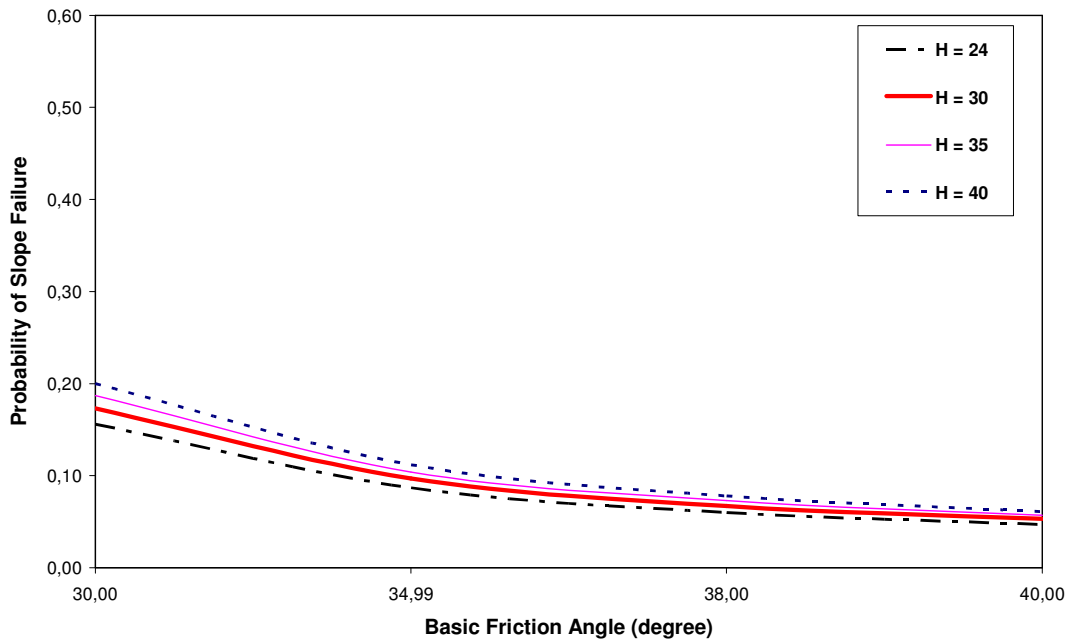


Figure 6.35 Friction angle versus probability of slope failure for different slope heights at 0.25 Normalized water pressure

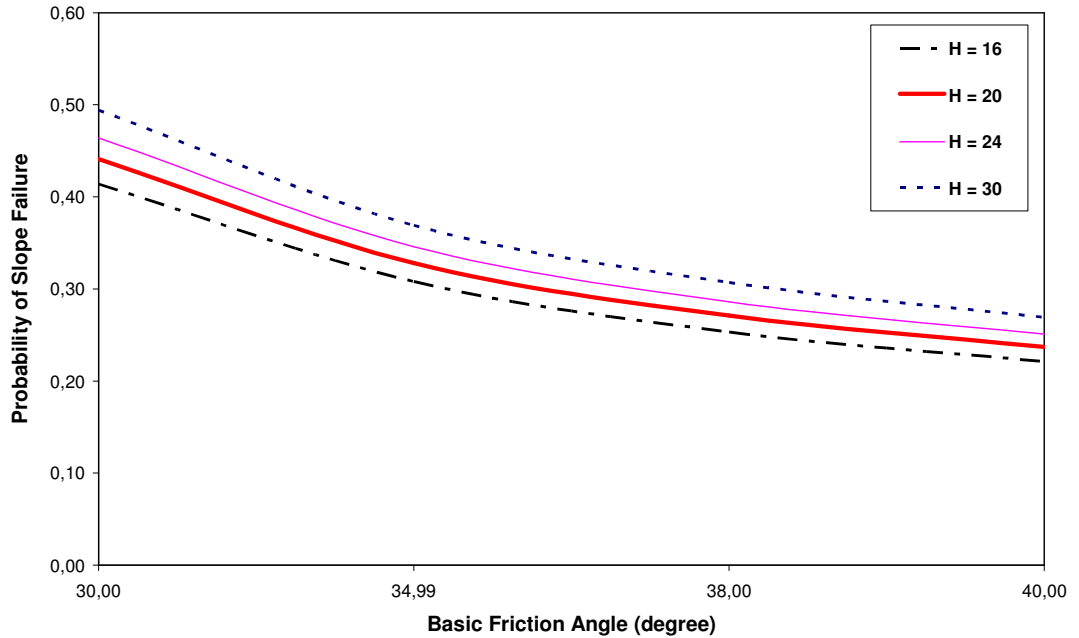


Figure 6.36 Friction angle versus probability of slope failure for different slope heights at 0.5 Normalized water pressure

6.6. Sensitivity Analysis Based on Distribution Function for PSA

This section is devoted to the application of PSA in investigating the sensitivity of reliability index (β) and consequently the probability of slope failure (P_F), to distribution functions of the parameters. PSA (Coulomb) and PSA (Barton Bandis) are used in this analysis.

6.6.1 Sensitivity analysis for PSA (Coulomb)

The parameters used in this study are as shown by Table 6.9 and 6.10.

Table 6.9 Summary of the basic variables for PSA (Coulomb)

Variable Name	Dip of slope surface (ψ_s , rad)	Dip of discontinuity plane (ψ_p , rad.)	Cohesion of the joint (C, ton/m ²)	Tangent of the friction angle of the joint (tan ϕ , rad.)	Height of water in tension crack (Zw, m)
Mean	1.396	0.541	15.000	0.700	10.000
Standard deviation	0.070	0.125	3.001	0.150	0.100

The constant parameters of the slope under consideration are shown in Table 6.10.

Table 6.10 Constant parameters for PSA

Slope height (H, m)	Unit weight of rock (y, ton/m ³)	Unit weight of water in (yw, ton/m ³)	Tension crack depth from the crest (Z, m)
60.000	2.700	1.000	40.000

From Figure 6.3 the maximum and minimum values of the parameters considered are needed if the distribution type is triangular (symmetric, upper, lower) or uniform. The values of these parameters are calculated utilizing Table (4.1) and equation (4.22). Then the results of this study are given in Tables 6.11.

Table 6.11 Results of the Plane Slope Analyzer (Coulomb)

	Normal	Uniform	Lognormal	Symmetric T.	Upper T.	Lower T.
β	1.5440	1.4192	1.7250	8.2221	1.3734	1.4267
P_F	0.0613	0.0779	0.0423	0.0000	0.0848	0.0768

6.6.2 Sensitivity analysis for PSA (Barton Bandis)

The basic variables used in this study are as shown in Table 6.12, while, the constant parameters are the same as those shown in Table 6.10. Then the results of the analysis are given in Tables 6.13.

Table 6.12 Summary of the basic variables for PSA (Barton Bandis)

Variable Name	Dip of slope surface (ψ_b , rad)	Dip of discontinuity plane (ψ_p , rad.)	Friction angle of the joint (ϕ , rad.)	Joint wall compressive strength (JCS, ton/m ²)	Height of water in tension crack (Z_w , m)	Joint roughness coefficient (JRC)
Mean	1.396	0.541	0.611	55682.957	10.000	10.000
Standard deviation	0.070	0.125	0.131	11136.591	0.100	0.100

Table 6.13 Results of the Plane Slope Analyzer (Barton Bandis)

	Normal	Uniform	Lognormal	Symmetric T.	Upper T.	Lower T.
β	4.0288	3.5108	8.9957	M	3.5940	3.8589
P_F	0.00003	0.00022	0.00000	0.00000	0.00016	0.00006

Where, M is a very large positive number.

From Tables 6.11 and 6.13 it is clear that the results of the symmetric triangular distribution are unreliable since they are always very large when compared with other results. The lognormal distribution, on the other hand, always gives results greater than the results of the normal distribution. The uniform and upper triangular

distributions give similar result to some extent. Finally, the lower triangular distribution is found to give the closest result to that of the normal distribution.

6.7. Discussion

The developed probabilistic models and their spreadsheets are verified by carrying out sensitivity analyses. That was done by investigating the variation affect of some parameters on reliability index (β), and probability of slope failure (P_F). In these analyses, one parameter is changed while the others are kept constant. The results of these analyses as shown in Figures 6.20 through 6.36 indicate the expected trend such that:

- a. The reliability index, Beta, decreases as the water level and the slope height increases whereas P_F increases.
- b. Beta increase as the cohesion, friction angle, or JCS increases whereas P_F decreases.

Based on these outcomes, it can be said that the developed models and the spreadsheets are verified and they can be used reliably by any practical engineers in their slope stability analysis.

The effect of Coulomb linear and Barton Bandis nonlinear failure criteria on probability of failure (P_F) is compared in both plane and wedge models. In these comparisons, the strength parameters used in those two different failure criteria were approximated in a manner representing each other. In this approximation the ratio of the compressive strength to cohesion, is taken as 4, as it is commonly utilized in practical applications. So, considering this practical usage, the ratio of JCS to cohesion is assumed to be 3.7 in these analyses.

The comparison of results presented in Tables 6.14 and 6.15 show that:

- For plane slopes, the results of Coulomb criterion are greater than those of Barton Bandis criterion (Table 6.14).
- For wedge slopes, the results of Barton Bandis criterion are greater than that of Coulomb criterion (Table 6.15).

Table 6.14 Probability of failure, P_F , of a plane with cohesion of 15 (ton/m²) for different slope heights at 10 m height of water table

	Coulomb	Barton Bandis
P_F at H = 60	0.061	2.78E-05
P_F at H = 70	0.077	3.36E-05
P_F at H = 80	0.091	3.99E-05

Table 6.15 Probability of failure, P_F , of a wedge with cohesion of 30 (kPa) for different slope heights at 0.5 Normalized water pressure

	Coulomb	Barton Bandis
P_F at H = 16	0.092	0.308
P_F at H = 20	0.157	0.328
P_F at H = 24	0.280	0.346

One reason for such differences in the results is the lack of uncertainty evaluation of the parameters in this thesis. Another reason is the estimation of the JCS that corresponds to a given cohesion value. This reduction in the ratio is due to the difficulty encountered in the estimation of JCS for in-situ rocks. Another reason is the distribution parameters which are found to have a great affect on the value of the reliability index.

For wedge slopes the system reliability approach is found more reliable than the conventional P_F which depends on the evaluation of P_F for each mode separately. That is because estimating the failure probability of a wedge slope depending on the failure probability of a single mode has a considerable amount of uncertainty.

According to the results shown in Tables 6.11 and 6.13 the type of distribution function has a remarkable affect on the value of reliability index and therefore on the probability of failure. The sensitivity analysis carried out showed that the results of lognormal distribution is greater than those of normal distribution as far as the reliability index is concerned, whereas, the results of uniform, upper triangular and lower triangular distributions are found to be smaller than those of the normal one. Additionally, the results of symmetric triangular distribution are found to be unreliable since they are always very large when compared with the results of other distribution types. The reason for such big results may be due to the transformation process involved, or as a result of PDF formulation of that distribution.

CHAPTER VII

CONCLUSIONS AND RECOMMENDATIONS

1. In this study, probabilistic models have been developed both for plane and wedge type of slope failures. The models utilize both linear form of Coulomb and non-linear form of Barton Bandis Failure criteria. Analyzer spreadsheets are developed to ease the usage of probabilistic models based on the AFOSM method in slope stability analyses.
2. The developed spreadsheets save time, yield accurate results and they are user friendly, therefore can be used by practical engineers.
3. The spreadsheets express the stability of slopes in terms of reliability index, and probability of slope failure and give the chance to compare them with the factor of safety.
4. The spreadsheets offer the choice of six different distribution types; normal, uniform, lognormal, symmetric triangular, upper triangular, and lower triangular distributions. They suggest that the symmetric triangular distribution is inappropriate for the calculation of the reliability index, while the lognormal distribution has greater effect than those of normal distribution as far as the reliability index is concerned.

5. For wedge slopes, the result of System reliability approach is found to be more reliable than the result of the conventional method, which depends on the failure probability of a single mode.

6. The developed models were verified by the sensitivity analyses and as expected the value of the reliability index decreases as the height of slope and/or the level of water table increases, while it increases as the cohesion, friction angle, and JCS increase. These parameters have the opposite effect on the probability of slope failure.

7. The results of Coulomb failure criterion for plane slopes are bigger than those of Barton Bandis failure criterion as far as P_F is concerned. However, for wedge slopes the results of Barton Bandis failure criterion are greater than those of Coulomb failure criterion.

Finally, based on this study the following recommended for further study:

1. In this thesis the uncertainties of the parameters which have a considerable affect on the result are not considered. Thus, it is recommended to carry out a detailed stability analysis considering the uncertainties as well as the variability of the parameters. That may reveal the ambiguity of the difference between the results of Coulomb and Barton Bandis failure criteria.
2. Wider application of AFOSM method is recommended, since it has overcome the drawbacks of other probabilistic methods.
3. The developed models should also be verified with an actual field data.

REFERENCES

Ang, A.H.S., and Tang, W.H., 1984. Probability Concepts in Engineering Planning and Design, Vol.2. Decision, risk, and reliability. John Wiley and Sons.

Barton, N. 1990. "Scale effects or sampling bias". In Pinto da Cunha A. (ed.), Scale effects in rock masses, Proc. 1st int. workshop, Leon. Balkema, Rotterdam, pp. 3-27.

Bolle, A. Bonnechere F. and Arnould R. 1987. "Aprobabilistic approach of slope stability in fractured rock", Proc. of 6th. Cong. Rock mechanics, pp. 301-303.

Brady, B.H.G. & Brown E.T. 1985. "Rock mechanics for underground mining". Allen and Unwin, London, pp. 527.

Cornell, C.A., 1969. "Structural Safety Specifications Based on Second Moment Analysis", Proc. Int. Assoc. Bridge and Structural Engineers, Symposium on Concepts of Safety of Structures and Methods of Design.

Ditlevsen, O., 1981. "Uncertainty modeling: with applications to multidimensional civil engineering systems". McGraw-Hill, New York.

Duzgun, H. S. B., 1994. "Plane failure analysis of rock slopes: A Reliability Approach". M.Sc. Thesis, Middle East Technical University, Turkey.

Duzgun, H. S. B., Bozdog, T. and Pasamehmetoglu, A.G., 1994. "Probabilistic Wedge Stability Analysis by Advanced First Order Second Moment (FOSM) Method", Proc. of Mine Planning and Equipment Selection'94, pp. 833-838.

Duzgun, H. S. B., Bozdog, T. and Pasamehmetoglu, A.G., 1995. "A Reliability Approach to Wedge Stability Analysis", Proc. of 8th ISRM Congress, pp. 389-392.

Duzgun, H. S. B., Yucemen, M. S., Karpuz, C. 2003. "A methodology for reliability-based design of rock slopes". Rock Mech. Rock Engng. 36 (2), pp. 95-120.

Duzgun, H. S. B., Karpuz, C. and Yucemen, M. S., 2005. "Probabilistic Modelling of Plane Failure in Rock Slopes", 9th International Conference on Structural Safety and Reliability, June 19-23, Rome, Italy.

Esterhuizen, G.S., 1990. "Combined Point Estimate and Monte Carlo Techniques for the Analysis of Wedge Failure in Rock Slopes". Proc. of Static and Dynamic Considerations in Rock Engineering Symp., pp. 125-132.

Feng P., 1997. "Probabilistic treatment of the sliding wedge". M.Sc. Thesis, University of Manitoba Winnipeg, Manitoba, Canada.

Giani, G.P., 1992. Rock Slope Stability Analysis, A.A. Balkema Publishing, Rotterdam.

Gökceoglu, C., Sonmez, H., and Ercanoglu, M., 2000. "Discontinuity controlled probabilistic slope failure risk maps of Altindag (settlement) region in Turkey". Engineering Geology, 55 (4), pp. 277-296.

Harr, M.E. 1981. "Mecanique des milieux formes de particules". Presses Polytechniques Romandes, Lausanne, pp. 514.

Hasofer, A.M. and Lind, N.C., 1974. "Exact and invariant second-moment code format". J.Engrg. Mech., ASCE, 100(1), pp. 111-121.

Hassan AM. Wolff TF. 1999. "Search algorithm for minimum reliability index of earth slopes". Journal of geotechnical and geoenvironmental engineering, ASCE; 125(04):301–8.

Hoek, E., Bray, J. W., and Boyd, J. M., 1973."The Stability of a Rock Slope Containing a Wedge Resting on Two Intersecting Discontinuities", Quarterly J. Engrg. Geol., 6(1), 1-55.

Hoek, E., Bray, J., 1977. Rock slope engineering. Institute of Mining and Metallurgy, London.

Hoek, E., Bray, J., 1981. Rock slope engineering. Institute of Mining and Metallurgy, 3rd edn., London.

Jimenez-Rodriguez, R., Sitar, N., and Chacon, J., 2006. "System reliability approach to rock slope stability". Int. J. Rock Mech. Min. Sci. 43 (6), pp. 847–859.

Kim, H.S., Major, G. and Ross, B.D., 1978. "A General Probabilistic Analysis for 3-Dimensional Wedge Failure", Pre-print Proc. 19th. U.S. Symp. Rock Mechanics, Makay School of Mines, Nevada.

Kimance, J. P., Howe, J. H., 1991. "A combined geostatistical and first order second moment reliability analysis of slopes in Kaolinsed granite". In: Proc., 7th ISRM Congress on Rock Mechanics, pp. 905–911.

Low, B. K., 1979. "Reliability of rock slopes with wedge mechanisms". M.Sc. thesis, Massachusetts Inst. Of Technol., Cambridge, Mass.

Low, B. K. and Einstein, H. H., 1992. "Simplified reliability analysis for wedge mechanisms in rock slopes". Proc., 6th Int. Symp. On Landslides, A. A. Balkema, Rotterdam, the Netherlands, pp. 499-507.

Low, B. K., 1996. "Practical probabilistic approach using spreadsheet". ASCE Geotechnical Special Publication No. 58, Proc., Uncertainty in the geologic Environment – From Theory to Practice, Madison, Wisconsin, July 31-August 3, Vol. 2, pp. 1284-1302.

Low, B. K., 1997. "Reliability analysis of rock wedges". J. Geotech. Geoenviron. Engng. 123 (6), pp. 498–505.

Low, B. K., 2002. "Practical First – Order Reliability Computations Using Spreadsheet". In Proceedings, Probabilistic In Geotechniques: Technical and Economic Risk Estimation. Verlag Gluckauf GmbH. Essen (Germany). pp. 39-46.

Low, B. K. 2003. "Practical Probabilistic Slope Stability Analysis". Proceedings, Soil and Rock America 2003. 12th Panamerican Conference on Soil Mechanics and Geotechnical Engineering and 39th U.S. Rock Mechanics Symposium. Verlag Gluckauf GmbH. Essen. Vol. 2, pp. 2777-2784.

Low, B. K., and Tang, W. H., 2004. "Reliability analysis using object-oriented constrained optimization." Struct. Safety, 26_1_, 69–89.

Major, G., Kim, H.S. and Ross, B.D., 1978. "Application of Monte Carlo Techniques to Stability Analysis", Pre-print Proc. 19th. U.S. Symp. Rock Mechanics, Makay School of Mines, Nevada.

McMahon, B.K., 1971."A Statistical Method for the Design of Rock Slopes", Proc. 1st. Australia-New Zeland Conference on Geomechanics.

Morris, P., and Stoter, H.J., 1983. "Open Cut Slope Design Using Probabilistic Methods", Proc. Of 5th ISRM Symposium, Vol. 1.

Mostyn, G.R., and Li K.S., 1993. "Probabilistic slope analysis-state of play". In Probabilistic Methods in Geotechnical Engineering, Li KS, Lo SC (eds). A.A. Balkema: Rotterdam-Brookfield.

Muralha, J. & Trunk, U., 1993. "Stability of Rock Slopes-Evaluation of Failure Probabilities by the Monte Carlo and First Order Reliability Methods". Proc. of Assessment and Prevention of Failure Phenomena in Rock Engineering, 759-765.

Nguyen, V.U., and Chowdhurym R.N., 1985. "Simulation for Risk Analysis with Correlated Variables", Geotechnique, 35.

Priest, S.D., and Brown, E.T., 1983. Probabilistic Stability Analysis of Variable Rock Slopes, Trans. Instn. Min. Metal., 92.

Rosenbleuth, E., 1975. "Point Estimates for Probability Moments", USA Proc. Nat. Acad. Sci., 70 (10).

Rosenbleuth, E., 1981. "Two Point Estimates in Probabilities", Applied Mathematical Modeling, 5.

Shinozuka, M., 1983. "Basic Analysis of Structural Safety", J. of Structural Division, ASCE, Vol. No. 3, 109.

USAGE (U.S. Army Corps of Engineers) (1999) document, "ETL 1110-2-556, Risk-based analysis in geotechnical engineering for support of planning studies", Appendix A, pages A11 and A12. <http://www.usace.army.mil/publications/eng-tech-ltrs/etl-ew.html>, (Retrieved January 15, 2007).

Wawersik W.R. and Fairhurst C., 1970. "A study of brittle rock fracture in laboratory compression experiments". Int. J Rock Mech. Min. Sci., 7, pp. 561-575.

Weisstein, Eric W., 2004. "Uniform Distribution." From MathWorld—A wolfram web resource.<http://mathworld.wolfram.com/UniformDistribution.html>, (Retrieved March 23, 2007).

Weisstein, Eric W., 2005. "Triangular Distribution." From MathWorld--A Wolfram web resource.<http://mathworld.wolfram.com/TriangularDistribution.html>, (Retrieved March 23, 2007).

Weisstein, Eric W., 2005. "Triangular Distribution." From MathWorld--A Wolfram web resource. <http://reference.wolfram.com/mathematica/ref/TriangularDistribution.html>, (Retrieved March 23, 2007).

APPENDIX A

PLANE SLOPE ANALYZER (COULOMB)

	A	B	C	D	E	F	G	H	I	J	K	L	M	
19	Inputs	Geometrical Parameters	Ψ_r	Dip of slope surface in (radians)										
20			Ψ_p	Dip of discontinuity plane in (radians)										
21			H	Slope height (m)										
22			Z	Tension crack depth from the crest (m)										
23														
24		Mechanical Parameters	γ	Unit weight of rock in (ton/m ³)										
25			γ_w	Unit weight of water in (ton/m ³)										
26			C	Cohesion of the joint in (ton/m ²)										
27			Z _w	Height water in tension crack (m)										
28			$\tan\theta$	Tangent of the friction angle of the joint in (radians)										
29			StDev	Standard deviation of the respective X_i (calculated in lab using the field data)										
30			Mean	Mean values of the respective X_i (calculated in lab using the field data)										
31			Min & Max	Minimum and maximum values of the parameters X_i (calculated in lab using the field data)										
32														
33	Outputs	F _s	Factor of safety											
34		β	Reliability index											
35		A	Area of the sliding surface for the rock block in (m ² /m)											
36		U	Uplift force due to pressure on the sliding surface in (ton/m)											
37		V	Force due to water pressure in the tension crack in (ton/m)											
38		W	Weight of sliding block in (ton/m)											
39		μ'' and σ''	Mean and standard deviation, respectively, of the equivalent normal distribution for x_i											
40		P(Failure)	Failure probability of the considered slope											
41														
42	Assumptions													
43														
44	Instruction:													
45														

Figure A.1 Plane Slope Analyzer (Coulomb) definitions and details worksheet (1)

APPENDIX B

THE USER DEFINED CODE IN THE DEVELOPED SPREADSHEETS

Function EquivalentNormal(DistributionName, paralist, x, code)

del = 0.1

para1 = paralist(1): para2 = paralist(2)

code1 = (μ N): code2 = (sigmaN)

Select Case UCase(Trim(DistributionName))

Case "NORMAL": If code = 1 Then EquivalentNormal = para1

If code = 2 Then EquivalentNormal = para2

Case "UNIFORM": Min = para1: Max = para2

If $x \leq \text{Min}$ Then $x = \text{Min} + \text{del}$

If $x \geq \text{Max}$ Then $x = \text{Max} - \text{del}$

If $\text{Min} < x < \text{Max}$ Then $\text{CDF} = (x - \text{Min}) / (\text{Max} - \text{Min})$: pdf = $1 / (\text{Max} - \text{Min})$

EquivalentNormal = EquivalentTransformed(x, CDF, pdf, code)

Case "SYMMETRIC TRIANGULAR":

Min = para1: Max = para2

$$\mu = (\text{Min} + \text{Max}) / 2$$

If $x \leq \text{Min}$ Then $x = \text{Min} + \text{del}$

If $x \geq \text{Max}$ Then $x = \text{Max} - \text{del}$

If $\text{Min} < x \leq \mu$ Then CDF = $(2 * ((x - \text{Min})^2)) / ((\text{Max} - \text{Min})^2)$: pdf = $4 * (x - \text{Min}) / ((\text{Max} - \text{Min})^2)$

If $\mu < x < \text{Max}$ Then CDF = $1 - ((2 * ((\text{Max} - x)^2)) / ((\text{Max} - \text{Min})^2))$: pdf = $4 * (\text{Max} - x) / ((\text{Max} - \text{Min})^2)$

EquivalentNormal = EquivalentTransformed(x, CDF, pdf, code)

Case "UPPER TRIANGULAR":

Min = para1: Max = para2

If $x \leq \text{Min}$ Then $x = \text{Min} + \text{del}$

If $x \geq \text{Max}$ Then $x = \text{Max} - \text{del}$

If $\text{Min} < x < \text{Max}$ Then CDF = $((x - \text{Min})^2) / ((\text{Max} - \text{Min})^2)$: pdf = $(2 * (x - \text{Min})) / ((\text{Max} - \text{Min})^2)$

EquivalentNormal = EquivalentTransformed(x, CDF, pdf, code)

Case "LOWER TRIANGULAR":

Min = para1: Max = para2

If $x \leq \text{Min}$ Then $x = \text{Min} + \text{del}$

If $x \geq \text{Max}$ Then $x = \text{Max} - \text{del}$

If $\text{Min} < x < \text{Max}$ Then CDF = $1 - (((\text{Max} - x)^2) / ((\text{Max} - \text{Min})^2))$: pdf = $(2 * (\text{Max} - x)) / ((\text{Max} - \text{Min})^2)$

EquivalentNormal = EquivalentTransformed(x, CDF, pdf, code)

Case "LOGNORMAL":

If $x < \text{del}$ Then $x = \text{del}$

Lamda = $\text{Log}(\text{para1}) - 0.5 * \text{Log}(1 + (\text{para2} / \text{para1})^2)$

If code = 1 Then EquivalentNormal = $x * (1 - \text{Log}(x) + \text{Lamda})$

```
If code = 2 Then EquivalentNormal = x * Sqr(Log(1 + (para2 / para1) ^ 2))
```

```
End Select
```

```
End Function
```

```
Function EquivalentTransformed(x, CDF, pdf, code)
```

```
delta = 10 ^ -16
```

```
If CDF <= delta Then CDF = delta
```

```
If CDF >= 1 - delta Then CDF = 1 - delta
```

```
EquivalentSigma = Application.NormDist(Application.NormSInv(CDF), 0, 1, False)
```

```
/ pdf
```

```
If EquivalentSigma < 0.000001 Then EquivalentSigma = 0.000001
```

```
If code = 1 Then EquivalentTransformed = x - EquivalentSigma *  
(Application.NormSInv(CDF))
```

```
If code = 2 Then EquivalentTransformed = EquivalentSigma
```

```
End Function
```

Note

The word “Application” in the code above stands for “Excel”.

APPENDIX C

PLANE SLOPE ANALYZER (BARTON BANDIS)

	A	B	C	D	E	F	G	H	I	J	K	L	M	
21	Inputs	Geometrical Parameters	Ψ_r	Dip of slope surface in (radians)										
22			Ψ_p	Dip of discontinuity plane in (radians)										
23			H	Slope height (m)										
24			Z	Tension crack depth from the crest (m)										
25														
26		Mechanical Parameters	γ	Unit weight of rock in (ton/m ³)										
27			γ_w	Unit weight of water in (ton/m ³)										
28			Z _w	Height water in tension crack (m)										
29			θ	Basic friction angles of the joint in (radians)										
30			JRC	Joint roughness coefficient (dimensionless)										
31			JCS	Joint wall compressive strength (ton/m ²)										
32			StDev	Standard deviation of the respective Xi (calculated in lab using the field data)										
33		Mean	Mean values of the respective Xi (calculated in lab using the field data)											
34		Min & Max	Minimum and maximum values of the parameters Xi (calculated in lab using the field data)											
35														
36	Outputs	F _s	Factor of safety											
37		β	Reliability index											
38		A	Area of the sliding surface for the rock block in (m ² /m)											
39		U	Uplift force due to pressure on the sliding surface (ton/m)											
40		V	Force due to water pressure in the tension crack (ton/m)											
41		W	Weight of sliding block (ton/m)											
42		μ'' and σ''	Mean and standard deviation, respectively, of the equivalent normal distribution for x_i											
43		θ	$\{JRC (\text{Log} (JCS/\sigma_n)) + \theta\}$											
44		P(Failure)	Failure probability of the given slope											
45														
46	Assumptions													
	Definitions and Details / Input & Output /													

Figure C.1 Plane Slope Analyzer (Barton Bandis) definitions and details worksheet (1)

	A	B	C	D	E	F	G	H	I	J	K	L	M	N
43		θ		{JRC (Log (JCS/on)) + ϕ }										
44		P(Failure)		Failure probability of the given slope										
46		Assumptions		For simplicity the variables are assumed to be uncorrelated										
48		Instruction:		<p>For each case;</p> <ol style="list-style-type: none"> 1. Choose the required distribution for each variable. When you do that the system will calculate the corresponding "μ^N" and "σ^N". 2. Start with x values = mean values (which means that you should copy the values of the "xi initial values" column and paste them in the "x" column (make sure that you choose "paste special" then click "values" then "ok" while pasting the values in "x" column). 3. Invoke the solver tool. Then make sure that in the dialogue box the β cell is set to value equal to minimum. 4. Press "Solve" to get the minimum value of β. 5. You can get answer, sensitivity, and limits reports if you select them. 6. Press "ok" after solving. 7. Close the spreadsheet and press no when you are asked to save the changes. (Make sure that you record all the data required before closing the spreadsheet). 										

Figure C.2 Plane Slope Analyzer (Barton Bandis) definitions and details worksheet (2)

	A	B	C	D	E	F	G	H	I	J	K	L	M	N
1	INPUTS							OUTPUTS						
3	Distribution	Symbol	para1	para2	DO NOT forget to input the values of (ψ_f , ψ_p , and θ_1) in RADIANS. Use the converter below.				x_i initial values	x	μ^N	σ^N	$(\mathcal{K})^2$	
4		ψ_f												
5		ψ_p												
6		ϕ												
7		Zw												
8		JRC												
9		JCS												
11	H	y	y_w	Z					A	U	V	W		
13	x_i initial values = IF(B="Normal",D,IF(B="Lognormal",D,IF(B="Upper Triangular",(D+2*E)/3,IF(B="Lower Triangular",2*D+E)/3,(D+E)/2))) "Copy" column " x_i initial values" and paste by clicking "Paste Special / values" in column x μ^N = EquivalentNormal(B,D,E,K,1) σ^N = EquivalentNormal(B,D,E,K,2) $(\mathcal{K})^2$ = (K-L)^2/(M)^2 A = (B13-E13)*(1/SIN(I5)) U = 0.5*D13*K*(B13-E13)*(1/SIN(I5)) V = 0.5*D13*((K7)^2) W = 0.5*C13*((B13)^2)*((E13/B13)^2)*(1/TAN(I5))-(1/TAN(I4)) σ_{n1} = ((N13*(COS(I5)))-(L13)-(M13*SIN(I5)))/K13 θ_1 = K8*(LOG10(D9/(IF(M16<=0.10^16,M16))))+DEGREES(K6) $\tan\theta_1$ = TAN(RADIANS(M17)) F(x) = (M16*M18)/((N13*SIN(I5))+(M13*COS(I5)))/K13 β = SQRT(SUM(N4:N9)) Final β = IF(M21>8.1;8.1;M21) P(failure) = 1-NORMSDIST(M22) The cells below: para1, para2, H, y, y_w , and Z do not contain formulas.													
24		σ_{n1}												
25		θ_1												
25		$\tan\theta_1$												
26		F(x)												
26		β												
26		Final β												
26		P(failure)												

Figure C.3 Plane Slope Analyzer (Barton Bandis) input & output worksheet

APPENDIX D

WEDGE SLOPE ANALYZER (COULOMB)

	A	B	C	D	E	F	G	H	I	J	K	L	
29	Inputs	Geometrical Parameters	$\beta_1, \delta_1, \beta_2, \delta_2$	Joint orientation angles (they are obtained from figure. 1 above) (in radians)									
30			α	Inclination of the slope face (in degrees)									
31			Ω	Inclination of the upper ground surface (in degrees)									
32			h	Height of the wedge (m)									
33													
34		Mechanical Parameters	γ	Unit weight of rock in kN/m ³									
35			S_y	Specific density of rock (dimensionless)									
36			C_1 and C_2	Cohesion of joints 1 and 2, respectively (in kPa)									
37			Gw_1 and Gw_2	Normalized water pressure parameters for joints 1 and 2, respectively (dimensionless and based on pyramidal water pressure conditions)									
38			$\tan\theta_1$ and $\tan\theta_2$	Tangent of the friction angle of joints 1 and 2, respectively (in radians)									
39	$StDev$		Standard deviation of the respective X_i (calculated in lab using the field data)										
40	$Mean$		Mean values of the respective X_i (calculated in lab using the field data)										
41	$Min \& Max$	Minimum and maximum values of the parameters X_i (calculated in lab using the field data)											
42													
43	Outputs	F_s	Factor of safety										
44		β	Reliability index										
45		μ^{II} and σ^{II}	Mean and standard deviation, respectively, of the equivalent normal distribution for X_i										
46		$P_f(\text{Failure})$	Total failure probability of the considered wedge slope										
47													
48													
49													
50	Assumptions												
51													
52	Instruction:												
53													
	Definitions and Details / Input & Output / BiPlane Failure / Plane 1 Failure / Plane 2 Failure / Floats / Summary												

Figure D.1 Wedge Slope Analyzer (Coulomb) definitions and details worksheet (1)

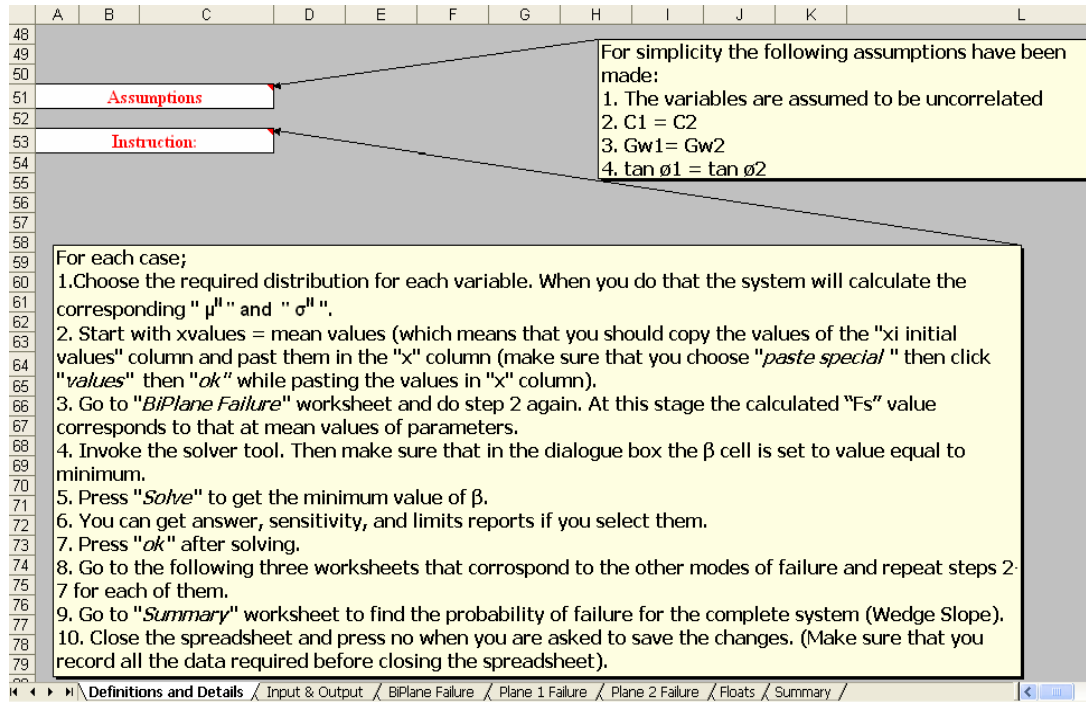


Figure D.2 Wedge Slope Analyzer (Coulomb) definitions and details worksheet (2)

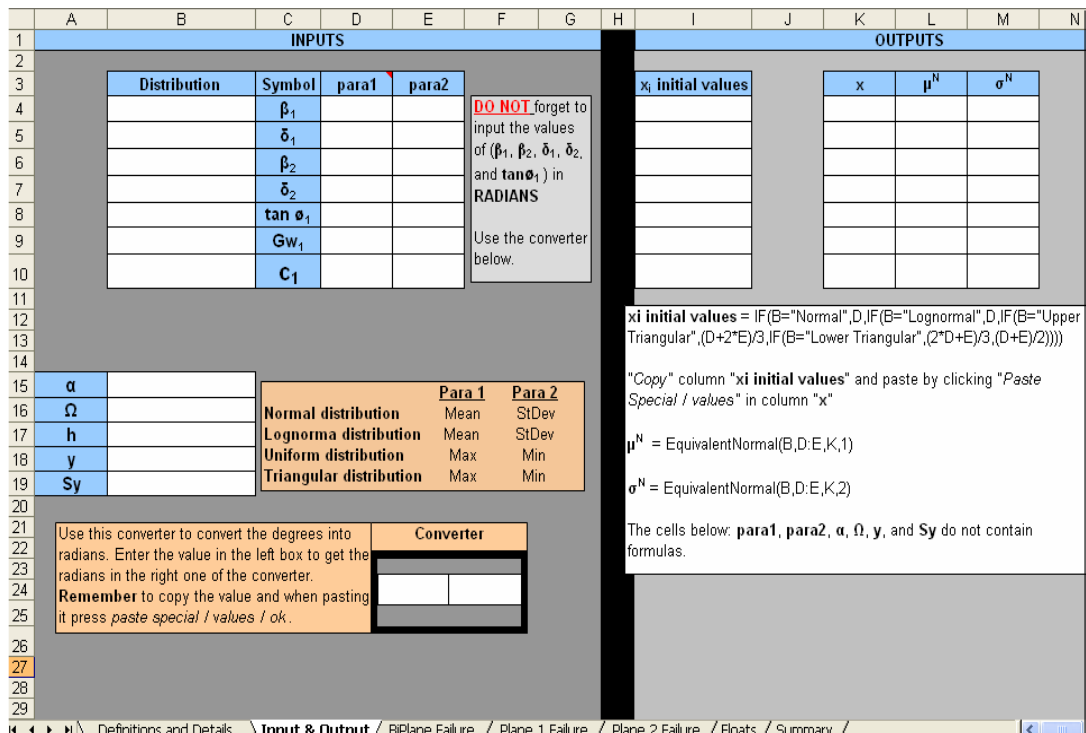


Figure D.3 Wedge Slope Analyzer (Coulomb) input & output worksheet

A	B	C	D	E	F	G	H	I	J	K	L	M	N
2	The Variables (X_i)	x	μ ^N	σ ^N	(X) ²			SinΨ			a ₀		
3	β ₁							κ			a ₁		
4	δ ₁							H			a ₂		
5	β ₂							ε					
6	δ ₂										b ₁		
7	tan φ ₁							cotδ ₁			b ₂		
8	Gw ₁							cotδ ₂			abG ₁		
9	C ₁							cota			abG ₂		
10	<p>"Copy" column "xi initial values" in "Input & Output" worksheet and paste by clicking "Paste Special / values" in column "x"</p> <p>μ^N = EquivalentNormal(Input & Output!B,Input & Output!D:E,C,1)</p> <p>σ^N = EquivalentNormal(Input & Output!B,Input & Output!D:E,C,2)</p> <p>(X)² = (C-D)^2/E^2</p> <p>SinΨ = ABS((1-(SIN(C4)*SIN(C6)*COS(C3+C5)+COS(C4)*COS(C6))^2)*0.5)</p> <p>κ = (1-((TAN(RADIANS(Input & Output!B16)))/TAN((RADIANS(Input & Output!B15))))/(1-(TAN(RADIANS(Input & Output!B16)))/J10))</p> <p>H = J3*Input & Output!B17</p> <p>ε = DEGREES(ATAN(J10))</p> <p>cotδ₁ = 1/TAN(C4)</p> <p>cotδ₂ = 1/TAN(C6)</p> <p>cota = 1/TAN(RADIANS(Input & Output!B15))</p> <p>tanε = (SIN(C3+C5)/(SIN(C3)*J8+SIN(C5)*J7))</p> <p>cote = 1/J10</p> <p>a₀ = (J2)/((SIN(C3+C5)*SIN(C4)*SIN(C6))^2*(J11-J9))</p> <p>Fs = ((M11*C7)+(M12*C7)+(3*Input & Output!B19*((M6*C9)+(M7*C9)))/(Input & Output!B19*Input & Output!B18*Input & Output!B17)</p> <p>β = SQRT(SUM(F3:F9))</p>												
11													
12													
13													
14													
15													
16													
17													
18													
19													
20													
21													
22													
23													
24													
25													
26													
27													
28													
29													
30													
31													
32													
33													
34													
35													
36													
37													
38													
39													
40													
41													
42													
43													
44													
45													
46													
47													
48													
49													
50													
51													
52													
53													
54													
55													
56													
57													
58													
59													
60													
61													
62													
63													
64													
65													
66													
67													
68													
69													
70													
71													
72													
73													
74													
75													
76													
77													
78													
79													
80													
81													
82													
83													
84													
85													
86													
87													
88													
89													
90													
91													
92													
93													
94													
95													
96													
97													
98													
99													
100													

Figure D.4 Wedge Slope Analyzer (Coulomb) Biplane failure worksheet

A	B	C	D	E	F	G	H	I	J	K	L	M
2	The Variables (X_i)	x	μ ^N	σ ^N	(X) ²			SinΨ			a ₀	
3	β ₁							κ			a ₁	
4	δ ₁							H			a ₂	
5	β ₂							ε			Z	
6	δ ₂										b ₁	
7	tan φ ₁							cotδ ₁			b ₂	
8	Gw ₁							cotδ ₂			abGZ ₁	
9	C ₁							cota			abGZ ₂	
10												
11												
12												
13												
14												
15												
16												
17												
18												
19												
20												
21												
22												
23												
24												
25												
26												
27												
28												
29												
30												
31												
32												
33												
34												
35												
36												
37												
38												
39												
40												
41												
42												
43												
44												
45												
46												
47												
48												
49												
50												
51												
52												
53												
54												
55												
56												
57												
58												
59												
60												
61												
62												
63												
64												
65												
66												
67												
68												
69												
70												
71												
72												
73												
74												
75												
76												
77												
78												
79												
80												
81												
82												
83												
84												
85												
86												
87												
88												
89												
90												
91												
92												
93												
94												
95												
96												
97												
98												
99												
100												

Figure D.5 Wedge Slope Analyzer (Coulomb) Plane 1 failure worksheet

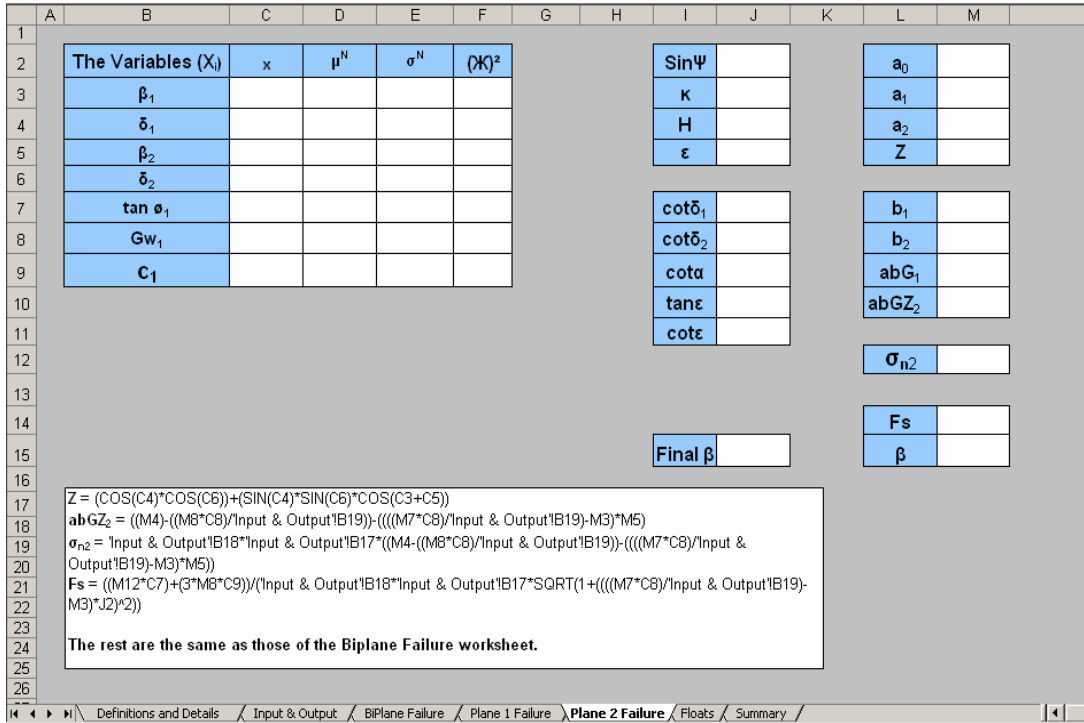


Figure D.6 Wedge Slope Analyzer (Coulomb) Plane 2 failure worksheet

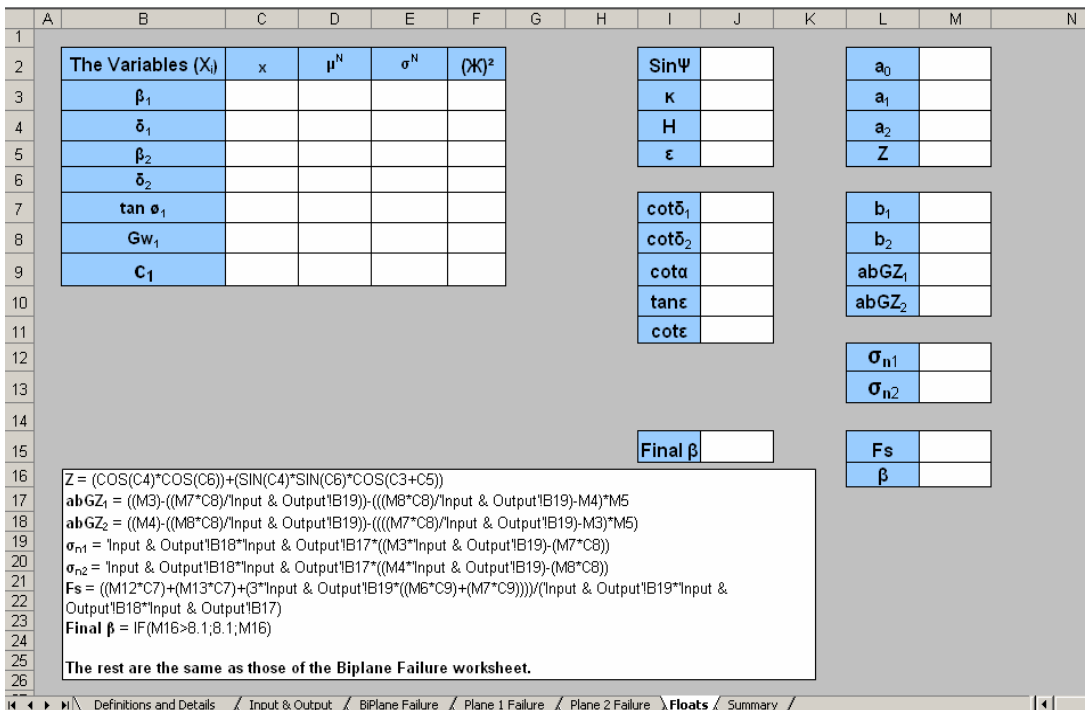


Figure D.7 Wedge Slope Analyzer (Coulomb) Floats worksheet

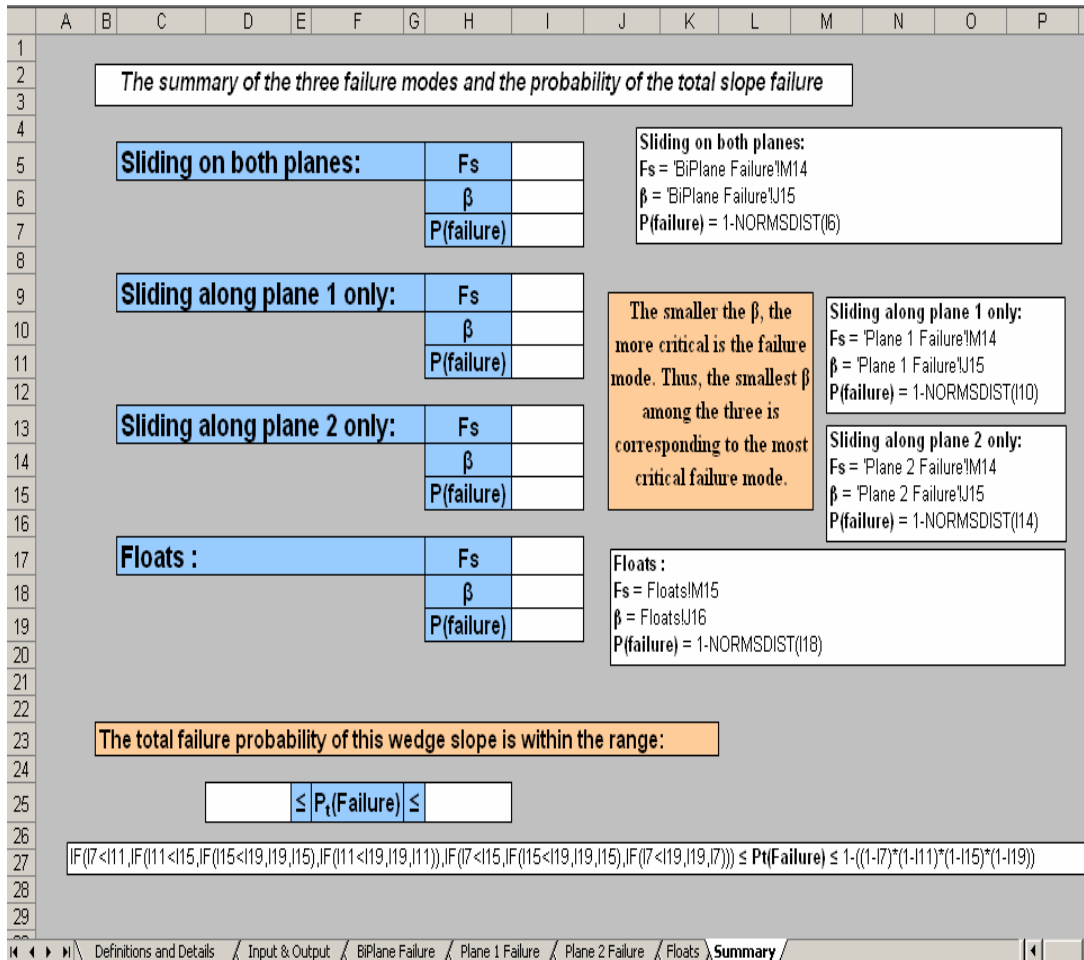


Figure D.8 Wedge Slope Analyzer (Coulomb) summary worksheet

APPENDIX E

WEDGE SLOPE ANALYZER (BARTON BANDIS)

	A	B	C	D	E	F	G	H	I	J	K	L
29	Inputs	Geometrical Parameters	$\beta_1, \delta_1, \beta_2, \delta_2$	Joint orientation angles (they are obtained from figure. 1 above) (in radians)								
30			α	Inclination of the slope face (in degrees)								
31			Ω	Inclination of the upper ground surface (in degrees)								
32			h	Height of the wedge (m)								
33		Mechanical Parameters	γ	Unit weight of rock in kN/m^3								
34			Sy	Specific density of rock (dimensionless)								
35			JRC	Joint roughness coefficient (dimensionless)								
36			JCS	Joint wall compressive strength in (kPa)								
37			Gw_1 and Gw_2	Normalized water pressure parameters for joints 1 and 2, respectively (dimensionless and based on pyramidal water pressure conditions)								
38			θ_1 and θ_2	Basic friction angle of joints 1 and 2, respectively (in radians)								
39	StDev		Standard deviation of the respective X_i (calculated in lab using the field data)									
40	Mean	Mean values of the respective X_i (calculated in lab using the field data)										
41	Min & Max	Minimum and maximum values of the parameters X_i (calculated in lab using the field data)										
42	Outputs	F_s	Factor of safety									
43		β	Reliability index									
44		μ'' and σ''	Mean and standard deviation, respectively, of the equivalent normal distribution for x_i									
45		ϵ	$\{JRC (\text{Log} (JCS/\sigma_n)) + \theta\}$									
46		$P_1(\text{Failure})$	Total failure probability of the given wedge slope									
47	Assumptions		For simplicity the following assumptions have been made: 1. the variables are assumed to be uncorrelated 2. $Gw_1 = Gw_2$ 3. $\theta_1 = \theta_2$									
48	Instruction:											
49												
Definitions and Details / Input & Output / BiPlane Failure / Plane 1 Failure / Plane 2 Failure / Floats / Summary /												

Figure E.1 Wedge Slope Analyzer (Barton Bandis) definitions and details worksheet

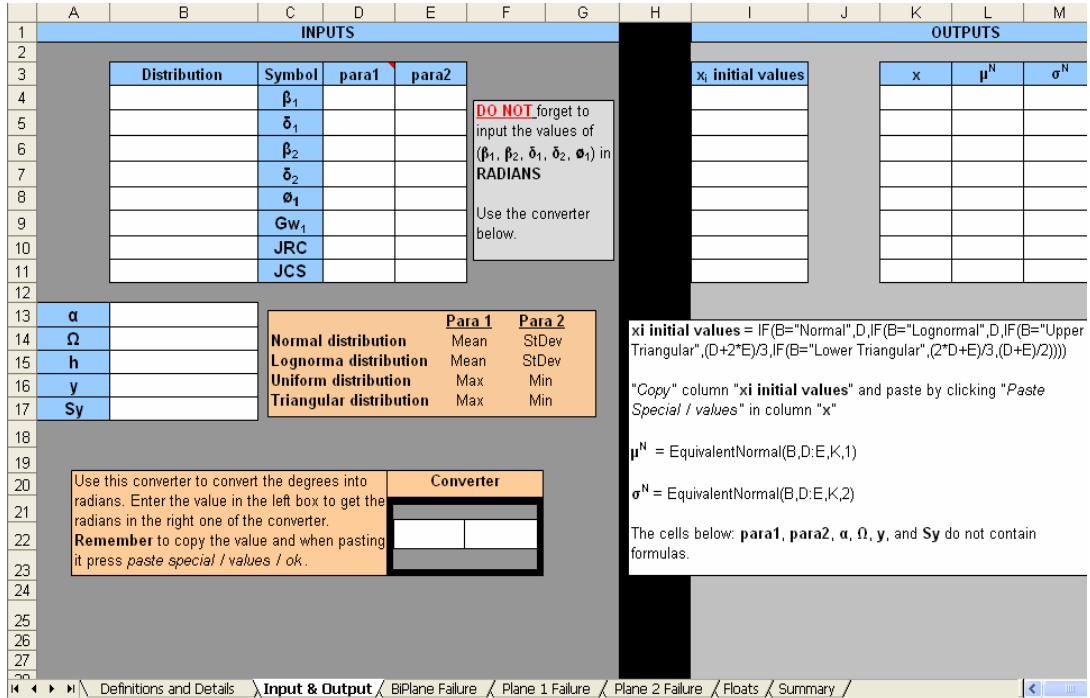


Figure E.2 Wedge Slope Analyzer (Barton Bandis) input & output worksheet

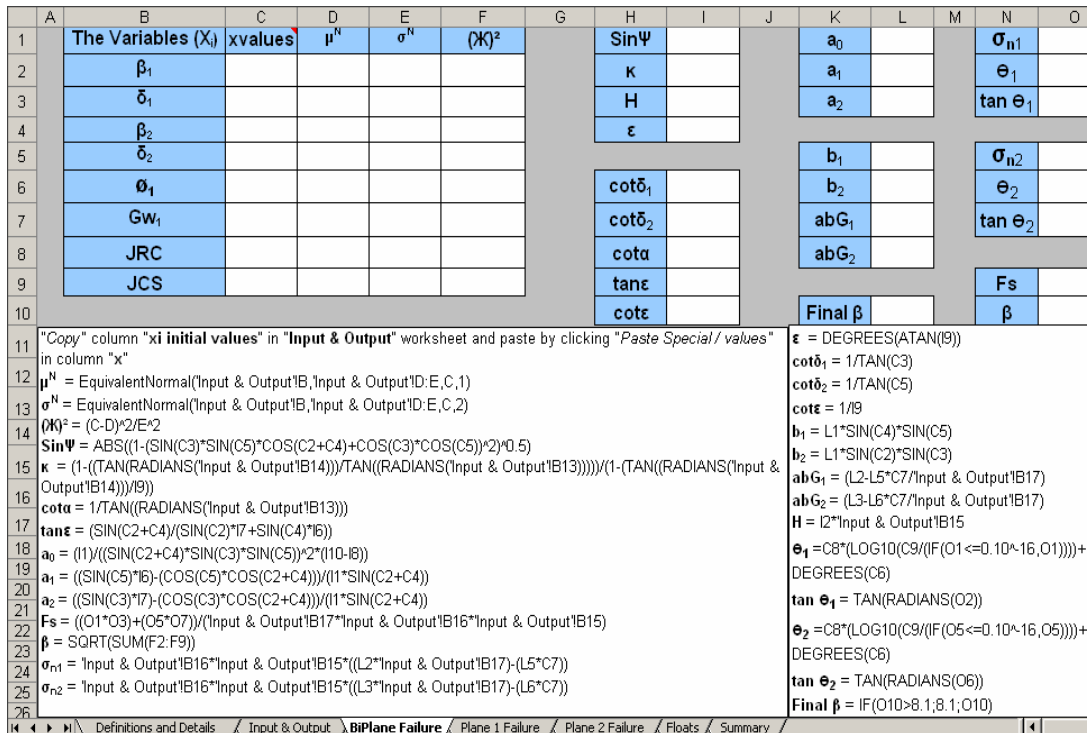


Figure E.3 Wedge Slope Analyzer (Barton Bandis) Biplane failure worksheet

	A	B	C	D	E	F	G	H	I	J	K	L	M	N	O
1		The Variables (X _i)	xvalues	μ^N	σ^N	$(X)^2$		Sin Ψ			a ₀			σ_{n1}	
2		β_1						κ			a ₁			θ_1	
3		δ_1						H			a ₂			tan θ_1	
4		β_2						ϵ			Z				
5		δ_2													
6		θ_1						cot δ_1			b ₁				
7		Gw ₁						cot δ_2			b ₂				
8		JRC						cota			abGZ ₁				
9		JCS						tan ϵ			abGZ ₂			Fs	
10								cote						β	
11											Final β				
12	$Z = (\cos(C3) \cdot \cos(C5)) + (\sin(C3) \cdot \sin(C5) \cdot \cos(C2 + C4))$														
13	$abGZ_1 = ((L2) - ((L6 \cdot C7) / \text{Input} \& \text{Output}!B17)) - (((L7 \cdot C7) / \text{Input} \& \text{Output}!B17) - L3) \cdot L4$														
14	$\sigma_{n1} = \text{Input} \& \text{Output}!B16 \cdot \text{Input} \& \text{Output}!B15 \cdot ((L2 - ((L6 \cdot C7) / \text{Input} \& \text{Output}!B17)) - (((L7 \cdot C7) / \text{Input} \& \text{Output}!B17) - L3) \cdot L4)$														
15	$\theta_1 = C8 \cdot ((\log_{10}(C9 / (IF(O1 <= 0.10 \wedge 16, O1)))) + \text{DEGREES}(C6))$														
16	$\tan \theta_1 = \text{TAN}(\text{RADIANS}(O2))$														
17	$Fs = (O1 \cdot O3) / (\text{Input} \& \text{Output}!B16 \cdot \text{Input} \& \text{Output}!B15 \cdot \text{SQRT}(1 + (((L7 \cdot C7) / \text{Input} \& \text{Output}!B17) - L3) \cdot (1) \cdot 2))$														
18	The rest are the same as those of the Biplane Failure worksheet.														
19															
20															
21															
22															
23															
24															
25															

Figure E.4 Wedge Slope Analyzer (Barton Bandis) Plane 1 failure worksheet

	A	B	C	D	E	F	G	H	I	J	K	L	M	N	O
1		The Variables (X _i)	xvalues	μ^N	σ^N	$(X)^2$		Sin Ψ			a ₀			σ_{n2}	
2		β_1						κ			a ₁			θ_2	
3		δ_1						H			a ₂			tan θ_2	
4		β_2						ϵ			Z				
5		δ_2													
6		θ_1						cot δ_1			b ₁				
7		Gw ₁						cot δ_2			b ₂				
8		JRC						cota			abG ₁				
9		JCS						tan ϵ			abGZ ₂			Fs	
10								cote						β	
11											Final β				
12	$Z = (\cos(C3) \cdot \cos(C5)) + (\sin(C3) \cdot \sin(C5) \cdot \cos(C2 + C4))$														
13	$abGZ_2 = ((L3) - ((L7 \cdot C7) / \text{Input} \& \text{Output}!B17)) - (((L6 \cdot C7) / \text{Input} \& \text{Output}!B17) - L2) \cdot L4$														
14	$\sigma_{n2} = \text{Input} \& \text{Output}!B16 \cdot \text{Input} \& \text{Output}!B15 \cdot ((L3 - ((L7 \cdot C7) / \text{Input} \& \text{Output}!B17)) - (((L6 \cdot C7) / \text{Input} \& \text{Output}!B17) - L2) \cdot L4)$														
15	$\theta_2 = C8 \cdot ((\log_{10}(C9 / (IF(O1 <= 0.10 \wedge 16, O1)))) + \text{DEGREES}(C6))$														
16	$\tan \theta_2 = \text{TAN}(\text{RADIANS}(O2))$														
17	$Fs = (O1 \cdot O3) / (\text{Input} \& \text{Output}!B16 \cdot \text{Input} \& \text{Output}!B15 \cdot \text{SQRT}(1 + (((L6 \cdot C7) / \text{Input} \& \text{Output}!B17) - L2) \cdot (1) \cdot 2))$														
18	The rest are the same as those of the Biplane Failure worksheet.														
19															
20															
21															
22															
23															
24															
25															

Figure E.5 Wedge Slope Analyzer (Barton Bandis) Plane 2 failure worksheet

	A	B	C	D	E	F	G	H	I	J	K	L	M	N	O
1		The Variables (X _i)	xvalues	μ ⁿ	σ ⁿ	(X) ²		SinΨ			a ₀			σ _{n1}	
2		β ₁						κ			a ₁			θ ₁	
3		δ ₁						H			a ₂			tan θ ₁	
4		β ₂						ε			Z				
5		δ ₂												σ _{n2}	
6		θ ₁						cotδ ₁			b ₁			θ ₂	
7		GW ₁						cotδ ₂			b ₂			tan θ ₂	
8		JRC						cota			abGZ ₁				
9		JCS						tanε			abGZ ₂			Fs	
10								cote						β	
11											Final β				
12		$Z = (\text{COS}(C3)*\text{COS}(C5))+(\text{SIN}(C3)*\text{SIN}(C5)*\text{COS}(C2+C4))$													
13		$abGZ_1 = ((L2)-((L6*C7)/\text{Input \& Output'IB17}))-(((L7*C7)/\text{Input \& Output'IB17}-L3)*L4$													
14		$abGZ_2 = ((L3)-((L7*C7)/\text{Input \& Output'IB17}))-(((L6*C7)/\text{Input \& Output'IB17}-L2)*L4$													
15		$\sigma_{n1} = \text{Input \& Output'IB16}*\text{Input \& Output'IB15}*((L2*\text{Input \& Output'IB17})-(L6*C7))$													
16		$\theta_1 = C8*((\text{LOG}10(C9/(\text{IF}(O1<=0.10^{\wedge}16,O1)))))+\text{DEGREES}(C6)$													
17		$\tan \theta_1 = \text{TAN}(\text{RADIANS}(O2))$													
18		$\sigma_{n2} = \text{Input \& Output'IB16}*\text{Input \& Output'IB15}*((L3*\text{Input \& Output'IB17})-(L7*C7))$													
19		$\theta_2 = C8*((\text{LOG}10(C9/(\text{IF}(O5<=0.10^{\wedge}16,O5)))))+\text{DEGREES}(C6)$													
20		$\tan \theta_2 = \text{TAN}(\text{RADIANS}(O6))$													
21		$Fs = ((O1*O3)+(O5*O7))/(\text{Input \& Output'IB17}*\text{Input \& Output'IB16}*\text{Input \& Output'IB15})$													
22		The rest are the same as those of the Biplane Failure worksheet.													
23															
24															
25															

Figure E.6 Wedge Slope Analyzer (Barton Bandis) Floats worksheet

	A	B	C	D	E	F	G	H	I	J	K	L	M	N	O	P				
1		The summary of the three failure modes and the probability of the total slope failure																		
2																				
3																				
4																				
5		Sliding on both planes:		Fs			Sliding on both planes: Fs = 'Biplane Failure'K13 β = 'Biplane Failure'L10 P(failure) = 1-NORMSDIST(I6)													
6				β																
7				P(failure)																
8																				
9		Sliding along plane 1 only:		Fs			The smaller the β, the more critical is the failure mode. Thus, the smallest β among the three is corresponding to the most critical failure mode.					Sliding along plane 1 only: Fs = 'Plane 1 Failure'N15 β = 'Plane 1 Failure'L11 P(failure) = 1-NORMSDIST(H10)								
10				β																
11				P(failure)																
12																				
13		Sliding along plane 2 only:		Fs								Sliding along plane 2 only: Fs = 'Plane 2 Failure'N15 β = 'Plane 2 Failure'L11 P(failure) = 1-NORMSDIST(H14)								
14				β																
15				P(failure)																
16																				
17		Floats :		Fs			Floats : Fs = FloatsN18 β = FloatsL11 P(failure) = 1-NORMSDIST(I18)													
18				β																
19				P(failure)																
20																				
21																				
22		The total failure probability of this wedge slope is within the range:																		
23				≤ P _t (Failure) ≤																
24																				
25																				
26		$\text{IF}((I7<I11, \text{IF}(I11<I15, \text{IF}(I15<I19, I19, I15)), \text{IF}(I11<I19, I19, I11))), \text{IF}(I7<I15, \text{IF}(I15<I19, I19, I15)), \text{IF}(I7<I19, I19, I7))) \leq \text{Pt}(\text{Failure}) \leq 1 - ((1-I7)^*(1-I11)^*(1-I15)^*(1-I19))$																		
27																				
28																				
29																				

Figure E.7 Wedge Slope Analyzer (Barton Bandis) summary worksheet

APPENDIX F

TABLES OF RESULTS FOR PSA (COULOMB)

Table F.1 Values of Pf for H = 60 m and at 0 m height of water table

	Cohesion (kPa)			
	15	25	35	45
Probability of Slope Failure (Pf)	0.016	0.002	0.00011	0.000

Table F.2 Values of Pf for H = 70 m and at 0 m height of water table

	Cohesion (kPa)			
	15	25	35	45
Probability of Slope Failure (Pf)	0.02272	0.0041	0.00046	0.00003

Table F.3 Values of Pf for H = 80 m and at 0 m height of water table

	Cohesion (kPa)			
	15	25	35	45
Probability of Slope Failure (Pf)	0.02897	0.007	0.00116	0.00013

Table F.4 Values of Pf for H = 100 m and at 0 m height of water table

	Cohesion (kPa)			
	15	25	35	45
Probability of Slope Failure (Pf)	0.03877	0.01316	0.00342	0.00068

Table F.5 Values of Pf for H = 60 m and at 10 m height of water table

	Cohesion (kPa)			
	15	25	35	45
Probability of Slope Failure (Pf)	0.06130	0.01145	0.00205	0.00043

Table F.6 Values of Pf for H = 70 m and at 10 m height of water table

	Cohesion (kPa)			
	15	25	35	45
Probability of Slope Failure (Pf)	0.07741	0.01899	0.00426	0.00101

Table F.7 Values of Pf for H = 80 m and at 10 m height of water table

	Cohesion (kPa)			
	15	25	35	45
Probability of Slope Failure (Pf)	0.09065	0.02694	0.00720	0.00194

Table F.8 Values of Pf for H = 100 m and at 10 m height of water table

	Cohesion (kPa)			
	15	25	35	45
Probability of Slope Failure (Pf)	0.11020	0.04172	0.01422	0.00468

Table F.9 Values of Pf for H = 60 m and at 0 m height of water table

	Friction angle (degree)			
	30	34.99202	36	38
Probability of Slope Failure (Pf)	0.04885	0.016	0.01246	0.00796

Table F.10 Values of Pf for H = 70 m and at 0 m height of water table

	Friction angle (degree)			
	30	34.99202	36	38
Probability of Slope Failure (Pf)	0.06762	0.02272	0.01812	0.0116

Table F.11 Values of Pf for H = 80 m and at 0 m height of water table

	Friction angle (degree)			
	30	34.99202	36	38
Probability of Slope Failure (Pf)	0.08263	0.02897	0.02319	0.0149

Table F.12 Values of Pf for H = 100 m and at 0 m height of water table

	Friction angle (degree)			
	30	34.99202	36	38
Probability of Slope Failure (Pf)	0.10321	0.03877	0.03123	0.02022

Table F.13 Values of Pf for H = 60 m and at 10 m height of water table

	Friction angle (degree)			
	30	34.99202	36	38
Probability of Slope Failure (Pf)	0.18396	0.06130	0.04884	0.031

Table F.14 Values of Pf for H = 70 m and at 10 m height of water table

	Friction angle (degree)			
	30	34.99202	36	38
Probability of Slope Failure (Pf)	0.22669	0.07741	0.06182	0.03949

Table F.15 Values of Pf for H = 80 m and at 10 m height of water table

	Friction angle (degree)			
	30	34.99202	36	38
Probability of Slope Failure (Pf)	0.26012	0.09065	0.07254	0.04646

Table F.16 Values of Pf for H = 100 m and at 10 m height of water table

	Friction angle (degree)			
	30	34.99202	36	38
Probability of Slope Failure (Pf)	0.30689	0.11020	0.88480	0.05693

APPENDIX G

TABLES OF RESULTS FOR PSA (BARTON BANDIS)

Table G.1 Values of Pf for H = 60 m and at 0 m height of water table

	JCS (kPa)			
	55682.96	92804.93	129926.90	167048.9
Probability of Slope Failure (Pf)	5E-6	1.16E-6	2.3E-9	0.000

Table G.2 Values of Pf for H = 70 m and at 0 m height of water table

	JCS (kPa)			
	55682.96	92804.93	129926.90	167048.9
Probability of Slope Failure (Pf)	6.8E-6	18E-6	3E-7	1.1E-12

Table G.3 Values of Pf for H = 80 m and at 0 m height of water table

	JCS (kPa)			
	55682.96	92804.93	129926.90	167048.9
Probability of Slope Failure (Pf)	9.3E-6	2.4E-6	1E-6	5.4E-9

Table G.4 Values of Pf for H = 100 m and at 0 m height of water table

	JCS (kPa)			
	55682.96	92804.93	129926.90	167048.9
Probability of Slope Failure (Pf)	1.46E-5	4E-6	1.6E-6	7E-7

Table G.5 Values of Pf for H = 60 m and at 10 m height of water table

	JCS (kPa)			
	55682.96	92804.93	129926.90	167048.9
Probability of Slope Failure (Pf)	2.78E-5	7.6E-6	3.1E-6	1.5E-6

Table G.6 Values of Pf for H = 70 m and at 10 m height of water table

	JCS (kPa)			
	55682.96	92804.93	129926.90	167048.9
Probability of Slope Failure (Pf)	3.36E-5	9.31E-6	3.8E-6	1.9E-6

Table G.7 Values of Pf for H = 80 m and at 10 m height of water table

	JCS (kPa)			
	55682.96	92804.93	129926.90	167048.9
Probability of Slope Failure (Pf)	0.0000399	0.0000112	0.0000046	0.0000023

Table G.8 Values of Pf for H = 100 m and at 10 m height of water table

	JCS (kPa)			
	55682.96	92804.93	129926.90	167048.9
Probability of Slope Failure (Pf)	0.0000527	0.0000150	0.0000063	0.0000032

Table G.9 Values of Pf for H = 60 m and at 0 m height of water table

	Basic Friction angle (degree)			
	22	26	30	34.99202
Probability of Slope Failure (Pf)	0.0000116	0.0000080	0.0000060	0.0000050

Table G.10 Values of Pf for H = 70 m and at 0 m height of water table

	Basic Friction angle (degree)			
	22	26	30	34.99202
Probability of Slope Failure (Pf)	0.0000209	0.0000133	0.0000095	0.0000068

Table G.11 Values of Pf for H = 80 m and at 0 m height of water table

	Basic Friction angle (degree)			
	22	26	30	34.99202
Probability of Slope Failure (Pf)	0.0000331	0.0000198	0.0000134	0.0000093

Table G.12 Values of Pf for H = 100 m and at 0 m height of water table

	Basic Friction angle (degree)			
	22	26	30	34.99202
Probability of Slope Failure (Pf)	0.0000641	0.0000353	0.0000224	0.0000146

Table G.13 Values of Pf for H = 60 m and at 10 m height of water table

	Basic Friction angle (degree)			
	22	26	30	34.99202
Probability of Slope Failure (Pf)	0.0001300	0.0000696	0.0000435	0.0000278

Table G.14 Values of Pf for H = 70 m and at 10 m height of water table

	Basic Friction angle (degree)			
	22	26	30	34.99202
Probability of Slope Failure (Pf)	0.0001710	0.0000887	0.0000540	0.0000336

Table G.15 Values of Pf for H = 80 m and at 10 m height of water table

	Basic Friction angle (degree)			
	22	26	30	34.99202
Probability of Slope Failure (Pf)	0.0002180	0.0001100	0.0000655	0.0000399

Table G.16 Values of Pf for H = 100 m and at 10 m height of water table

	Basic Friction angle (degree)			
	22	26	30	34.99202
Probability of Slope Failure (Pf)	0.0003240	0.0001570	0.0000898	0.0000527